

**NUMERICAL MODELING OF UNSTEADY AND
NON-EQUILIBRIUM SEDIMENT TRANSPORT IN
RIVERS**

**A Thesis Submitted to
The Graduate School of Engineering and Sciences of
İzmir Institute of Technology
In Partial Fulfillment of the Requirements for the Degree of
MASTER OF SCIENCE
in Civil Engineering**

**by
Aslı BOR**

**December 2008
İZMİR**

We approve the thesis of **Aslı BOR**

Prof. Dr. Gökmen TAYFUR
Supervisor
Department of Civil Engineering
İzmir Institute of Technology

Asist. Prof. Dr. Şebnem ELÇİ
Department of Civil Engineering
İzmir Institute of Technology

Prof. Dr. M. Şükrü GÜNEY
Department of Civil Engineering
Dokuz Eylül University

.....
.....

.....
.....

04.12.2008

Date

Prof. Dr. Gökmen TAYFUR
Head of the Department of
Civil Engineering

Prof. Dr. Hasan BÖKE
Dean of the Graduate School of
Engineering and Science

ACKNOWLEDGEMENTS

I would like to thank my advisor Prof. Dr. Gökmen TAYFUR for making this work possible. I am very grateful for his constant guidance, support and encouragement throughout my masters program. I would like to extend a note of thanks to Asst. Prof. Dr. Şebnem ELÇİ for taking her valuable time out and agreeing to be on my thesis committee and also helping me out in times of need.

This study would not be possible without the support of The Scientific and Technical Research Council of Turkey (TUBİTAK Project number 106M274). I also would like to special thanks to Prof. Dr. M. Şükrü GÜNEY, who is the principle investigator of the project and he is the member of thesis committee for his valuable assistance throughout this project. I would also like to thank Prof. Dr. Turhan ACATAY and Gökçen BOMBAR for all the assistance they have provided.

Thanks to research assistants at IYTE Department of Civil Engineering who helped me in anyway along this study. Thanks to my colleagues Anıl ÇALIŞKAN, Ramazan AYDIN and Sinem ŞİMŞEK for their help. Also special thanks to Nisa KARTALTEPE for her encouragement and good friendship.

I would like to extend a note of thanks to my sister Gizem BOR, my cousins Alptuğ TATLI, Altuğ TATLI and İsmail KESKİN for all their continuous support and endless love. A special thank to Fatih YAVUZ for his assistance and encouragement. Finally, I would like to give a special thanks to my parents and all other extend family members for their love and support, which always inspired me through my research period.

ABSTRACT

NUMERICAL MODELING OF UNSTEADY AND NON-EQUILIBRIUM SEDIMENT TRANSPORT IN RIVERS

Management of soil and water resources is one of the most critical environmental issues facing many countries. For that reason, dams, artificial channels and other water structures have been constructed. Management of these structures encounters fundamental problems: one of these problems is sediment transport.

Theoretical and numerical modeling of sediment transport has been studied by many researchers. Several empirical formulations of transported suspended load, bed load and total load have been developed for uniform flow conditions. Equilibrium sediment transport under unsteady flow conditions has been just recently numerically studied. The main goal of this study is to develop one dimensional unsteady and nonequilibrium numerical sediment transport models for alluvial channels.

Within the scope of this study, first mathematical models based on the kinematic, diffusion and dynamic wave approach are developed under unsteady and equilibrium flow conditions. The transient bed profiles in alluvial channels are simulated for several hypothetical cases involving different particle velocity and particle fall velocity formulations and sediment concentration characteristics. Three bed load formulations are compared under kinematic and diffusion wave models. Kinematic wave model was also successfully tested by laboratory flume data. Secondly, a mathematical model developed based on kinematic wave theory under unsteady and nonequilibrium conditions. The model satisfactorily simulated transient bed forms observed in laboratory experiments. Finally, nonuniform sediment transport model was developed under unsteady and nonequilibrium flow based on diffusion wave approach. The results implied that the sediment with mean particle diameter and the sediments with nonuniform particle diameters gave different solutions under unsteady flow conditions.

ÖZET

NEHİRLERDE KARARSIZ VE DENGESİZ SEDİMENT TAŞINIMININ NÜMERİK MODELLENMESİ

Toprak ve su kaynakları yönetimi birçok ülkenin karşılaştığı en ciddi çevre sorunlarından biridir. Bu nedenle barajlar, su kanalları ve diğer su yapıları inşa edilmektedir. Bu yapıların yönetimi, birçok problemle karşı karşıya kalmaktadır. Bu problemlerin biri de katı madde taşınımıdır.

Teorik ve nümerik katı madde taşınımı birçok araştırmacı tarafından çalışılmaktadır. Kararlı akım koşulları altında, askıda katı madde, çökmüş katı madde ve toplam katı madde taşınımı deneysel formüller yardımıyla geliştirilmiştir. Son yıllarda, kararsız akım şartları altında dengede katı madde taşınımı nümerik modellenmesi çalışılan konular arasındadır. Bu çalışmanın amacı da nehirlerde 1 boyutlu, kararsız ve dengesiz sediment taşınımının nümerik modellenmesidir.

Bu amaç çerçevesinde, önce kararsız ve dengeli akım koşulları altında kinematik, difüzyon ve dinamik dalga yaklaşımına göre üç farklı model geliştirilmiştir. Alluvial nehirlerdeki geçici yatak profilleri, farklı parçacık hızı ve parçacık düşüm hızı formülleri ve katı madde karakteristiklerini içeren farklı farazi durumlar için oluşturulmuştur. Kinematik ve difüzyon dalga yaklaşımı altında üç farklı yatak yükü formülü karşılaştırılmıştır. Ayrıca kinematik dalga modeli laboratuvar verileri ile test edilmiştir ve sonuçlar başarılı olmuştur. Daha sonraki aşamada, kinematik dalga yaklaşımını kullanarak kararsız akım şartları altında dengesiz model kurulmuştur. Kurulan model laboratuvar verileri ile test edilmiş ve gözlemlenen yatak profilleri, model ile başarıyla elde edilmiştir. Son olarak, üniform olmayan katı madde karışımı, difüzyon dalga yaklaşımı ile kararsız ve dengesiz akım şartları altında modellenmiştir. Sonuçlara göre katı madde ortalama çapı ile kurulan model ve üniform olmayan katı madde karışımı ile kurulan model, kararsız akım şartlarında farklı sonuçlar vermiştir. Bu sonuçlar ayrıca laboratuvar verileri ile desteklenmelidir.

TABLE OF CONTENTS

LIST OF FIGURES	x
LIST OF TABLES	xiii
CHAPTER 1. INTRODUCTION	1
CHAPTER 2. LITERATURE REVIEW	6
2.1. Physical Studies	6
2.2. Mathematical Studies	8
2.2.1. Analytical Studies	8
2.2.2. Numerical Studies	9
2.2.2.1. One Dimensional Model Studies	11
2.2.2.2. Two Dimensional Model Studies	12
2.2.2.3. Three Dimensional Model Studies	14
2.3. Measurement Surveys	14
CHAPTER 3. MECHANICS OF SEDIMENT TRANSPORT	16
3.1. Physical Properties of Water	16
3.1.1. Specific Weight	16
3.1.2. Density	16
3.1.3. Viscosity	17
3.2. Physical Properties of Sediment	17
3.2.1. Size	18
3.2.2. Shape	18
3.2.3. Particle Specific Gravity	19
3.2.4. Fall Velocity	19
3.2.4.1. Dietrich Approach	21
3.2.4.2. Yang Approach	23
3.3. Bulk Properties of Sediment	23
3.3.1. Particle Size Distribution	23

3.3.2. Specific Weight.....	24
3.3.3. Porosity	24
3.4. Incipient Motion Criteria	25
3.4.1. Shear Stress Approach	26
3.4.2. Velocity Approach	27
3.4.3. Meyer – Peter and Müller Criterion	28
3.5. Resistance to Flow with Rigid Boundary	28
3.5.1. Darcy – Weisbach, Chezy and Manning formulas.....	29
3.6. Bed Forms	31
3.7. Mechanism of Sediment Transport.....	32
3.7.1. Bed Load Transport Formulas	33
3.7.1.1. DuBoys Approach	33
3.7.1.2. Meyer – Peter’s Approach.....	34
3.7.1.3. Schoklitsch Formula	35
3.7.1.4. Shields Approach.....	36
3.7.1.5. Meyer – Peter and Müller’s Approach	36
3.7.1.6. Regression Approach.....	37
3.7.1.7. Chang, Simons and Richardson’s Approach	38
3.7.1.8. Parker et al. (1982) Approach	39
3.7.1.9. Tayfur and Singh’s Approach	40
3.7.2. Suspended Load Transport Formulas.....	41
3.7.2.1. The Rouse Equation	41
3.7.2.2. Lane and Kalinske’s Approach	43
3.7.2.3. Einstein’s Approach	44
3.7.3. Total Load Transport Formulas	45
3.7.3.1. Einstein’s Approach	45
3.7.3.2. Laursen’s Approach.....	46
3.7.3.3. Bagnold’s Approach.....	47
3.7.3.4. Engelund and Hansen’s Approach	48
3.7.3.5. Ackers and White’s Approach.....	49
 CHAPTER 4. ONE DIMENSIONAL HYDRODYNAMIC MODEL.....	 51
4.1. de Saint Venant Equations	51
4.1.1. Continuity Equation in Unsteady Flows	52

4.1.2. Momentum Equation in Unsteady Flows.....	54
4.2. Kinematic Wave Approximation	59
4.3. Diffusion Wave Approximation	60
4.4. Dynamic Wave Approximation	61
CHAPTER 5. ONE DIMENSIONAL SEDIMENT TRANSPORT MODEL	63
5.1. One Dimensional Numerical Model for Sediment Transport	
under Unsteady and Equilibrium Conditions	63
5.1.1. Kinematic Wave Model of Bed Profiles in Alluvial	
Channels under Equilibrium Conditions.....	63
5.1.1.1. Numerical Solution of Kinematic Wave Equations	67
5.1.1.2. Model Testing for Hypothetical Cases	70
5.1.1.2.1. Hypothetical Case I: Effect of Inflow	
Concentration	71
5.1.1.2.2. Hypothetical Case II: Effect of Particle	
Velocity and Effect of Particle Fall Velocity	73
5.1.1.2.3. Hypothetical Case III: Effect of Maximum	
Concentration	79
5.1.2. Diffusion Wave Model of Bed Profiles in Alluvial	
Channels under Equilibrium Conditions.....	81
5.1.2.1. Numerical Solution of Diffusion Wave Equation	82
5.1.3. Dynamic Model of Bed Profiles in Alluvial Channels	
under Equilibrium Conditions	82
5.1.3.1. Numerical Solution of Dynamic Wave Equations	83
5.1.3.2. Model Testing: Comparing the Kinematic, Diffusion	
and Dynamic Models for Hypothetical Cases	84
5.1.3.3. Hypothetical Case I: Comparing Three Bed Load	
Formulas under Kinematic and Diffusion Wave	
Models	87
5.1.3.4. Model Testing Using Experimental Data	88
5.1.3.4.1. Test I	88
5.1.3.4.2. Test II	91
5.2. One Dimensional Numerical Model for Sediment	
Transport under Unsteady and Nonequilibrium Conditions	95

5.2.1. Governing Equations.....	95
5.2.1.1. Numerical Solution of Kinematic Wave Equations	100
5.2.1.2. Model Application.....	102
5.2.1.3. Model Testing Using Experimental Data	105
5.2.1.4. Model Testing: Comparing the Equilibrium and Nonequilibrium models for Hypothetical Cases	107
5.3. One Dimensional Numerical Model for Nonuniform Sediment Transport under Unsteady and Nonequilibrium Conditions	109
5.3.1. Governing Equations.....	109
5.3.1.1. Numerical Solutions of Nonuniform Model.....	110
5.3.1.2. Model Application.....	111
 CHAPTER 6. SUMMARY AND CONCLUSION	 116
6.1. Summary	116
6.2. Conclusion	116
 REFERENCES	 118
 APPENDICES	
 APPENDIX A.....	 129

LIST OF FIGURES

<u>Figure</u>	<u>Page</u>
Figure 1.1. Different modes of sediment transport	3
Figure 3.1. Settling of sphere in still water	25
Figure 3.2. Shields diagram for incipient motion	27
Figure 3.3. Bed forms of sand bed channels	32
Figure 3.4. Movement types of sediment particles	33
Figure 4.1. Definition sketch for continuity equation.....	52
Figure 4.2. Definition sketch for momentum equation.....	55
Figure 5.1. Definition sketch of two layer system	64
Figure 5.2. Finite – difference grid	68
Figure 5.3. (a) Inflow hydrograph (b) Inflow concentration.....	71
Figure 5.4. Transient bed profile at (a) rising period (b) equilibrium period (c) recession period (d) post recession period of inflow hydrograph and concentration	72
Figure 5.5. Transient bed profile under different particle velocities at (a) rising period (b) equilibrium period (c) recession period (d) postrecession period of inflow hydrograph and concentration. (Source: under Rouse 1938, Dietrich 1982, Yang 1996 formula).....	77
Figure 5.6. Transient bed profiles under different fall velocities at (a) rising period (b) equilibrium period (c) recession period (d) postrecession period of inflow hydrograph and concentration. (Source: under Chien and Wan 1999, Bridge and Dominic 1984, Kalinske 1947 formulation.	78
Figure 5.7. Transient bed profile under different z_{max} values at (a) rising period (b) equilibrium period (c) recession period (d) postrecession period of inflow hydrograph and concentration.....	80
Figure 5.8. Comparison of numerical solution of Diffusion and Kinematic waves at distance (a) $x = 200m$ (b) $x = 500m$ (c) $x = 800m$ of the channel.....	85

Figure 5.9. Comparison of numerical solution of Dynamic, Diffusion and Kinematic waves at distance (a) $x = 200m$ (b) $x = 500m$ (c) $x = 800m$ (assuming clear water ($c = 0$))	86
Figure 5.10. (a) Comparison of Tayfur and Singh, Meyer – Peter and Schoklitsch bed load formulations under Kinematic wave model at time 160 min. (b) Comparison of Tayfur and Singh, Meyer – Peter and Schoklitsch bed load formulations under Kinematic wave model at distance $x = 200m$ of the channel	87
Figure 5.11. (a) Comparison of Tayfur and Singh, Meyer – Peter and Schoklitsch bed load formulations under Diffusion wave model at time 160 min. (b) Comparison of Tayfur and Singh, Meyer – Peter and Schoklitsch bed load formulations under Diffusion wave model at distance $x = 200m$ of the channel	88
Figure 5.12. (a) The input hydrograph a) Rising limb = 90 second (b) Rising limb = 120 second	89
Figure 5.13. Measured and computed water depths at (a) 10.5 m (b) 14 m (the hydrograph that has 90 second in rising limb)	90
Figure 5.14. Measured and computed water depths at (a) 10.5 m (b) 14 m (the hydrograph that has 120 second in rising limb)	90
Figure 5.15. Simulation of measured bed profile at (a) 30 min (b) 60 min (c) 90 min.....	92
Figure 5.16. Simulation of measured bed profile at (a) 15 min (b) 45 min (c) 75 min (d) 105 min.....	94
Figure 5.17. Definition Sketch of two layer system in nonequilibrium condition	96
Figure 5.18. (a) Inflow hydrograph. (b) Inflow concentration.....	103
Figure 5.19. Transient bed profile at (a) rising period (b) equilibrium period (c) recession period (d) post recession period of inflow hydrograph and concentration	104
Figure 5.20. Simulation of bed profiles along a channel bed at (a) 30 h, (b) 60 h, (c) 90 h and (d) 120 h of the laboratory experiment.....	106

Figure 5.21. Simulation of bed profiles in time during the laboratory experiment at six different locations of the experimental channel. Location #1 is 10 m away from the upstream end.....	107
Figure 5.22. (a) Inflow hydrograph. (b) Inflow concentration.....	108
Figure 5.23. Comparing the equilibrium and nonequilibrium models.....	108
Figure 5.24. Multiply – layer model for bed load column.....	109
Figure 5.25. (a) Inflow hydrograph. (b) Inflow concentration	112
Figure 5.26. Transient bed profiles of nonuniform sediment and uniform sediment model at (a) rising period (b) equilibrium period (c) recession period (d) post recession period of inflow hydrograph and concentration in unsteady flow conditions.....	113
Figure 5.27. Transient bed profiles of nonuniform sediment and uniform sediment model at (a) rising period (b) equilibrium period (c) recession period (d) post recession period of inflow hydrograph and concentration in steady flow conditions	114

LIST OF TABLES

<u>Figure</u>	<u>Page</u>
Table 3.1. Properties of water	18
Table 5.1. Computed <i>RMSE</i> , <i>MAE</i> , <i>MRE</i>	91
Table 5.2. Computed <i>RMSE</i> , <i>MAE</i> , <i>MRE</i>	93
Table 5.3. Computed <i>RMSE</i> , <i>MAE</i> , <i>MRE</i>	107
Table 5.4. Sediment Characteristics.....	112

CHAPTER 1

INTRODUCTION

River management is as old as human civilization. Since ancient times, rivers have been used for water supply, flood control, irrigation, tourism, navigation, fishing, waste disposal and power generation by civilizations. Water is the source of life and soil is the root of existence. The life cannot exist without water and soil. Water and soil resources are the most fundamental materials on which people rely for existence and development. Development of society is determined by its capacity to use its resources. Some of these resources may in time become exhausted and deteriorate (World Meteorological Organization 2003). Soil and water are limited and irreplaceable resources. Especially in developing countries, due to the industrial growth and urbanization quality and quantity of natural water resources have been rapidly decreased. This may lead to water resources come to an end.

Soil and water losses cause the deterioration of ecology and changes in river morphology have a direct impact on earth's landscape. By human activities, as inappropriate land and water resources usage, land desertification occurs and it makes the farmland useless forever. Sedimentation is the consequence of a complex natural process involving soil detachment, entrainment, transport and deposition. It is common in rivers because of the difference between sediment load and the real sediment transportation capacity of flow. When sediments are deposited in river basins, the water level rises and it brings ecological problems such as landslides and slope collapses, debris flow and flow disasters. It also causes economical problems nationwide. On the other hand, transport of sediment reduces reservoirs life-time and hydrodynamic potential of dams and can contribute to contamination of drinking water supplies (Bor, et al. 2007). Reservoirs are limited, precious and non renewable resources. Reducing the capacity of the reservoir, affects factors of design aims such as water supply, flood control, irrigation, and power generation. Sediment accumulation has been estimated to decrease worldwide reservoir storage by 1% per year (Mahmood 1987). On the other hand, erosion can cause scouring under the river training works, so it brings some safety problems for river and it affects water supply and navigation along the rivers. Furthermore, aggregation and degradation affect the stability of a dam.

Sediment particles in water, might behave as a carrier for heavy metals which have affinity to attach to cohesive sediments. They serve as the major pollutant and can cause disruption of ecosystems. Sediment particles such as nitrogen, organic compounds, residues, pathogenic bacteria, pesticides and viruses are carried into a reservoir, deteriorate water quality and cause different illness (World Meteorological Organization 2003).

Sedimentation and soil erosion are the modern world's environmental topics. These subjects have been studied for centuries by engineers. There are different approaches for solving engineering problems. Sediment deposition deals with water and sediment particles so, the physical properties of water and sediment particles should be studied to understand sediment transport mechanism. Sediments are transported as suspended and bed load as shown in Figure 1.1 depending upon fundamental properties of water and sediment particle size, density, etc.

In a river system, loose surface can erode from basin by water and be transported by stream. Sediment particles can be transported in four modes rolling, sliding, saltation and suspension. While sediment particles are sliding and rolling, particles continue to be at contact with the bed. Saltation means that jumping motion along the bed in a series of low trajectories. Rolling and sliding particles move along the bed surface under the force of the overlying flow of water. It is often unimportant to distinguish saltation from rolling or sliding because saltation is restricted to only a few grain diameters in height (Dyer 1986). A saltating grain may only momentarily leave the bed and rise no higher than a few (<4) grain diameters. These three modes are bed load transport. Sometimes sediments stay in suspension for an appreciable length of time called suspended load transport. Suspension of a sediment grain is one of the modes in water systems that occurs when the magnitude of the vertical component of the turbulent velocity is greater than the settling speed of the grain. Bagnold (1966) argued that the major distinction in sediment transport modes is between suspended and unsuspended (bed load) transport. Bed load sediment grains and aggregates are transported under the combined processes of saltation, rolling, and sliding, and receive insufficient hydrodynamic impulses to overcome gravitational settling. Their only significant upward impulse is derived from successive contacts with the bed (Dyer 1986). When the flow conditions satisfy or exceed the criteria for incipient motion, sediment particles along an alluvial bed will start to move (Yang 1996).

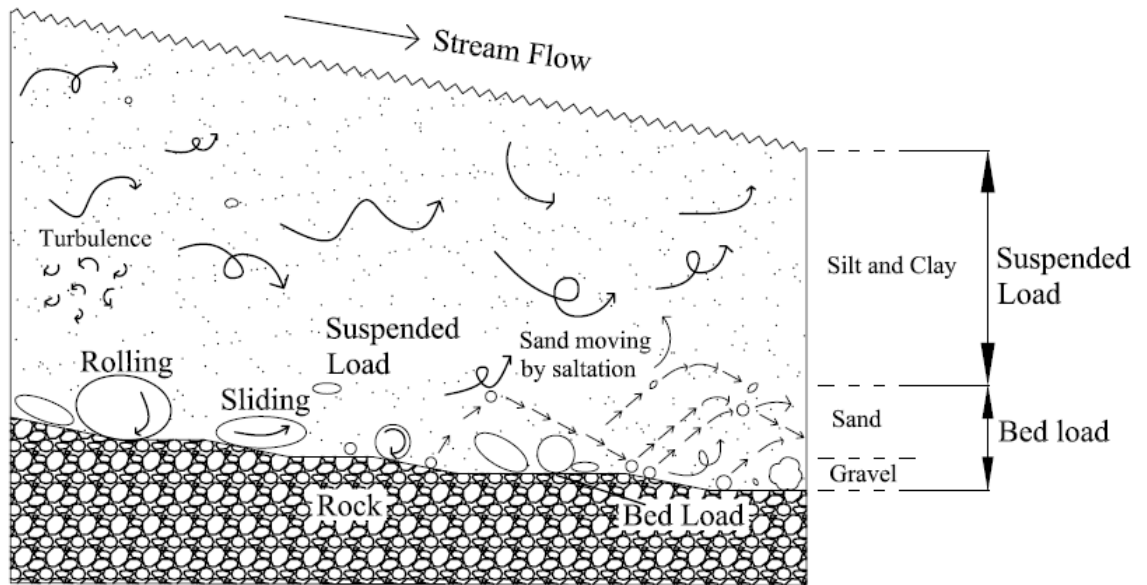


Figure 1.1. Different modes of sediment transport
(Source: Singh 2005)

It is essential to predict effects of sedimentation and loss of storage capacity in advance for better operation of the reservoirs. Current research on reservoir sedimentation prediction is mainly based on numerical modeling of sediment transport methodologies (Hotchkiss and Parker 1991) and investigation of transport parameters in the laboratory (Guy, et. al. 1966, Soni 1981a).

Free-surface flows can be classified into various types using criteria of their classification (Chaudhry 1993). Steady and unsteady flows based on changes with respect to time. In steady flow regimes, depth and velocity do not vary with time. If depth and velocity at a point vary with time, the flow regime is classified as unsteady. It is possible to transform an unsteady flow into a steady flow by having coordinates with respect a moving reference in some cases. Studying steady flow is easier than unsteady flows in governing mathematical models although the real world situation is unsteady flow. Such a transformation is possible only if the wave shape does not change as the wave propagates.

One of the other classifications based on changes with respect to space. If the flow velocity at a given instant of time does not change within a given length of channel, it is uniform flow. It means that the convective acceleration is zero. If the flow velocity at a time varies with respect to distance, it is non-uniform flow. Steady and

unsteady flows are characterized by the variation with respect to time at a given location, whereas the uniform and nonuniform flows are characterized by the variation at a given instant of time with respect to distance.

The flow can be classified based on Reynolds number. If the liquid particles appear to move in definite smooth paths and the flow appears to be as a movement of thin layers on top each other, it is laminar flow. In natural channels, in laminar flow Reynolds number is low than 500 ($Re < 500$). The flow is characterized by the irregular movement of particles of the fluid in turbulent flow, Reynolds number is greater than 600 ($Re > 600$). If the flow is that $500 < Re < 600$ it is called transient flow.

The other classification is based on Froude number. The Froude Number is a dimensionless parameter measuring of the ratio of the inertia force on an element of fluid to the weight of the fluid element - the inertial force divided by gravitational force. If the flow velocity is equal to celerity, it is critical flow ($F_r = 1$). If the flow velocity is less than the critical velocity, it is subcritical flow ($F_r < 1$). If the flow is supercritical the flow velocity is greater than the critical velocity ($F_r > 1$).

Hydraulic engineers generally treat channel in one dimension (1D). 1D flow means that the longitudinal acceleration is significant, whereas transverse and vertical accelerations are negligible.

Modeling of sediment transport can be assumed in equilibrium or non equilibrium conditions. If detachment rate and deposition rate are equal, the flow is in equilibrium condition. In non equilibrium condition, there is difference between detachment rate and deposition rate. There is no doubt that natural rivers are mostly in non equilibrium state. Because the real river systems behave as unsteady flow in non equilibrium state, treating the system with steady flow in equilibrium state is a simplification.

The main objective of this study is to develop unsteady and non equilibrium one dimensional numerical model for sediment transport in rivers. For that aim, first of all three numerical models were developed using the kinematic wave, diffusion wave and dynamic wave, for describing the bed profile evolution and movement in alluvial channels under equilibrium conditions. The models were evaluated by simulating bed profiles for several hypothetical scenarios. The scenarios involve solving the equations with different formulations of particle velocity, particle fall velocity, sediment flux and

different values of maximum bed elevation. Also, the models tested against measured flume data and the solutions were compared.

This thesis includes six chapters. Chapter 1 aims to present a brief introductory background to the research subject. Previous relevant physical and mathematical studies are reviewed in Chapter 2. Sediment transport formulations are summarized in Chapter 3. The one dimensional hydrodynamic model is described by the governing equations in Chapter 4. In Chapter 5, one dimensional sediment transport equations are governed in two categories: equilibrium and nonequilibrium. Also three different wave approaches were discussed: kinematic, diffusion and dynamic waves. The boundary conditions of the numerical model used in the study, and the testing of the model are described. Finally, in Chapter 6, the main results and the conclusions of the study are summarized.

CHAPTER 2

LITERATURE REVIEW

Sediment related disasters such as debris flow, landslides and slope collapses are known to occur naturally, causing social and economically problems in the world. Hence, the human civilizations study sediment transport to reduce the damages of the disasters and to maximize the benefits of the water resources structures. The studies of the sediment transport can be classified in two categories. Physical studies are related to extensive flume and field observations. Mathematical studies are related to develop theoretical and numerical methods.

2.1. Physical Studies

Physical studies are done by doing experiments in laboratory flumes or by taking field observations. It is difficult to represent a river by a laboratory flume; so many assumptions are usually incorporated in laboratory studies. The laboratory studies are still important for understanding of basic concepts of river flow and sediment transport. Many investigators have developed empirical methods to represent sediment transport phenomena using data obtained in laboratory.

Taking real time observations are better to understand the complex real life river systems. However it is very difficult to take real time data in the field and sometimes it is even impossible.

Experimental studies have been mostly done with laboratory flume experiments (Guy, et al. 1966, Langbein and Leopold 1968, Soni 1981a, Wathen and Hoey 1998, Lisle, et al. 1997, Lisle, et al. 2001). Also laboratory studies are easier than field measurements and provide control to particular combinations of initial and boundary conditions (Curran and Wilcock 2005).

Newton (1951) studied, with a series experiments, degradation with uniform sediment size. He saw that the bed elevation and bed slope decreased asymptotically with time.

Leopold and Maddock (1953) obtained field data showing the relationship between total sediment discharge and water discharge.

Lane and Borland (1954) conducted experiments to study riverbed scour during floods. Laboratory data were obtained for degradation in alluvial channels by Suryanarayana (1969).

Colby and Hembree (1955) compared the results of total sediment discharge and water discharge between computed and measured from the Niobrara River near Cody, Nebraska. Yang (1973) unit stream power equation gave the best agreement with those measurements.

Bhamidipaty et al. (1971) studied with Newton's analysis and combined their own extensive laboratory flume studies for three different particle sizes with uniform sediment grain sizes. They observed that the bed elevation in a degrading channel decreases exponentially with time. Soni et al. (1980) conducted a similar experiment using mobile bed under equilibrium conditions before the aggradation started. Hence they formed experiment conditions to better present the real river systems and developed a mathematical model for aggradation in an infinitely long channel. In 1980 Mehta (1980) improved studies by Soni et al. (1980) research with different sediment size particles.

Vanoni (1971) compared the computed sediment discharges from different equations with the measured results from natural rivers. Yang and Stall (1976) and Yang (1977) reported his comparisons.

For aggradation and degradation of non uniform sediments, Little and Mayer (1972) conducted a series of experiments. They studied the variations of sediment gradation on the bed surface during the armoring.

Ribberink (1985) studied the vertical sorting phenomenon of sediment having an idealized gradation under the equilibrium conditions. He also proposed a transport layer concept.

Yen et al. (1985) and Yen et al. (1988a) conducted a series of overloading experiments using uniform coarse sediment and found that the mean sediment transport velocity and aggradation wave speed increase with the initial equilibrium bed slope and decrease with loading ration.

Wilcock and Southard (1989) did careful measurements and observations in equilibrium conditions and investigated the interaction between the transport, bed surface texture and bed configuration. Also, Wilcock et al. (2001) conducted five different sediments in a laboratory flume by carrying out 48 sets of experiments of flow, transport and bed grain size.

Yen et al. (1992) also did flume studies with constant median sediment particle diameter but varying geometric standard deviation, so that the effect of non uniformity in rivers could be taken into account. They investigated that aggradation and degradation depends on materials vary so that the effect of non uniformity in rivers could be taken into account.

Tang and Knight (2006) investigated the effect of flood plain roughness on bed form geometry, bed load transport and dune migration rate.

Experimental flume studies have the limitations due to the complexity of representing a real life river conditions. However, it helps us to understand basic concepts of river flow and it provides a detailed analysis for parameters related to physics of the problem.

2.2. Mathematical Studies

Both experimental flume studies and field observations have limitations in predicting sediment transport capacity. Laboratory studies do not represent real life river conditions, besides taking the survey data sometimes impossible. Due to these restrictions, investigators have made many assumptions during the research. To study the sediment transport mechanism, many investigators developed mathematical equations for real life situations. All the sediment transport mathematical models developed so far are based on five basic physical equations. These equations have been developed by many researches that can be solved both analytically and numerically.

Solving the complex differential equations, numerical solutions are more appropriate than analytical solutions. On the other hand analytical solutions can be developed and applied only in very simplified and simple cases.

2.2.1. Analytical Studies

When flow conditions are very simplified in one dimensional case analytical solution can be developed. Developing the solution is very complex for generalized two or three dimensional cases with complex conditions. Some of the well known analytical sediment models are summarized below.

Tinney (1955) solved one dimensional differential equation analytically to simulate the degradation of bed composed of uniform sediment in open channel and compared his result with Newton (1951).

Al-Khalif (1965) developed a bed load function which explains the aggradation using Einstein (1950) approach.

de Vries (1971) and de Vries (1973) developed a linear hyperbolic bed elevation change model using convection – acceleration and depth gradients.

Soni et al. (1980) used a linear diffusion model to predict the transient bed profiles due to sediment overloading.

Jain (1985) studied the process with appropriate boundary conditions.

Begin et al. (1981) computed longitudinal profiles that produced by base- level lowering using diffusion model.

Jaramillo (1983) estimate bed load discharge for a finite and semi finite domain using linear parabolic sediment transport model. The bed elevation was estimated using sediment transport equation. Jaramillo and Jain (1984) developed a nonlinear parabolic sediment model for non uniform flow and solved the model by using the method of weighted residuals (Jain 1985). The results were compared with experimental data obtained by Newton (1951).

Gill (1983a) and Gill (1983b) used Fourier series by the error function methods and a linear parabolic bed elevation for a finite length channel to solve the linear diffusion equation for aggradation and degradation.

Zhang and Kahawita (1987) and Gill (1987) solved a nonlinear parabolic aggradation and degradation model and compared the solutions with experimental and linear solutions. They presented that the bed elevation is a function of square root of time.

Mosconi (1988) developed a linear hyperbolic analytical model for aggradation in the case of increase of sediment discharge and nonlinear parabolic analytical model for degradation in the case of reduction of sediment discharge.

2.2.2. Numerical Studies

The linear and non linear parabolic equations are generally based on the assumption of steady state or quasi state water flow. Unsteady water flow makes the

system complex and analytical solution is difficult to develop for the complex systems. Numerical sediment transport models have been developed in one, two or three dimensional have been listed below.

Lyn and Altinakar (2002) predicted bed elevation using quasi – steady model.

Curran and Wilcock (2005) studied constant flow rate and flow depth while varying the sand supply.

Mathematical sediment transport models have been based on generally diffusion wave and dynamic wave to predict bed profiles in alluvial channels. Whereas many researchers (de Vries 1973, Soni 1981b, Soni 1981c, Ribberink and Van Der Sande 1985, Lisle, et al. 2001) studied diffusion equations, others (Ching and Cheng 1964, Vreugdenhil and de Vries 1973, de Vries 1975, Ribberink and Van Der Sande 1985, Pianese 1994, Lyn and Altinakar 2002, Cao and Carling 2003, Singh, et al. 2004, Mohammadian, et al. 2004, Li and Millar 2007) studied dynamic equations. The sediment transport function has been expressed as a function of water flow variables and the bed formation and the bed movement has been treated as having diffusion characteristics in literature (Tayfur and Singh 2006). On the other hand the experimental studies by Langbein and Leopold (1968) provided that movement of bed profiles behaves as kinematic wave, a function of sediment transport rate and concentration. Kinematic wave theory applicability to unsteady flow routing problems is discussed by Tsai (2003). Tayfur and Singh (2006) used the kinematic wave theory under equilibrium conditions and modeled transient bed profiles.

Other mathematical approaches are equilibrium and nonequilibrium sediment transport models. In equilibrium models, the actual sediment transport rate is assumed to be equal to the sediment transport capacity at every cross section whereas in many cases the inflow sediment discharge imposed at the inlet is different than the transport capacity which might lead to difficulties in the calculation of bed changes near the inlet, thus solved by non- equilibrium models. Calculation of the equilibrium models are easier than non- equilibrium models. In many studies it was assumed that detachment rate and deposition rate are equal. This assumption may be valid only if conditions such as channel geometry, water and sediment properties are constant for a long period of time. Natural rivers are mostly in non – equilibrium state. Wu et al. (2004) developed one dimensional numerical model in unsteady flows under non – equilibrium conditions. Tayfur and Singh (2007) developed a mathematical model using kinematic wave theory under non – equilibrium conditions in alluvial rivers.

2.2.2.1. One Dimensional Model Studies

In rivers, the accelerations in lateral and vertical directions are mostly assumed negligible and therefore, acceleration in longitudinal direction is generally utilized in one dimensional models. This assumption simplifies the solution as it involves few equations only in one direction. These models have been mostly solved based on finite difference method to obtain bed elevation and water surface profiles (Perdreau and Cunge 1971, Cunge and Perdreau 1973, Chang 1982, Krishnappan 1985, Rahuel, et al. 1989, Holly and Rahuel 1990a, Holly and Rahuel 1990b, Correia, et al. 1992, Holly, et al. 1993).

de Vries (1965) has developed one dimensional model using explicit finite difference scheme to compute bed and water elevation profiles.

Cunge et al. (1980) has developed one dimensional model simulations of alluvial hydraulics.

Rahuel et al. (1989) studied unsteady flow models and have applied in river conditions. Cui et al. (1996), Kassem and Chaudhry (1998), Cao and Egiashira (1999), Capart (2000), Cao et al. (2001), Capart and Young (2002) and Di Cristo et al. (2002) have studied similar models in recent years, many numerical models.

The majority of one dimensional unsteady models can be divided into two categories in the literature: ⁽¹⁾uncoupled flow models that water flow equations and sediment continuity equation are solved separately and ⁽²⁾quasi-steady flow models that energy equation solved with sediment continuity equation. Only a few models are coupled in literature. Lyn and Goodwin (1987) presented an approach to model fully coupled unsteady water flow equations and sediment continuity equation. They compared the solutions between stability of coupled and uncoupled models and concluded that the coupled model is more stable. Other one dimensional coupled sediment transport models presented by Rahuel and Holly (1989), Holly and Rahuel (1990a, 1990b) simulating process between bed load and suspended load. Correria et al. (1992), studied with full explicit coupling models using water continuity equation, so it gives the permission to change the bed roughness depending on flow regime. Bhallamudi and Chaudhry (1989) have presented one dimensional, unsteady and coupled deformable bed model using Mac Cormack second order accurate explicit scheme. They compared the results with experimental laboratory flumes data and saw

that the results are satisfactory. Singh et al. (2004) have developed a fully coupled one dimensional alluvial river model and governed system of partial differential equations using Preissmann finite difference scheme. The tests presented by simulating the Quail Creek failure in Washington, USA. Wu et al. (2005) proposed one dimensional model simulates under unsteady flow conditions in dendritic channel networks with hydraulic structures. The equations solved in a coupling model and tested in several cases.

Although in uncoupled models, there is strong interaction between solid and water phases of the flow, only the flow continuity and momentum equations are solved simultaneously (Singh, et al. 2004). Park and Jain (1986) used Preissmann linearized implicit scheme for simulating the governing equations in unsteady and uncoupled models. Lyn (1987) studied uncoupled models and suggested that complete coupling between the full unsteady flow equations and sediment continuity equation is desirable in cases where the conditions change rapidly at the boundaries.

2.2.2.2. Two Dimensional Model Studies

Sediment concentration is averaged only along one direction, generally vertical direction (depth – integrated) where vertical variations are not significant depending on the flow characteristics in two dimensional models. One of the advantages of the 2D simulation of flow and sediment transport is depth – averaged subsystem for river flow. In depth – averaged models, all the model parameters are assumed to be same everywhere the water column. The depth - integrated equations of motion and continuity are linked to a depth - integrated sediment transport model (Boer, et al. 1984, McAnally, et al. 1991). The two dimensional models are more difficult than the one dimensional models and they provide more information about flow conditions.

Although the best mathematical model is the three dimensional it is not practical since it requires much more computational time especially in longer river stretches. In addition, enough experimental data cannot be available in general for model calibration.

Struiksma (1985) and Shimizu and Itakura (1989) developed a two dimensional model for the simulation of the large scale bed change in alluvial channels.

Mohapatra and Bhallamudi (1994) developed two dimensional model using a false transient principle with the quasi – steady uncoupled approach in a transformed coordinate system and McCormack scheme was used for the numerical solution.

Chaudhary (1996) developed the model for straight and meandering channels.

MIKE21 (DHI 2003), TABS-MD (Thomas and McAnally 1990), CCHE2D (Wu 2001) and HSCTM2D (Hayter 1995) are the widely used two dimensional sediment transport models.

MIKE21C is the curvilinear finite difference model. It has been developed at the Danish Hydraulic Institute (DHI) for river morphology (Langendoen 1996). The effects of secondary flow are taken into account by introducing quasi – steady approach in curved channels. In bends, the direction of sediment transport has been determined by using this secondary flow. Also, the model has been used to simulate critical morphological and hydrodynamic conditions.

One of the depth – integrated two dimensional sediment transport model is CCHE2D (Wu 2001). This model is based on variation of the finite element method using depth – average $k-\varepsilon$ models to estimate the turbulent eddy viscosity. The secondary flow effects were modeled on bed load direction in curved channels although fluid momentum and sediment transport rate effects were not. This model is applicable for morphological problems in rivers.

HSCTM2D (Hydrodynamic, Sediment and Contaminant Transport Model) model was developed for U. S. Environmental Protection Agency which based on the finite element method and vertically integrated in cohesive sediments.

Other well known models for simulation of sediment transport are TRIM-2D (Casulli 1990) based on finite difference approach and was adapted for practical applications. MOBED2 (Spasojevic and Holly 1990) models with finite difference and applicable in natural rivers, and TELEMAC2D with its module TSEF based on standard equilibrium bed load formulations as Meyer – Peter Müller (1948) uses $k-\varepsilon$ models with finite element model.

Minh Duc et al. (2004) developed a depth – averaged model using a finite volume method to calculate bed deformation in alluvial channels.

Li and Millar (2007) studied two dimensional hydrodynamic bed model to simulate bed load transport.

2.2.2.3. Three Dimensional Model Studies

The sediment transport process in alluvial channels could be described best by three dimensional models that include all the space dimensions. Since the full equations of motion are solved, the model is the most complicated and resource consuming in implementation. When the flow is stratified in salinity or temperature, mostly three dimensional models are applicable.

Demuren and Rodi (1986) used $k - \varepsilon$ models to develop neutral tracer transport model.

Wan and Adefeff (1986) developed finite element method for unsteady flow.

Van Rijn (1987) developed equations for mass balance using three dimensional equations and combined them with two dimensional depth integrated model.

Lin and Falconer (1996) developed a three dimensional sediment transport model for estuaries and coasts.

Hamrick (1996) developed EFDC and tested numerical model. EFDC can simulate flow processes in all three dimensions in rivers, lakes, reservoirs, estuaries, wetlands and coastal regions.

Wu (2000) studied three dimensional models for straight channels.

Delft-3D (Delft Hydraulics 2002) and ECOMSED (HydroQual Inc. 2003) are general three dimensional models that are used widely.

ECOMSED is the sediment transport model that was developed by HydroQual, Inc. and Delft Hydraulics (Blumberg and Mellor 1987) for estuaries and oceans. This model is applicable only up to a diameter size of $500 \mu m$ and cannot be applied for bed load transport. HydroQual, Inc. developed the SED module of ECOMSED (2002). A three dimensional suspended sediment transport model is SED formed for non cohesive sediments using implicit scheme.

2.3. Measurement Surveys

The geomorphologic data of river can be obtained by a topographic survey, including a land survey and groundwater surveying, or by repetitive surveying with pre-determined ranges, since samples size distribution can be found and determined the dry density or unit weight. Also, surveying of reservoirs are required to determine

sedimentation rates and to assess overall capacity of the reservoir. For surveying, manual sounding poles, sounding weights and echo sounders are commonly used. For reasons of economy, accuracy and expediency, sedimentation surveys were carried out in small reservoirs or cross small river reaches. More advanced instruments have been adopted as electronic distance measuring systems for large reservoirs. Sedimentation surveys are best reliable for the accurate positioning of measuring points where no deposition or erosion takes place, the elevation of the bed surface should coincide with that measured in a previous survey (Bor, et al. 2008). This is a good check of the accuracy and reliability of the sedimentation surveys. In addition to this detailed bathymetry map, thickness and long-term average accumulation rates of the lake can be determined by using echo sounder systems (Odhiambo and Boss 2004). Other studies in literature about surveying using acoustic methods include the technical details of scanning (Urick 1983), techniques used for sediment mapping (Higginbottom, et al. 1994), and the comparison of different echoes on sediment type (Collins and Gregory 1996).

Also, in hydrometric stations for sediment measurement, suspended sediment discharge and sediment concentration, size gradation of suspended sediment and bed material can be measured the whole year around.

Taking real time observations can explain the real life systems better than flume experiments but it is very difficult to take real time data in the field even sometimes it is impossible.

CHAPTER 3

MECHANICS OF SEDIMENT TRANSPORT

Sediment transport mechanism is concerned about water and sediment particles. An understanding of the sediment transport mechanism requires the learning of the physical properties of water and sediment particles. Fundamental properties of water and sediment particles are described below.

3.1. Physical Properties of Water

The fundamental properties of water are important in sediment transport studies. They are summarized below.

3.1.1. Specific Weight

Specific weight is defined as weight per unit volume. Specific weight can be expressed as (Yang 1996):

$$\gamma = \rho g \quad (3.1)$$

where,

γ = specific weight (M/L²/T²)

ρ = density (M/L³)

g = gravitational acceleration (L/T²)

3.1.2. Density

Quantity of matter contained in a unit volume of the substance.

$$\rho = m/v \quad (3.2)$$

where,

m =mass (M)

v =volume (L^3)

3.1.3. Viscosity

Due to cohesion and interaction between molecules, resistance to deformation is observed. Viscosity of the property defines the rate of this resistance to deformation. Newton's law of viscosity relates shear stress and velocity gradient by dynamic viscosity.

$$\tau = \mu \frac{du}{dy} \quad (3.3)$$

where,

τ =shear stress (M/L^2)

μ =dynamic viscosity (M / (LT))

$\frac{du}{dy}$ =velocity gradient

Kinematic viscosity is the ratio between dynamic viscosity and fluid density (Yang 1996).

$$\nu = \frac{\mu}{\rho} \quad (3.4)$$

where,

ν =kinematic viscosity (L^2/T)

The properties of water are summarized in Table 3.1.

3.2. Physical Properties of Sediment

Particle size, shape specific gravity and fall velocity are important for understanding of sediment transport mechanism.

3.2.1. Size

Particle size clearly describes the physical properties of the sediment particle, so it is the most important parameter for many practical purposes. The sediment size can be measured by various methods such as sieve analysis, optical methods or visual accumulation tube analysis. The sediment grade scale suggested by Lane (1947), as shown in Table 3.1. It was adopted by American Geophysical Union and is still used by hydraulic engineers.

Table 3.1. Properties of water
(Source: Yang 1996)

Temperature (°C)	Specific Weight γ (kN/m ³)	Density ρ (kg/m ³)	Dynamic Viscosity $\mu \times 10^3$ (N-s/m ²)	Kinematic Viscosity $\nu \times 10^{-6}$ (m ² /s)
0	9.805	999.8	1.781	1.785
5	9.807	1000.0	1.518	1.519
10	9.804	999.7	1.307	1.306
15	9.798	999.1	1.139	1.139
20	9.789	998.2	1.002	1.003
25	9.777	997.0	0.890	0.893
30	9.764	995.7	0.798	0.800
40	9.730	992.2	0.653	0.658
50	9.689	988.0	0.547	0.553
60	9.642	983.2	0.466	0.474
70	9.589	977.8	0.404	0.413
80	9.530	971.8	0.354	0.364
90	9.466	965.3	0.315	0.326
100	9.399	958.4	0.282	0.294

3.2.2. Shape

Particle shape is the second most significant sediment property in natural sediments. The geometric configuration defines shape parameter regardless of sediment particle size and composition. Grains are usually considered to have with long diameter

a, intermediate diameter b and short diameter c. Corey (Schulz, et al. 1954) investigated several shape factors and defined the shape factor as:

$$CSF = \frac{c}{\sqrt{ab}} \quad (3.5)$$

Corel shape factor was the most significant expression of shape. The shape factor for a sphere would be 1.0. Natural sediment typically has a shape factor of about 0.7 (US Army Corps of Engineers 2008).

3.2.3. Particle Specific Gravity

Specific gravity is defined as the ratio of the specific weight of the sediment to that of water. It usually ranges numerically from 2.6 to 2.8 in natural solids. While the lower values of specific gravity are typical of the coarser soils, higher values are typical of the fine – grained soil types. Due to its resistance to weathering and abrasion, quartz, which has a specific gravity of 2.65, is the most common mineral found in natural noncohesive sediments. Typically, the average specific gravity of a sediment mixture is close to that of quartz. Therefore, in sedimentation studies, specific gravity is frequently assumed to be 2.65, although whenever possible, site-specific particle specific gravity should be determined (US Army Corps of Engineers 2008).

3.2.4. Fall Velocity

Fall velocity or settling velocity is the most fundamental property governing the motion of the sediment particle in a fluid. It is a function of the volume, shape and density of the particle and the viscosity and density of the fluid. The fall velocity of any naturally worn sediment particle may be calculated if the characteristics of the particle and fluid are known. Fall velocity is related to relative flow conditions between the sediment particle and water during conditions of sediment entrainment, transportation and deposition. Fall velocity can be calculated from a balance between the particle buoyant weight or submerged weight and the resulting force from fluid drag (Yang 1996). The general drag equation is

$$F_D = C_D \rho A \frac{v_f^2}{2} \quad (3.6)$$

where,

F_D = drag force

C_D = drag coefficient

ρ = density of water

A = the projected area of particle in the direction of fall

v_f = the fall velocity

The particle buoyant weight or submerged weight of a spherical sediment particle is

$$W_s = \frac{4}{3} r^3 \pi (\rho_s - \rho) g \quad (3.7)$$

where,

W_s = submerged weight

r = particle radius

ρ_s and ρ = densities of sediment and water respectively.

For very slow, steady moving sphere, the drag coefficient thus obtained is

$$C_D = \frac{24}{\text{Re}} \quad (3.8)$$

This equation is acceptable for Reynolds numbers less than 1.0 where;

$$\text{Re} = \frac{v_f d_s}{\nu} \quad (3.9)$$

where,

ν = kinematic viscosity of water

d_s = sediment diameter

From Equation 3.6 and Equation 3.8, Stokes (1851) equation can be obtained;

$$F_D = 3\pi d\rho v_f v \quad (3.10)$$

Equality of Equation 3.7 and Equation 3.10, the fall velocity for a sediment particle can be obtained as below:

$$v_f = \frac{1}{18} \frac{\gamma_s - \gamma_w}{\gamma_w} g \frac{d_s^2}{\nu} \quad (3.11)$$

where,

γ_s and γ_w = specific weights of sediment and water respectively.

This equation is acceptable for the particle diameter equal to or less than 0.1 mm.

The drag coefficient of a sphere depends on the Reynolds number. When the particle Reynolds number is greater than 2.0, the particle fall velocity is determined experimentally. Rouse (1937) gave $v_f = 0.024m/s$ for most natural sands, the shape factor is 0.7 and $d_s = 0.2mm$.

There are many approaches about fall velocity in literature. Some of them summarized below:

3.2.4.1. Dietrich Approach

Dietrich (1982) developed the following equation for fall velocity analyzing empirical relation.

$$W_* = R_3 10^{(R_1 + R_2)} \quad (3.12)$$

where,

W_* = the dimensionless fall velocity

$$W_* = \frac{\rho v_f^3}{(\rho_s - \rho)g\nu} \quad (3.13)$$

$$R_1 = -3.767 + 1.929(\log D_*) - 0.0982(\log D_*)^2 - 0.00575(\log D_*)^3 + 0.00056(\log D_*)^4 \quad (3.14)$$

$$R_2 = \log \left[1 - \frac{(1 - CSF)}{0.85} \right] - (1 - CSF)^{2.3} \tanh[\log D_* - 4.6] + 0.3(0.5 - CSF)(1 - CSF)^2 (\log D_* - 4.6) \quad (3.15)$$

$$R_3 = \left[0.65 - \left(\frac{CSF}{2.83} \tanh[\log D_* - 4.6] \right) \right]^{\left[1 + \frac{(3.5 - P)}{2.5} \right]} \quad (3.16)$$

where,

D_* = the dimensionless particle size

CSF = the Corey shape factor

The dimensionless particle size D_* is expressed as (Dietrich 1982):

$$D_* = \frac{(\rho_s - \rho)gd_s^3}{\rho v^2} \quad (3.17)$$

The Corey shape factor (CSF) is expressed as (Dietrich 1982):

$$CSF = \frac{c}{(ab)^{0.5}} \quad (3.18)$$

where,

a,b,c= the longest intermediate and shortest axes of the particle respectively and mutually perpendicular.

* $CSF \approx 0.5 - 0.8$ (Dietrich 1982)

P = Powers value of roughness (P is between 3.5 and 6 (Dietrich 1982))

3.2.4.2. Yang Approach

Yang (1996) expressed the fall velocity of particle (for the particle Reynolds number ($R_{pn} = v_f d_s / \nu$) is less than 2.0):

$$v_f = \begin{cases} \frac{1}{18} \frac{(\gamma_s - \gamma_w) g d_s^2}{\gamma_w \nu} & d_s \leq 0.1mm \\ F \left[\frac{g d_s (\gamma_s - \gamma_w)}{\gamma_w} \right]^{0.5} & \text{for } 0.1mm < d_s \leq 2.0mm \\ 3.32 \sqrt{d_s} & d_s > 2.0mm \end{cases} \quad (3.19)$$

where,

$$F = \begin{cases} \left[\frac{2}{3} + \frac{36\nu^2 \gamma_w}{g d_s^3 (\gamma_s - \gamma_w)} \right]^{0.5} - \left[\frac{36\nu^2 \gamma_w}{g d_s^3 (\gamma_s - \gamma_w)} \right]^{0.5} & 0.1mm < d_s \leq 1.0mm \\ 0.79 & 1.0mm < d_s \leq 2.0mm \end{cases} \quad (3.20)$$

3.3. Bulk Properties of Sediment

Three important bulk properties are described below, particle size distribution, specific weight and porosity.

3.3.1. Particle Size Distribution

Particle sizes are determined using a variety of methods. Diameters of particles larger than 256 mm may be obtained by measuring the mean diameter. Templates with square openings can be used to determine a size equivalent to the sieve diameter for particles between 32 and 256 mm. Sieve analyses are generally used for particles between 0.0625 and 32 mm. For sediments less than 0.0625 mm hydrometer analysis can be utilized.

The variation in particle sizes in a sediment mixture is described with a gradation curve, which is a cumulative size-frequency distribution curve showing particle size versus accumulated percent finer, by weight. It is common to refer to particle sizes according to their position on the gradation curve. d_{50} is the geometric mean particle size; that is, 50 percent of the sample is finer, by weight; $d_{84.1}$ is 1 standard deviation larger than the geometric mean size in practice and it is rounded to d_{84} , while $d_{15.9}$ is 1 standard deviation smaller than the geometric mean size and it is rounded to d_{16} in practice (US Army Corps of Engineers 2008).

3.3.2. Specific Weight

Specific weight of deposited sediment is the weight per unit volume. It is expressed as dry weight.

$$\gamma_d = (1 - p)SG\gamma_w \quad (3.21)$$

or

$$\gamma_d = (1 - p)\gamma_s \quad (3.22)$$

where,

γ_d = specific weight of deposited sediment

SG = specific gravity of sediment particle

p = porosity

Specific weight increases with time after initial deposition. It also depends on the composition of the sediment mixture (US Army Corps of Engineers 2008).

3.3.3. Porosity

It is defined as the ratio of volume of voids to total volume of sample. Porosity is affected by particle size, shape and degree of compaction.

$$p = \frac{V_v}{V_t} \quad (3.23)$$

where,

V_v = void volume

V_t = total volume of sample

3.4. Incipient Motion Criteria

The concept of incipient motion of sediment particles from the bed is important to understand the aggradation and degradation forces acting on a spherical sediment particle shown in Figure 3.1. The component of gravitational force in the direction of flow can be neglected compared to other forces acting on a spherical sediment particle because the channel slopes are small enough in most natural rivers. Other forces are drag force F_D , lift force F_L , submerged weight W_S and resistance force F_R . A sediment particle starts the incipient motion when the conditions are satisfied below (Yang 1996).

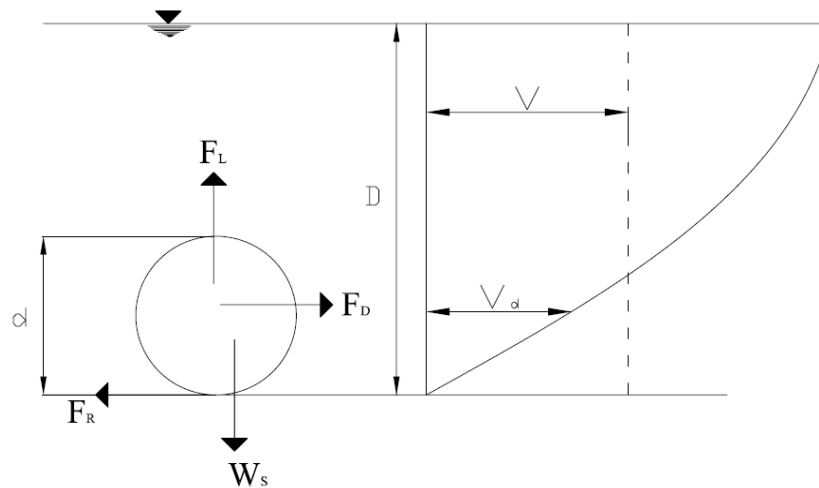


Figure 3.1. Settling of sphere in still water
(Source: Yang 1996)

where,

$$F_L = W_S$$

$$F_D = F_R$$

$$M_O = M_R$$

M_O =overturning moment due to F_D and F_R

M_R =resisting moment due to F_L and W_s

Different researchers developed several approaches defining the incipient motion of sediment particles.

3.4.1. Shear Stress Approach

In early 1936, Shields (1936) derived a function for incipient motion of sediment particles where balance of forces acting on a particle on a bed was considered. He applied dimensional analysis to determine dimensionless parameters and investigated the relationship between these two parameters by experimental studies.

$$\frac{\tau_c}{(\gamma_s - \gamma_w)d_s} = f\left(\frac{U_*d_s}{\nu}\right) \quad (3.24)$$

$$\text{Re} = \frac{U_*d_s}{\nu} \quad (3.25)$$

where,

Re=Reynolds number

U_* = shear velocity

τ_c = critical shear stress at initial motion

Vanoni (1975) developed diagram fitting the curve to the data provided by Shields (Figure 3.2). Figure 3.2. shows the results of experiments about relationship between dimensional shear stress and particle Reynolds number.

Shields simplified the problem by neglecting the lift force and considered only the drag force. The American Society of Civil Engineers Task Committee on the Preparation of Sediment Manual modified diagram and uses a third parameter as shown in Figure 3.2. The parameter is

$$\frac{d_s}{\nu} \left[0.1 \left(\frac{\gamma_s}{\gamma_w} - 1 \right) g d_s \right]^{1/2} \quad (3.26)$$

This parameter allows determination of intersection with the Shields diagram and its corresponding values of shear stress. Many investigators have proposed different options which are more or less the same.

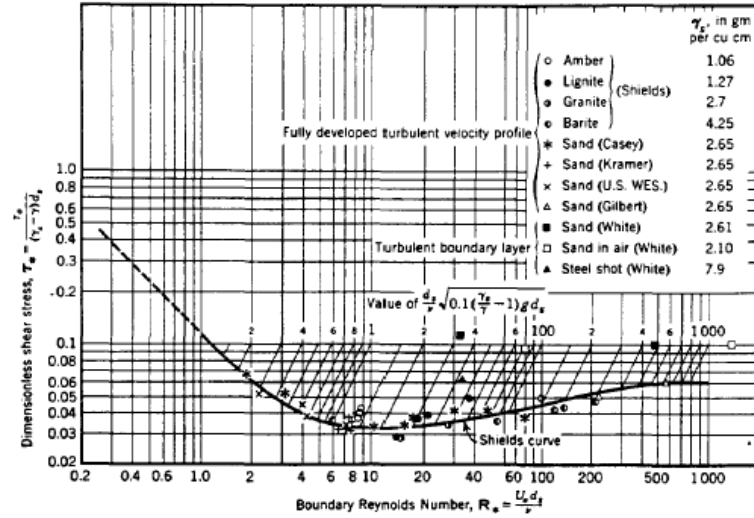


Figure 3.2. Shields diagram for incipient motion

(Source: Vanoni 1975)

3.4.2. Velocity Approach

Velocity approach uses the relationship between the velocity field and shear stress field. It means that the velocity for incipient motion can be calculated if the drag force for incipient motion is known.

Yang (1973) obtained incipient motion criteria using laboratory data collected by different investigators. The relationship between dimensionless critical average flow velocity and Reynolds number follows a hyperbola when the Reynolds number is less than 70 summarized in Equation 3.27. When the Reynolds number greater than 70, V_{cr} / ω becomes a constant, as shown Equation 3.28. (Singh 2005).

$$\frac{V_{cr}}{v_f} = \frac{2.5}{\log(U_* d_s / \nu) - 0.06} + 0.06, \quad 1.2 < \frac{U_* d_s}{\nu} < 70 \quad (3.27)$$

$$\frac{V_{cr}}{v_f} = 2.05, \quad 70 \leq \frac{U_* d_s}{\nu} \quad (3.28)$$

3.4.3. Meyer – Peter and Müller Criterion

Meyer – Peter and Müller (1948) obtained bed load equation and sediment size at incipient motion as formulated from bed load equation (Yang 1996).

$$d_s = \frac{SD}{K_1 \left(n / d_{90}^{1/6} \right)^{3/2}} \quad (3.29)$$

where,

d_s = sediment size in the armor layer (in mm)

S = channel slope

D = mean flow depth

K_1 = constant (=0.9 when D is in ft and 0.058 when D is in m)

n = channel bottom roughness or Manning's roughness coefficient

d_{90} = bed material size where 90% of the material is finer (in m)

3.5. Resistance to Flow with Rigid Boundary

Prandtl's (1926) mixing theory depends on velocity distribution approach. Velocity at distance y is

$$u = \left(8.5 + 5.75 \log \frac{y}{k_s} \right) U_* \quad (3.30)$$

and

$$u = \left(5.5 + 5.75 \log \frac{y U_*}{\nu} \right) U_* \quad (3.31)$$

where,

u = velocity at a distance y above the bed

$U_* = \sqrt{gDS}$ = shear velocity

D = depth of flow

S = slope

k_s = equivalent roughness defined by Schlichting (1955)

For sand bed channels,

$k_s = d_{65}$ (Einstein 1950),

$k_s = d_{90}$ (Meyer – Peter and Müller 1948),

$k_s = d_{85}$ (Simons and Richardson 1966, Yang 1996).

3.5.1. Darcy – Weisbach, Chezy and Manning formulas

The Darcy – Weisbach formula for pipe flow is

$$h_f = f \frac{L}{D} \frac{V^2}{2g} \quad (3.32)$$

For open channel flow,

$$R = \frac{A}{P} = \frac{\frac{\pi D^2}{4} / 2}{\pi D / 2} = \frac{D}{4} \quad (3.33)$$

and

$$S = \frac{h_f}{L} \quad (3.34)$$

So we can express the f value;

$$f = \frac{8gRS}{V^2} \quad (3.35)$$

$$gRS = U_*^2 \quad (3.36)$$

$$\frac{V}{U_*} = \left(\frac{8}{f} \right)^{1/2} \quad (3.37)$$

where,

h_f = friction loss

f = Darcy – Weisbach friction factor

L = pipe length

D = pipe diameter

V = average flow velocity

R = hydraulic radius

S = energy slope

The Chezy formula is

$$V = C_z \sqrt{RS} \quad (3.38)$$

Shear stress along the boundary is

$$\tau_0 = \frac{1}{8} f \rho V^2 \quad (3.39)$$

From relationship between τ_0, U_*, R and V , Chezy coefficient can be obtained by

$$C_z = \left(\frac{8\gamma}{f\rho} \right)^{1/2} \quad (3.40)$$

The Manning formula is

$$V = \frac{1}{n} R^{2/3} S^{1/2} \quad (3.41)$$

where,

n = Manning coefficient and can be obtained by the formula below;

$$n = \frac{d^{1/6}}{21.1} \quad (3.42)$$

where,

d = sediment diameter of uniform sand in m (Yang 1996).

3.6. Bed Forms

Rate of sediment transport mainly depends on resistance to flow and bed configuration. Simons and Richardson (1960) summarized bed forms as shown in Figure 3.3. below (Yang 1996).

Ripples begin to form, as current velocity picks up in lower flow regime. These are small bed forms, generally wavelengths less than 30 cm and heights less than 5 cm. In faster currents, ripples grow into dunes. Dunes are similar to bars but larger than ripples. Their profile height is limited by depth of flow, so they can be several meters tall in deep water. Bars are bed forms having lengths the same as channel width and height same as channel height. In higher velocities dunes are destroyed and plane bed forms occur. In very high velocities anti dune bed forms occurs. Water surface forms waves that move upstream and so anti dunes move upstream. These are also called standing waves. In large slopes, high velocities and sediment concentrations chutes and pools occur. They consist of large elongated mounds of sediment. In transition zone, bed configurations range from dunes to plane beds or to anti dunes.

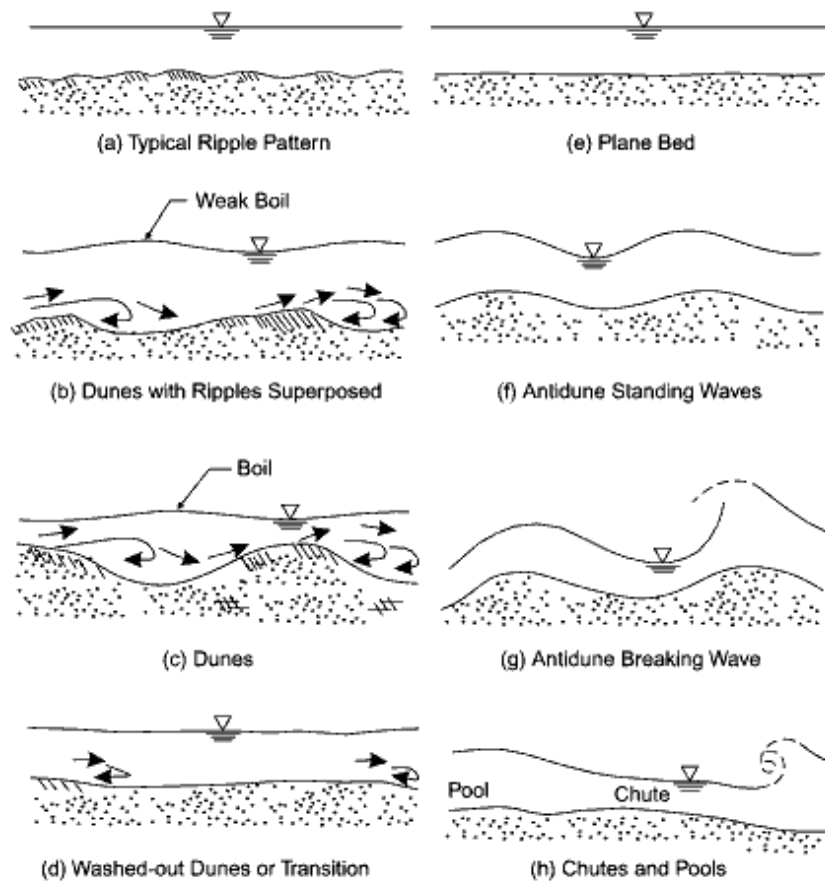


Figure 3.3. Bed forms of sand bed channels
 (Source: Simon and Richardson 1966)

3.7. Mechanism of Sediment Transport

Sediments are eroded from basin by water and transported by stream when the flow conditions exceed the criteria for incipient motion. The motion can be rolling, sliding or jumping along the bed which is called bed load transport. Sometimes sediments stay in suspension for an appreciable length of time called suspended load transport. In addition, wash load is a bed material load according the particle size and mainly moves as suspended load. So, sediment can be classified as bed material load and wash load or bed load and suspended load. Wash load transport is a function of basin characteristics, whereas bed load transport is a function of flow characteristics (Yang 1996) (Figure 3.4).

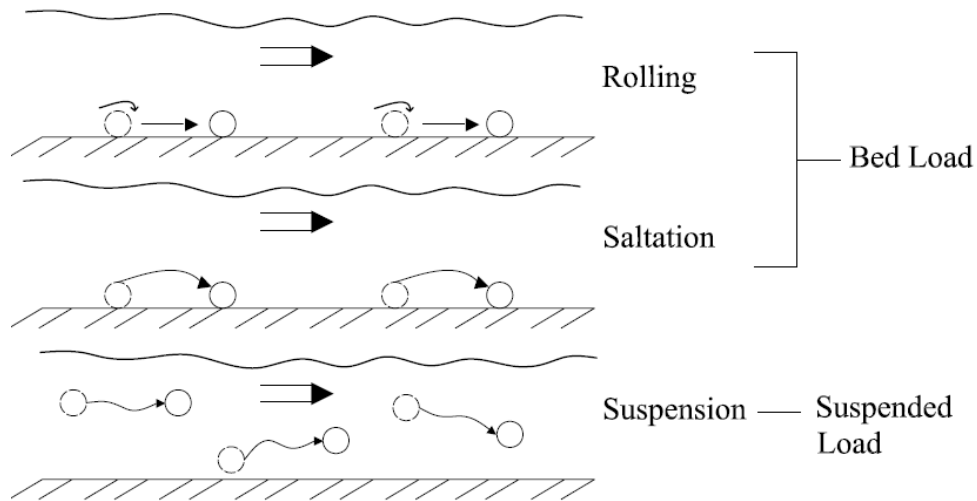


Figure 3.4. Movement types of sediment particles

3.7.1. Bed Load Transport Formulas

Bed load motion starts when critical conditions are exceeded. The motion concerned with two phase (solid + liquid) flow near the bed. Generally, the bed load transport rate of a river is about 5-25% of that in suspension. Bed load measurement is difficult, so it is estimated by sediment transport formulas based on different modes of motion employing different parameters, including shear stress and flow velocity. The approaches for prediction of bed load are briefly summarized as follows.

3.7.1.1. DuBoys Approach

Dubois (1879) developed a bed load model using shear stress approach. This model consists of sediment particles moving in layers because of the tractive force acting along at the bed. The bed load capacity formula is given as;

$$q_b = K\tau(\tau - \tau_c) \quad (3.43)$$

where; Straub (1935) defined K coefficient depending on the sediment particle characteristics.

$$K = \frac{0.173}{d^{3/4}} \quad (3.44)$$

Thus DuBoys equation can be rewritten as,

$$q_b = \frac{0.173}{d_s^{3/4}} \tau(\tau - \tau_c) \quad (3.45)$$

where,

d_s = sediment particle diameter in mm

τ and τ_c = bed and critical shear stress respectively in lb/ft²

q_b = bed load transport capacity in (ft³/sec)/ft

3.7.1.2. Meyer – Peter’s Approach

Meyer-Peter et al. (1934) developed the following bed load formula using the energy slope approach in metric system;

$$\frac{0.4q_b^{2/3}}{d_s} = \frac{q^{2/3}S}{d_s} - 17 \quad (3.46)$$

where,

q_b = bed load [in (kg/s)/m]

q = water discharge [in (kg/s)/m]

S = Slope

d_s = particle size (in m)

Meyer – Peter formula is valid only for coarse material sediment particle diameters greater than 3 mm. For mixtures of non uniform material, d should be replaced by d_{35} , where 35% of the mixture is finer than d_{35} (Yang 1996).

3.7.1.3. Schoklitsch Formula

There are two Schoklitsch bed load formulas which were developed from discharge approach. The first was published in 1934 in metric units.

$$q_b = 7000 \frac{S^{3/2}}{d_s^{1/2}} (q - q_c) \quad (3.47)$$

where,

q_b = bed load [in (kg/s)/m]

q and q_c = water discharge and critical discharge at incipient motion [in m³/s)/m] respectively

For sand with specific gravity 2.65, critical water discharge can be calculated by plotting for given flow and grain diameter curve of bed load as ordinate against slope as abscissa and then extrapolating the curve to zero bed load to obtain the intercept with abscissa.

$$q_c = \frac{0.00001944d_s}{S^{4/3}} \quad (3.48)$$

where,

d_s = particle size (in m)

S = energy slope

The second bed load formula was published in 1943 in metric units.

$$q_b = 2500S^{3/2}(q - q_c) \quad (3.49)$$

For sand with specific gravity 2.65 critical water discharge can be calculated by

$$q_c = \frac{0.6d_s^{3/2}}{S^{7/6}} \quad (3.50)$$

3.7.1.4. Shields Approach

Shields (1936) conducted laboratory studies and obtained the flow conditions corresponding to incipient motion when sediment transport greater than zero. Shield's measurements provided semi empirical equation for estimating bed load transport capacity (with English units);

$$\frac{q_b \gamma_s}{q \gamma_w S} = 10 \frac{\tau - \tau_c}{(\gamma_s - \gamma_w) d_s} \quad (3.51)$$

where,

q_b and q = bed load and water discharge per unit channel width, respectively

$$\tau = \gamma D S$$

τ_c can be obtained from Shields diagram (Yang 1996).

3.7.1.5. Meyer – Peter and Müller's Approach

Meyer-Peter and Müller (1948) transformed the Meyer-Peter bed load formula by isolating involved parameters one by one.

$$\gamma \left(\frac{K_s}{K_r} \right)^{3/2} R S = 0.047 (\gamma_s - \gamma_w) d + 0.25 \rho^{1/3} q_b^{2/3} \quad (3.52)$$

where,

R = hydraulic radius (in m)

S = energy slope

d = mean particle diameter (in m)

ρ = specific mass of water (in metric ton – s/m⁴)

q_b = bed-load rate in underwater weight per unit time and width [in (metric ton / s)/m]

$(K_s / K_r) S$ = the kind of slope which is adjusted for energy loss due to grain resistance

S_r , is responsible for the bed-load motion.

Energy slope can be calculated by Strickler (1923) formula:

$$S = \frac{V^2}{K_s^2 R^{4/3}} \quad (3.53)$$

Energy loss due to grain resistance can be calculated by Strickler's formula as:

$$S_r = \frac{V^2}{K_r^2 R^{4/3}} \quad (3.54)$$

So;

$$\frac{K_s}{K_r} = \left(\frac{S_r}{S} \right)^{1/2} \quad (3.55)$$

The formula is based on a large quantity of experimental data. Test results showed the relationship to be of the form;

$$\left(\frac{K_s}{K_r} \right)^{3/2} = \frac{S_r}{S} \quad (3.56)$$

And

$$K_r = \frac{26}{d_{90}^{1/6}} \quad (3.57)$$

where,

d_{90} = the size of sediment for which 90% of the material is finer (Yang 1996).

3.7.1.6. Regression Approach

Rottner (1959) expressed bed load discharge in terms of the flow parameters based on regression analysis. The formula is dimensionally homogeneous (Yang 1996).

$$q_b = \gamma_s [(\xi_s - 1)gD^3]^{1/2} \times \left\{ \frac{V}{[(\xi_s - 1)gD]^{1/2}} \left[0.667 \left(\frac{d_{50}}{D} \right)^{2/3} + 0.14 \right] - 0.778 \left(\frac{d_{50}}{D} \right)^{2/3} \right\}^3 \quad (3.58)$$

where,

q_b = bed load discharge (in lb/s per ft of width)

γ_s = specific weight of sediment (in lb/ft³)

ξ_s = specific gravity of the sediment (=2.65)

g = acceleration of gravity (in ft/s²)

D = mean depth (in ft)

V = mean velocity (in ft/s)

d_{50} = particle size at which 50% of the bed material by weight is finer (in ft)

3.7.1.7. Chang, Simons and Richardson's Approach

Chang, Simons and Richardson (1965) suggested that the bed load discharge by weight can be determined using shear stress approach;

$$q_b = \frac{K_b \gamma_s V (\tau - \tau_c)}{(\gamma_s - \gamma) \tan \phi} \quad (3.59)$$

$$q_b = K_t V (\tau - \tau_c) \quad (3.60)$$

where,

K_b = constant

K_t = obtained by graph in English unit

ϕ = angle of repose of submerged material

q_b = bed load transport capacity in lb/ft/s (Yang 1996).

3.7.1.8. Parker et al. (1982) Approach

Parker et al. (1982) developed bed load transport formula using the hypothesis of equal mobility.

$$W_i^* = \frac{(\gamma_s / \gamma - 1)q_{bi}}{p_i (gD_s)^{1/2} D_s} \quad (3.61)$$

$$\phi = \frac{\tau^*}{\tau_r^*} \quad (3.62)$$

$$\phi_i = \frac{\tau_i^*}{\tau_{ri}^*} \quad (3.63)$$

$$\phi_{50} = \frac{\tau_{50}^*}{\tau_{r50}^*} \quad (3.64)$$

where,

D_s = grain size

γ and γ_s = specific weights of water and sediment

q_{bi} = bed-load per unit channel with in size fraction d_i

p_i = friction by weight in size d_i

g =gravitational acceleration

τ = bed stress

$\tau^* = \tau / \rho R g D_s$: Shields stress for grain size D_s

$\tau_i^* = \tau / \rho R g D_i$: Shields stress for i th grain size range

$\tau_{50}^* = \tau / \rho R g D_{50}$: Shields stress for median diameter of subpavement

τ_r^* = reference value of τ^* at which $W^* = W_r^*$

τ_{ri}^* = reference value of τ_i^* at which $W_i^* = W_r^*$

$\tau_{r50}^* = 0.0876$ reference value of τ_{50}^*

\mathfrak{R} = *Submerged* specific gravity of sediment

ρ = density of water

$$\phi_i = \frac{D_s}{(\gamma_s / \gamma - 1)d_i \tau_{ri}^*} \quad (3.65)$$

The value of τ_{ri}^* based on d_{50} is 0.0875

$$\tau_{ri}^* = 0.0875d_{50} / d_i \quad (3.66)$$

$$W^* = 0.0025 \exp[14.2(\phi_{50} - 1) - 9.28(\phi_{50} - 1)^2] , \quad 0.95 < \phi_{50} < 1.65 \quad (3.67)$$

or

$$W^* = 1.2 \left(1 - \frac{0.822}{\phi_{50}} \right)^{4.5} , \quad \phi_{50} > 1.65 \quad (3.68)$$

where,

W_i^* = dimensionless bed-load in i th grain size sub range

W^* = dimensionless total bed-load

3.7.1.9. Tayfur and Singh's Approach

Tayfur and Singh (2006) derived sediment flux equation from Langbein and Leopold (1968) sediment flux concentration equation. Tayfur and Singh obtained following equation from the kinematic wave theory approach.

$$q_{bs} = pV_s z \left[1 - \frac{z}{z_{\max}} \right] \quad (3.69)$$

where,

q_{bs} = the sediment flux in movable bed layer (L^2/T)

V_s = the velocity of sediment particles as concentration approaches zero (L/T)

z_{max} = the maximum bed elevation

z = the mobile bed layer elevation

p = porosity of the bed layer

3.7.2. Suspended Load Transport Formulas

Settling velocities are balanced by upward component of turbulent velocity and stays in suspension. While particles fall, some of them are carried away with high flow velocity and then returning near the bed region. Others particles caught in an upward moving eddy are lifted again. The higher the turbulence, the smaller the particle size and the greater the portion of the particles is lifted up. Thus some sediment is kept in suspension. Some basic suspended load formulas are summarized below.

3.7.2.1. The Rouse Equation

The downward transport rate is settling by gravity and the upward transport rate is rising by diffusion must be balanced under steady equilibrium conditions. Settling by gravity and the rising by diffusion components in opposite direction, respectively are

ωC and $\varepsilon_s \frac{dC}{dy}$ where;

ω = fall velocity of sediment particles

C = sediment concentration

$\frac{dC}{dy}$ = concentration gradient

ε_s = momentum diffusion coefficient for sediment. It is function of y .

In the form of balance;

$$\omega C + \varepsilon_s \frac{dC}{dy} = 0 \quad (3.70)$$

Assuming the mass transfer coefficient is equal to momentum transfer coefficient;

$$\varepsilon_s = \beta \varepsilon_m \quad (3.71)$$

where,

ε_m = momentum transfer coefficient

β = a factor of proportionality

In turbulent flows, the turbulent shear stress is;

$$\tau_y = \varepsilon_m \rho \frac{du}{dy} \quad (3.72)$$

A distance y above the bed is

$$\tau_y = \gamma S(h - y) = \tau \left(1 - \frac{y}{h}\right) \quad (3.73)$$

Assuming logarithmic velocity distribution;

$$\frac{du}{dy} = \frac{U_*}{ky} \quad (3.74)$$

where,

u = local velocity at a distance y above the bed

U_* = shear velocity

k = Prandtl-von Karman universal constant

From the equations below, ε_m and ε_s can be obtained:

$$\varepsilon_m = kU_*y \left(1 - \frac{y}{h}\right) \quad (3.75)$$

$$\varepsilon_s = \beta kU_*y \left(1 - \frac{y}{h}\right) \quad (3.76)$$

To integrate Equation 3.70 a to y by substituting ε_s ,

$$\int_a^y \frac{dC}{C} = -\int_a^y \frac{\omega dy}{\beta k U_* y \left(1 - \frac{y}{h}\right)} \quad (3.77)$$

For fine sediments β can be assumed 1,

$$\ln \frac{C}{C_a} = -\int_a^y \frac{\omega h}{k U_* y (h - y)} dy \quad (3.78)$$

When α is equal to;

$$\alpha = \frac{\omega}{k U_* y (h - y)} \quad (3.79)$$

So;

The Rouse (1937) equation becomes

$$\frac{C}{C_a} = \left(\frac{h - y}{y} \frac{a}{h - a} \right)^\alpha \quad (3.80)$$

3.7.2.2. Lane and Kalinske's Approach

Lane and Kalinske (1941) assumed $\beta = 1$ and obtained sediment concentration in English units as;

$$q_{sw} = q C_a P_L \exp\left(\frac{15 \omega a}{U_* h}\right) \quad (3.81)$$

where,

P_L can be obtained by function of $\frac{n}{D^{1/6}}$ and $\frac{\omega}{U_*}$ with the results shown in Yang (1996)

book Figure 5.6.

3.7.2.3. Einstein's Approach

Einstein (1950) replaced U_* with U_*' and assumed $\beta = 1$ and obtained α as;

$$\alpha = \frac{\omega}{0.4U_*'} \quad (3.82)$$

Suspended load transported rate is

$$q = \int_a^h u \bar{c} dy \quad (3.83)$$

For any unit system

$$q = \int_a^h C_a \left(\frac{h-y}{y} \frac{a}{h-a} \right)^\alpha 5.75U_*' \log \left(\frac{30.2y}{\Delta} \right) dy \quad (3.84)$$

where,

$$\Delta = k_s / x = d_{65} / x$$

Einstein (1950) obtain x and $\frac{k_s}{\delta}$ that shown in Yang (1996) book Figure 3.9.

After substituting the logarithm velocity distribution formula simplifying one obtains:

$$q = 11.6U_*' C_a a \left[2.303 \log \left(\frac{30.2h}{\Delta} \right) I_1 + I_2 \right] \quad (3.85)$$

Clearly, I_1 and I_2 functions of A and their values can be obtained by numerical integration with the results shown in Yang (1996) book Figure 5.7. and Figure 5.8. Einstein (1950) assumed that $a = 2d$, d is the representative grain size of bed material. The concentration at $y = a$ is

$$C_a = \frac{A_5 i_{BW} q_{bw}}{au_B} \quad (3.86)$$

where,

$i_{BW} q_{bw}$ = bed load transport rate by weight of size i_{BW}

U_B = average bed load velocity which was assumed by Einstein to be proportional to U_*'

A_5 = a correction factor (=1/11.6)

Einstein's equations can be applied to compute the suspended load discharge.

3.7.3. Total Load Transport Formulas

Total sediment load includes both bed load and suspended load. The transported total bed material also consists of bed material load and wash load. However methods for calculating the bed material load and wash load are different. The wash load is estimated by measurements but since the bed surface is changing with incoming flow continuously, it is difficult to predict the wash load in rivers. When comparing the measured and computed total bed load, wash load should be removed from measurements. Below, some basic total load formulas introduced.

3.7.3.1. Einstein's Approach

Einstein (1950) obtained the bed load transport rate for per unit channel width;

$$i_{BW} q_{bw} = \phi_* i_{bw} \rho_s g \left[\frac{\rho}{(\rho_s - \rho) g d^3} \right]^{-1/2} \quad (3.87)$$

Suspended load transport rate for per unit channel is

$$i_{sw} q_{sw} = i_{BW} q_{bw} (P_E I_1 + I_2) \quad (3.88)$$

The total bed load for the size fraction i_t ,

$$\begin{aligned} i_t q_t &= i_{BW} q_{bw} + i_{sw} q_{sw} \\ &= i_{BW} q_{bw} (1 + P_E I_1 + I_2) \end{aligned} \quad (3.89)$$

3.7.3.2. Laursen's Approach

Laursen (1958) developed relationship between flow condition and sediment discharge. ASCE Task Committee (1971) denoted Laursen's formula in dimensionally homogeneous form;

$$C_t = 0.01\gamma \sum_i p_i \left(\frac{d_i}{D} \right)^{7/6} \left(\frac{\tau'}{\tau_{ci}} - 1 \right) f \left(\frac{U_*}{\omega_i} \right) \quad (3.90)$$

where,

C_t = total average sediment concentration by weight per unit volume

$$U_* = \sqrt{gDS}$$

p_i = percentage of materials available in size fraction i

ω_i = fall velocity of particles of mean size d_i in water

τ_{ci} = critical tractive force for sediment size d_i as given by the Shields diagram,

$$\tau' = \frac{\rho V^2}{58} \left(\frac{d_{50}}{D} \right)^{1/3} \quad (3.91)$$

The bed material load is

$$q_t = q C_t \quad (3.92)$$

where,

q = flow discharge per unit width

q_t = dry weight of sediment discharge per unit time and width.

Laursen's formula is applicable for fine sediment (Yang 1996).

3.7.3.3. Bagnold's Approach

Bagnold (1966) estimated sediment transport capacity in submerged weight for bed load and suspended load respectively as bellows:

$$\frac{\gamma_s - \gamma_w}{\gamma_w} q_{bw} \tan \alpha = \tau V e_b \quad (3.93)$$

$$\frac{\gamma_s - \gamma_w}{\gamma_w} q_{sw} \frac{\omega}{u_s} = \tau V 0.01 \quad (3.94)$$

where,

γ_s and γ_w = specific weights of sediment and water, respectively

q_{bw} = bed load transport rate by weight per unit channel width

q_{sw} = suspended load discharge in dry weight per unit time and channel width

$\tan \alpha$ = ratio of tangential to normal shear force (can be obtained in graph that showed a function of $\tau / [(\gamma_s - \gamma_w)d]$ and $\tan \alpha$ with grain size d in Yang (1996) book Figure 6.5.b.)

τ = shear force acting along the bed

V = average flow velocity

e_b = efficiency coefficient (can be obtained in graph that showed a function of V and e_b with grain size d in Yang (1996) book Figure 6.5.a.)

ω = fall velocity for suspended sediment

\bar{u}_s = mean transport velocity of suspended load

Transport function is based on stream power concept. Bagnold's formula expresses the bed load transport capacity by using energy concept as a function of work

done by system for transporting sediment (Yang 1996). The total load is sum of the bed load as given the equation;

$$q_z = q_{bw} + q_{sw} = \frac{\gamma_w}{\gamma_s - \gamma_w} \tau V \left(\frac{e_b}{\tan \alpha} + \frac{0.01V}{\omega} \right) \quad (3.95)$$

where,

q_z = total load [in (lb / s / ft)]

3.7.3.4. Engelund and Hansen's Approach

Engelund and Hansen (1972) carried out Bagnold's stream power concept and obtained the sediment transport formula with similarity principle (Yang 1996);

$$f' \cdot \phi = 0.1 \theta^{5/2} \quad (3.96)$$

where,

$$f' = \frac{2gSD}{V^2} \quad (3.97)$$

$$\phi = q_t \left[\gamma_s \left(\frac{\gamma_s - \gamma}{\gamma} \right) g d^3 \right]^{-1/2} \quad (3.98)$$

$$\theta = \frac{\tau}{(\gamma_s - \gamma)d} \quad (3.99)$$

where,

g = gravitational acceleration

S = energy slope

V = average flow velocity

q_t = total sediment discharge by weight per unit weight

d =median particle diameter

τ =shear stress along the bed

Engelund and Hansen's formula is applicable only to dune beds and median particle diameter is greater than 0.15 mm.

3.7.3.5. Ackers and White's Approach

Ackers and White (1973) transport capacity formula based on Bagnold's stream power concept and applied dimensional analysis for uniform sediment. The dimensionless sediment transport function is

$$G_{gr} = \frac{XD}{d \frac{\gamma_s}{\gamma}} \left(\frac{U_*}{V} \right)^n \quad (3.100)$$

where,

X =rate of sediment transport in terms of mass flow per unit mass flow rate (unitless)

D =water depth

U_* =shear velocity

d =sediment particle size

V =average flow velocity

Ackers and White (1973) expressed the mobility number for sediment is

$$F_{gr} = U_*^n \left[gd \left(\frac{\gamma_s}{\gamma} - 1 \right) \right]^{-1/2} \left[\frac{V}{\sqrt{32} \log(\alpha D / d)} \right]^{1-n} \quad (3.101)$$

where,

n =transition exponent, depending on sediment size

α =coefficient in rough turbulent equation (=10)

The sediment size by a dimensionless grain diameter is

$$d_{gr} = d \left[\frac{g(\gamma_s / \gamma - 1)}{v^2} \right]^{1/3} \quad (3.102)$$

where,

v = kinematic viscosity

The generalized dimensionless sediment transport function is

$$G_{gr} = C \left(\frac{F_{gr}}{A} - 1 \right)^m \quad (3.103)$$

The values, n , A , m and C can be obtained from laboratory data.

$$\text{If } d_{gr} > 60 \quad (3.104)$$

$$n = 0.0$$

$$A = 0.17$$

$$m = 1.5$$

$$C = 0.025$$

$$\text{If } 1 < d_{gr} \leq 60 \quad (3.105)$$

$$n = 1.00 - 0.56 \log(d_{gr})$$

$$A = 0.23 d_{gr}^{-1/2} + 0.14$$

$$m = \frac{9.66}{d_{gr}} + 1.34$$

$$\log C = 2.86 \log(d_{gr}) - \log^2(d_{gr}) - 3.53$$

Ackers and White's approach applicable to $d > 0.04mm$ and $F_r < 0.8$.

where,

F_r = Froude number

CHAPTER 4

ONE DIMENSIONAL HYDRODYNAMIC MODEL

The hydrodynamic model is described by equations of motion in open channel flows. The flow model is developed to solve governing equations based on conservation of mass and momentum. The flow depth and velocity of flow are sufficient to define the flow conditions at a channel cross section, so two governing equations can be solved for a typical flow situation.

In this Chapter, the continuity and momentum equations are derived that are usually referred to as the Saint Venant equations.

4.1. de Saint Venant Equations

The one dimensional modeling of unsteady flow in open channels is most often performed by supplementing de Saint Venant equations that describe the propagation of a wave. In unsteady modeling, two flow variables, such as the flow depth and velocity or the flow depth and the rate of flow are calculated to define the flow conditions at a channel cross section. Therefore, two governing equations must be used to analyze a typical flow situation. The required equations are the continuity equation and the momentum equation derived with many assumptions (Roberson, et al. 1997, Chaudry 1993):

- The streamlines do not have sharp curves, so that the pressure distribution is hydrostatic.
- As the channel bottom slope is small, the measured lateral and vertical velocity are approximately same, so the lateral velocity and acceleration component can be neglected.
- No lateral, secondary circulation occurs. The flow velocity distribution is uniform over any channel cross section.
- The channel is prismatic with the same cross section and slope thorough out the distance.

- The head losses in unsteady flow can be simulated by using the steady – state resistance laws, so Chezy and Maning equations can be used also in unsteady flow model. Water has uniform density and flow is generally subcritical (Chaudhry 1993).

4.1.1. Continuity Equation in Unsteady Flows

According to the law of conservation of mass, both the difference of the rate of mass inflow through area dA_1 at section 1 and the rate of mass outflow through area dA_2 at section 2 and the lateral inflow or outflow through Δx in the same dt time space, must be equal to changing of volume.

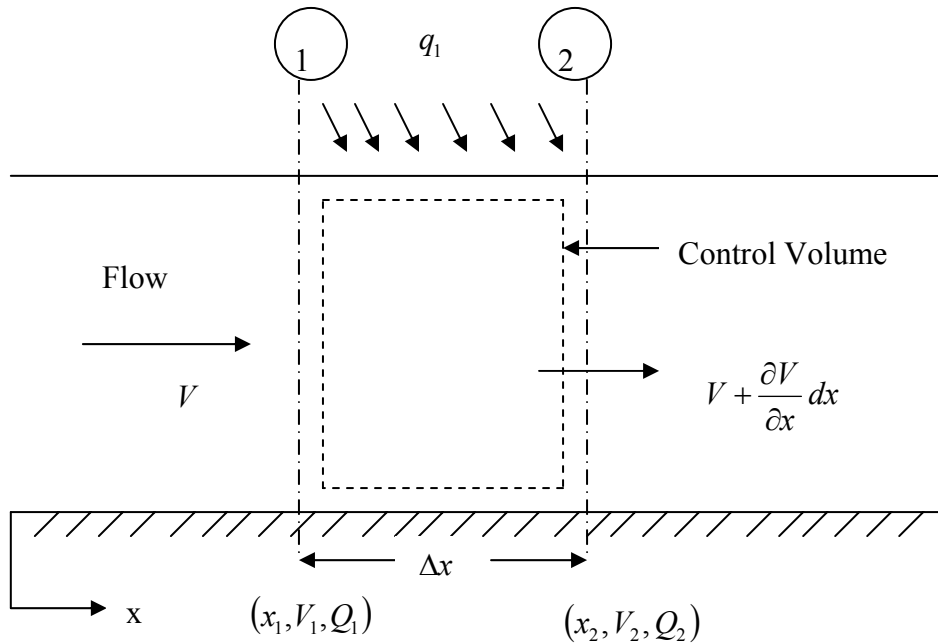


Figure 4.1. Definition sketch for continuity equation

$$\frac{\partial M}{\partial t} = \frac{d}{dt} \int_{x_1}^{x_2} (\rho A + \rho A_2 V_2 - \rho A_1 V_1 - \rho q_1 (x_2 - x_1)) dx = 0 \quad (4.1)$$

where,

M =mass

A =flow area

V =flow velocity

ρ =mass density of water

q_1 =volumetric rate of lateral inflow or outflow per unit length of the channel between sections 1 and 2. (inflow q_1 is positive, outflow q_1 is negative)

If water is assumed incompressible, mass density can be taken constant. Therefore Equation (4.1) becomes,

$$\frac{d}{dt} \int_{x_1}^{x_2} (A + A_2 V_2 - A_1 V_1 - q_1 (x_2 - x_1)) dx = 0 \quad (4.2)$$

By rearranging Equation (3.2) with average flow area and average flow velocity in channel cross section and applying the *Leibnitz's rule* *, the equation becomes,

$$B \Delta x \frac{\partial h}{\partial t} dt - AV dt + \left[A + \frac{\partial A}{\partial x} \Delta x \right] \left[V + \frac{\partial V}{\partial x} \Delta x \right] dt - q_1 \Delta x dt \quad (4.3)$$

where,

h =flow depth

The $\left(\frac{\partial A}{\partial x} \frac{\partial V}{\partial x} \right)$ can be neglected because it is small and with other simplifiers it

becomes,

$$B \frac{\partial h}{\partial t} + A \frac{\partial V}{\partial x} + V \frac{\partial A}{\partial x} - q_1 = 0 \quad (4.4)$$

or

$$\frac{\partial h}{\partial t} + \frac{A}{B} \frac{\partial V}{\partial x} + V \frac{\partial h}{\partial x} = \frac{q_1}{B} \quad (4.5)$$

or

$$\frac{\partial h}{\partial t} + h \frac{\partial V}{\partial x} + V \frac{\partial h}{\partial x} = \frac{q_1}{B} \quad (4.6)$$

For a wide rectangular section the conservation of mass equation for water on a unit width can be written as:

$$\frac{\partial h}{\partial t} + \frac{\partial hu}{\partial x} = \frac{q_{1w}}{B} \quad (4.7)$$

where,

h = the flow depth (L)

u = the flow velocity (L/T)

q_{1w} = the lateral flow flux (L²/T)

x = independent variable representing the coordinate in the longitudinal direction (flow direction) (L)

t = independent variable of time (T)

*Leibnitz's rule

$$\frac{d}{dt} \int_{f_1(t)}^{f_2(t)} F(x, t) dx = \int_{f_1(t)}^{f_2(t)} \frac{\partial}{\partial t} F(x, t) dx + F(f_2(t), t) \frac{df_2}{dt} - F(f_1(t), t) \frac{df_1}{dt}$$

4.1.2. Momentum Equation in Unsteady Flows

The second required equation is derived by considering how the forces on the control volume affect the movement of water through the control volume. The momentum equation states that the rate of change of momentum is equal to the resultant force acting on the control volume $\sum F = \frac{d(mv)}{dt}$. In Figure 4.2 there is an element which has mass m and length Δx . The rate of changing of total momentum for that element for the incompressible flows is,

$$\sum F = \frac{d}{dt} \int_{x_1}^{x_2} (V \rho A dx + V_2 \rho A_2 V_2 - V_1 \rho A_1 V_1 - V_x \rho q_1 (x_2 - x_1)) \Delta x \quad (4.8)$$

where,

V_x = the component of the velocity of lateral inflow in the x - direction

q_1 = is positive in lateral inflow and negative in lateral outflow.

The Leibnitz's rule must be applied to Equation (4.8) and $Q = VA$,

$$\sum F = \int_{x_1}^{x_2} \left(\rho \frac{\partial Q}{\partial t} dx + \rho Q_2 V_2 - \rho Q_1 V_1 - V_x \rho q_1 (x_2 - x_1) \right) dx \quad (4.9)$$

The mean value theorem can save the Equation (4.9) to differential form, so dividing the terms by $\rho(x_2 - x_1)$,

$$\frac{\sum F}{\rho(x_2 - x_1)} = \frac{\partial Q}{\partial t} + \frac{\partial(QV)}{\partial x} - V_x q_1 \quad (4.10)$$

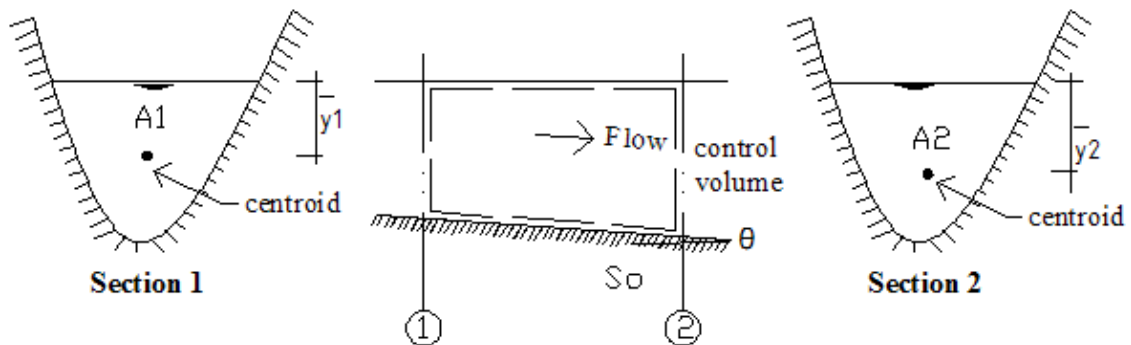


Figure 4.2. Definition sketch for momentum equation

For the typical hydraulic engineering applications the shear stress on the flow surface due to the wind and the effects of the Coriolis acceleration can be neglected. The forces acting on the control volume are the pressure forces, the gravity force in the x - direction and the frictional force which are explained below.

On the upstream end, the pressure force is;

$$F_1 = \rho g A_1 \bar{h}_1 \quad (4.11)$$

On the downstream end, the pressure force;

$$F_2 = \rho g A_2 \bar{h}_2 \quad (4.12)$$

where,

\bar{h}_1 and \bar{h}_2 = depth of the centroid of flow area A_1 and A_2 , respectively

The weight of the water in the control volume in the x - direction is;

$$F_3 = \rho g \int_{x_1}^{x_2} A S_0 dx \quad (4.13)$$

where,

S_0 = The channel bottom slope

The frictional force due to water and the channel sides and channel bottom is;

$$F_4 = \rho g \int_{x_1}^{x_2} A S_f dx \quad (4.14)$$

where,

S_f = The friction slope

The resultant force acting on the control volume is;

$$\sum F = F_1 - F_2 + F_3 - F_4 \quad (4.15)$$

By inserting terms in the Equation (4.15) and dividing by $\rho(x_2 - x_1)$,

$$\frac{\sum F}{\rho(x_2 - x_1)} = \frac{g(A_1 \bar{h}_1 - A_2 \bar{h}_2)}{x_2 - x_1} + \frac{g}{x_2 - x_1} \int_{x_1}^{x_2} A(S_0 - S_f) dx \quad (4.16)$$

The mean value theorem can save the Equation (4.16) to differential form,

$$\frac{\partial Q}{\partial t} + \frac{\partial(QV)}{\partial x} - V_x q_1 = -g \frac{\partial}{\partial x} (A\bar{h}) + gA(S_0 - S_f) \quad (4.17)$$

By rearranging gives,

$$\frac{\partial Q}{\partial t} + \frac{\partial}{\partial x} (QV + gA\bar{h}) = gA(S_0 - S_f) + V_x q_1 \quad (4.18)$$

The Equation 4.18 is the momentum equation of water flow. If the right – hand side of this equation is zero, it means that mass is conserved along any closed contour in the $x-t$ plane unless it is zero, this term acts like a source or a sink depending on q_1 (Cunge, et al. 1980).

$$\Delta(A\bar{h}) = \left[A(\bar{h} + \Delta h) - \frac{1}{2} B(\Delta h)^2 \right] - A\bar{h} \quad (4.19)$$

So the higher – order terms can be neglected. Assuming $\Delta h \rightarrow 0$, we can obtain $(\partial/\partial h)(A\bar{h}) = A$ and that can be rearranged as:

$$\frac{\partial}{\partial x} (gA\bar{h}) = g \frac{\partial}{\partial h} (A\bar{h}) \frac{\partial h}{\partial x} = gA \frac{\partial h}{\partial x} \quad (4.20)$$

The Equation 4.18 becomes,

$$\frac{\partial Q}{\partial t} + \frac{\partial(QV)}{\partial x} + gA \frac{\partial h}{\partial x} = V_x q_1 + gA(S_0 - S_f) \quad (4.21)$$

The acceleration can be an increase in velocity at one point over time (local acceleration) or an increase in velocity over space (acceleration may occur as water moves along the control volume). These concepts lead to the de Saint Venant Equations, the momentum equation, which when written in its conservation form is (Chaudhry 1993).

hydrodynamic form until the 1950s, although they were derived in the early nineteenth century. A number of simplifications were performed by different researchers, being more appropriate in particular situations. Consideration of the implications of the different simplifications can also lead to a better understanding of the full equations so de Saint Venant equations were described by the propagation of a wave. In wave approximations, the continuity equation is solved simultaneously with approximate form of the momentum equation. Their differences are all in momentum equation assumptions. The three types of simplifications for wave models studied in this research are summarized below.

4.2. Kinematic Wave Approximation

The kinematic wave approximation represents the change of flow with distance and time by neglecting the local and convective acceleration terms of the momentum equation. The assumption is that the water surface is parallel to the channel bed (uniform flow assumption) in the kinematic wave approximation. It means there is no way to represent backwater effects. These assumptions reduce the momentum equation to the following.

$$S_0 = S_f \quad (4.25)$$

The remaining terms represent the resistance equation for steady, uniform flow as described by Manning's or Chezy's equation but can be taken into consideration the effects of unsteadiness by an increase or decrease in the flow depth.

The resistance equation can be written as:

$$Q = f(A) \quad (4.26)$$

By applying the chain rule we can write,

$$\frac{\partial A}{\partial t} = \frac{\partial A}{\partial Q} \frac{\partial Q}{\partial t} \quad (4.27)$$

$$\frac{\partial A}{\partial t} = \frac{\partial Q}{\partial t} \frac{\partial A}{\partial Q} \Big|_{x=x_0} \quad (4.28)$$

Substituting this equation into Equation 4.6, assuming $q_1 = 0$,

$$\frac{\partial Q}{\partial t} + a \frac{\partial Q}{\partial x} = 0 \quad (4.29)$$

where,

$a = dQ/dA$ Represents the velocity of flood wave (L^2/T)

This equation represents the kinematic wave which's combined with continuity equation. While Q is dependent variable, x and t are independent variables in this first – order partial differential equation. If a is constant, the equation becomes linear. The general solution of this linear equation by D'Alembert is,

$$Q = f(x - at) \quad (4.30)$$

While $t = 0$, it represents initial conditions. The function creates a curve that describes the variation of discharge Q with distance x . Assuming that t changes such as, t_1, t_2 and t_3 at velocity a in the downstream direction, the discharge occurs Q_1, Q_2 and Q_3 drawing a curve. It can be said that this curve always appears as $f(x)$, so it shows a flood hydrograph in kinematic wave as it travels in the positive x - direction at velocity a , the shape of the hydrograph does not change and its peak does not attenuate (assuming a is constant). The kinematic wave equation describes the propagation of a flood wave along a river reach but doesn't account for any backwater effects. This implies that water may only flow downstream. The solution may be analytical or numerical (Chaudhry 1993).

4.3. Diffusion Wave Approximation

The diffusion wave approximation is a simplified form of the dynamic wave approximation. In addition, it is a significant improvement over the kinematic wave

model. In the diffusion wave approach, the $\partial h/\partial t$ term from de Saint Venant equation allows the water – surface slope to differ from the bed slope. This pressure differential term allows the diffusion model to describe the attenuation of the floodwave. It also allows the specification of a boundary condition at the downstream extremity of the routing reach to account for backwater effects. The simplified form of the momentum equation includes the convective acceleration term representing the spatial change in the flow depth as well as the source terms, but neglects the temporal derivative term as well as the convective acceleration terms due to spatial change in the flow velocity (Chaudhry 1993). The simplified form of the momentum equation is,

$$\frac{\partial h}{\partial x} = (S_0 - S_f) \quad (4.31)$$

Combining the simplified momentum equation with the continuity equation gives the single equation called the diffusion wave equation.

$$D \frac{\partial^2 Q}{\partial x^2} = \frac{\partial Q}{\partial t} + a \frac{\partial Q}{\partial x} \quad (4.32)$$

where,

$$D = Q/2BS_0$$

$$a = dQ/dA$$

The first term of the right side in this equation is the same as the equation for kinematic model. The first term of the left side in Equation 4.32 represents the diffusion of a flood wave as it travels in the channel. The coefficients D and a determined from the observed hydrographs. By using them the attenuation of a flood wave due to storage and friction can be included in the analysis (Chaudhry 1993).

4.4. Dynamic Wave Approximation

The dynamic wave equations are most accurate and comprehensive solution for one dimensional unsteady flow problems in open channels under the specific assumptions. The dynamic wave equations can be applied to wide range of one dimensional flow problems such as dam break flood wave routing, evaluating flow

conditions due to tidal fluctuations, and routing flows through irrigation and canal systems. The full equations can be solved by several numerical methods for incremental times t and incremental distances x along the water way. The specific terms in the momentum equation are small in comparison to the bed slope. In dynamic wave approximation, the continuity equation is solved simultaneously with approximate form of the momentum equation. If we reorganize the momentum equation Equation 4.24 the full dynamic wave approximation can be defined by,

$$\frac{\partial u}{\partial t} + u \frac{\partial u}{\partial x} + g \frac{\partial h}{\partial x} = g(S_0 - S_f) \quad (4.33)$$

where,

u =the flow velocity (L/T)

h =the flow depth (L)

S_f = friction slope

S_0 = bed slope

g =acceleration due to gravity (L/T^2)

t =independent variable of time (T)

x =independent variable representing the coordinate in the longitudinal direction (flow direction) (L)

CHAPTER 5

ONE DIMENSIONAL SEDIMENT TRANSPORT MODEL

The bed of the channel may aggrade or degrade in natural streams if the balance of the water discharge or sediment is destroyed by natural or manmade factors. Eroding loose surface from the basin by water deteriorates the ecology and changes the river morphology. The water level rises and brings ecological problems when sediments are deposited in river basins. It is essential to predict effects of sediment transport for river management. Current research on river sediment transport prediction is mainly based on numerical modeling of sediment transport. One dimensional unsteady sediment transport models studied in two categories in this research: equilibrium and nonequilibrium.

5.1. One Dimensional Numerical Model for Sediment Transport under Unsteady and Equilibrium Conditions

Bed material transportation is mathematically divided into two independent processes: erosion and deposition. When the erosion and the deposition rates are equal then there is equilibrium. It means that there is no interchange of sediment particles between suspended and bed load sediment transport (Tayfur and Singh 2007). The equilibrium condition exists when the same number of a given type and size of particles are deposited on the bed as are entrained from it. In the literature, most of the studies are based on equilibrium approach although natural rivers are mostly in nonequilibrium state. When flow and sediment discharges, channel geometry and sediment properties do not change substantially a long period of time, assuming the equilibrium sediment transport conditions is appropriate.

5.1.1. Kinematic Wave Model of Bed Profiles in Alluvial Channels under Equilibrium Conditions

The kinematic wave model neglects the local acceleration, convective acceleration and pressure terms in the momentum equation for dynamic wave model.

Tayfur and Singh (2006) represented transport movement in a wide rectangular alluvial channels as a system involving two layers: water flow layer and movable bed layer, as shown in Figure 5.1. The water flow layer may contain suspended sediment. The movable bed layer consists of both water and sediment particles, so the movable bed layer includes porosity. The basic one dimensional partial differential equations for unsteady and equilibrium nonuniform transport can be expressed as (Tayfur and Singh 2006):

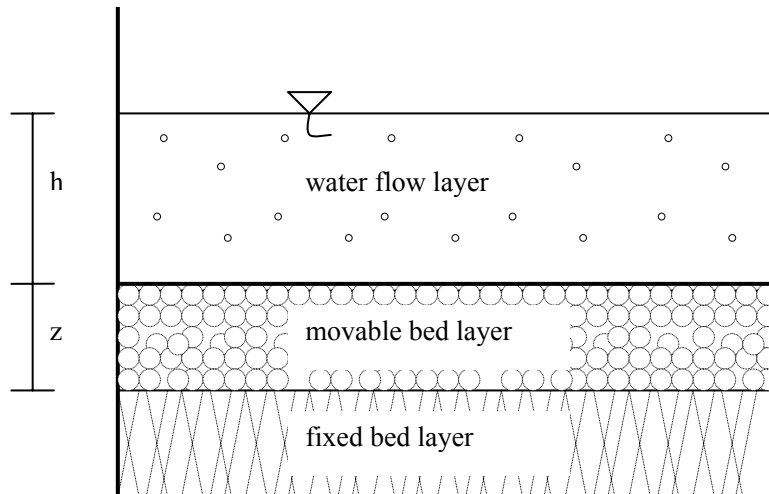


Figure 5.1 Definition sketch of two layer system
(Source: Tayfur and Singh 2006)

- Continuity equation for water:

$$\frac{\partial h(1-c)}{\partial t} + \frac{\partial hu(1-c)}{\partial x} + p \frac{\partial z}{\partial t} = q_{1w} \quad (5.1)$$

where,

u = flow velocity (L/T)

h = flow depth (L)

z = mobile bed layer elevation (L)

c = volumetric sediment concentration in the water flow phase (in suspension) (L^3 / L^3)

q_{1w} = volumetric rate of lateral inflow or outflow of water (L/T)

p = porosity of the bed layer (L^3 / L^3)

t = independent variable of time (T)

x = independent variable representing the coordinate in the longitudinal direction (flow direction) (L)

- Continuity equation for sediment:

$$\frac{\partial hc}{\partial t} + \frac{\partial huc}{\partial x} + (1-p) \frac{\partial z}{\partial t} + \frac{\partial q_{bs}}{\partial x} = q_{ls} \quad (5.2)$$

where,

q_{bs} = the sediment flux in the movable bed layer (L^2/T)

q_{ls} = volumetric rate of lateral inflow or outflow of sediment (L/T)

For simplicity, if there is no lateral inflow of water and sediment, the terms on the right hand sides of Equation 5.1 and Equation 5.2 vanish (Tayfur and Singh 2006).

Equations 5.1 and 5.2 contain five unknowns: h, u, c, z and q_{bs} . It means that there must be three additional equations. One equation is obtained from momentum equation for kinematic wave which is given as follows:

- Momentum equation for water:

$$S_f = S_o \quad (5.3)$$

Friction slope is taken as equal to bed slope employing Chezy's equation for the friction slope, yields;

$$u = \alpha h^{\beta-1} \quad (5.4)$$

where,

$$\alpha = C_z S_f^{0.5}$$

$$\beta = 1.5$$

The second equation is obtained from Velikanov (1954), relating suspended sediment concentration to flow variables as;

$$c = \frac{\kappa u^3}{g v_f h} \quad (5.5)$$

where,

g = gravitational acceleration (L/T²)

v_f = average fall velocity of sediments (L/T)

κ = coefficient of sediment transport capacity

By rearranging the equation with $\delta = \frac{\kappa}{gv_f}$, the equation becomes,

$$c = \delta u^3 h^{-1} \quad (5.6)$$

The third equation is obtained from Langbein and Leopold (1968) who proposed a sediment flux concentration relation as:

$$q_{st} = v_s C_b \left[1 - \frac{C_b}{C_{b_{\max}}} \right] \quad (5.7)$$

where,

q_{st} = sediment transport rate (M/L/T)

v_s = velocity of sediment particles as concentration approaches zero (L/T)

C_b = areal sediment concentration (M/L²)

$C_{b_{\max}}$ = maximum areal sediment concentration (M/L²)

The sediment transport rate q_{st} is in (M/L/T) (Equation 5.7) and the sediment flux q_{bs} is in (L²/T) (Equation 5.2), so q_{st} is related to q_{bs} as:

$$q_{st} = \rho_s q_{bs} \quad (5.8)$$

where,

ρ_s = mass density of sediment (M/L³)

Areal concentration can be related to bed level as (Tayfur and Singh 2006):

$$C_b = (1 - p)z\rho_s \quad (5.9)$$

By substituting Equations 5.8 and 5.9 into the Equation 5.7;

$$q_{bs} = (1-p)v_s z \left[1 - \frac{z}{z_{\max}} \right] \quad (5.10)$$

where,

z_{\max} = maximum bed elevation (L)

By using the chain rule, derivative of q_{bs} can be obtained as:

$$\frac{\partial q_{bs}}{\partial x} = (1-p)v_s \left[1 - \frac{2z}{z_{\max}} \right] \frac{\partial z}{\partial x} \quad (5.11)$$

Hence the unknowns h, u, c, z and q_{bs} can be obtained by the system of Equations 5.1, 5.2, 5.4, 5.5 and 5.11. After algebraic manipulation, the equations can be written in compact form as:

$$\left[1 - 1.5\delta\alpha^3 h^{0.5} \right] \frac{\partial h}{\partial t} + \left[1.5\alpha h^{0.5} - 1.5\delta\alpha^4 h \right] \frac{\partial h}{\partial x} + p \frac{\partial z}{\partial t} = 0 \quad (5.12)$$

$$\left[1.5\delta\alpha^3 h^{0.5} \right] \frac{\partial h}{\partial t} + \left[2\delta\alpha^4 h \right] \frac{\partial h}{\partial x} + (1-p) \frac{\partial z}{\partial t} + (1-p)v_s \left[1 - \frac{2z}{z_{\max}} \right] \frac{\partial z}{\partial x} = 0 \quad (5.13)$$

(note that $\beta = 1.5$)

5.1.1.1. Numerical Solution of Kinematic Wave Equations

In this model, a finite difference scheme developed by Lax (1954) is used. This scheme can capture shocks, since all the governing equations are solved simultaneously. There is no need for iterations when gradients are large. The Lax scheme is an explicit scheme and does not require large matrices, so it is easy for solving general empirical equations for roughness and sediment discharge. With reference to the finite difference

grid as shown in Figure 5.2, the partial derivatives and other variables are approximated as follows.

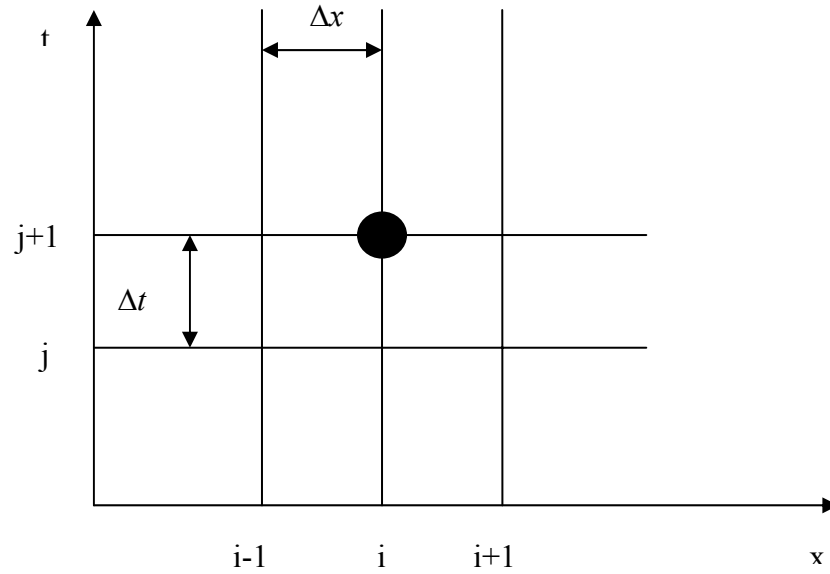


Figure 5.2. Finite – difference grid

$$\frac{\partial f}{\partial t} = \frac{f_i^{j+1} - 0.5(f_{i+1}^j + f_{i-1}^j)}{\Delta t} \quad (5.14)$$

$$\frac{\partial f}{\partial x} = \frac{f_{i+1}^j - f_{i-1}^j}{2\Delta x} \quad (5.15)$$

where,

i = the node in space

j = the node in time

Δx and Δt = the distance and steps, respectively.

Based on the finite difference approximation of Equations 5.14 and 5.15, 5.12 and 5.13 may be written as follows for determining the values h^{j+1} and z^{j+1} .

$$h_i^{j+1} = 0.5(h_{i+1}^j + h_{i-1}^j) - \frac{[1.5\alpha h_{ij}^{0.5} - 1.5\delta\alpha^4 h_{ij}]}{[1 - 1.5\delta\alpha^3 h_{ij}^{0.5}]} \frac{\Delta t}{2\Delta x} (h_{i+1}^j - h_{i-1}^j) - \left[\frac{P}{[1 - 1.5\delta\alpha^3 h_{ij}^{0.5}]} [z_i^{j+1} - 0.5(z_{i+1}^j - z_{i-1}^j)] \right] \quad (5.16)$$

$$z_i^{j+1} = 0.5(z_{i+1}^j + z_{i-1}^j) - \frac{[2\delta\alpha^4 h_{ij}]}{p} \frac{\Delta t}{2\Delta x} (h_{i+1}^j - h_{i-1}^j) - \frac{[1.5\delta\alpha^3 h_{ij}^{0.5}]}{(1-p)} [h_i^{j+1} - 0.5(h_{i+1}^j - h_{i-1}^j)] - v_s \left[1 - \frac{2z_{ij}}{z_{\max}} \right] \frac{\Delta t}{2\Delta x} (z_{i+1}^j - z_{i-1}^j) \quad (5.17)$$

The hydrodynamic part of the model is:

$$h_i^{j+1} = 0.5(h_{i+1}^j + h_{i-1}^j) - \frac{[1.5\alpha h_{ij}^{0.5} - 1.5\delta\alpha^4 h_{ij}]}{[1 - 1.5\delta\alpha^3 h_{ij}^{0.5}]} \frac{\Delta t}{2\Delta x} (h_{i+1}^j - h_{i-1}^j) \quad (5.16a)$$

$$u_i^{j+1} = \alpha (h_i^{j+1})^{\beta-1} \quad (5.16b)$$

By using the presented algorithm, the unknown values of h and z at the new time level $j+1$ (future time) are determined from every interior node ($i = 2, \dots, N-1$). The values of the dependent variables h and z at the boundary nodes 1 and $N+1$ are determined by using boundary conditions. Also, at the time level $j=1$, initial conditions are already known.

Initial conditions can be specified as:

$$h(x,0) = h_o \quad (5.18)$$

$$z(x,0) = z_o \quad (5.19)$$

where,

h_o and z_o = the initial flow depth (L) and the bed level (L), respectively.

The upstream boundary conditions can be specified as inflow hydrograph and inflow sedimentograph.

$$h(0,t) = h(t) \quad (5.20)$$

$$z(0, t) = z(t) \quad (5.21)$$

The downstream boundary conditions can be specified as:

$$\frac{\partial h((N, t))}{\partial x} = 0 \quad (h_{N+1}^{j+1} = h_{N-1}^{j+1}) \quad t > 0.0 \quad (5.22)$$

$$\frac{\partial z((N, t))}{\partial x} = 0 \quad (z_{N+1}^{j+1} = z_{N-1}^{j+1}) \quad t > 0.0 \quad (5.23)$$

•Stability

The numerical scheme has to satisfy the stability conditions. For this reason, the Courant – Friedrichs – Lewy (CFL) condition was used. Since the water waves travel at a much higher velocity than the bed transients this condition is given by:

$$C_n = \frac{(u + \sqrt{gh})\Delta t}{\Delta x} \leq 1 \quad (5.24)$$

where,

C_n = Courant number (it was taken $C_n = 0.2$ in this research)

Equations 5.16 and 5.17 are solved simultaneously for each time step.

5.1.1.2. Model Testing for Hypothetical Cases

The hypothetical cases were analyzed assuming inflow hydrograph and concentration at the upstream of the channel, shown in Figures 5.3a and 5.3b.

The channel was assumed to have a 1000 m length and 20 m width with 0.0025 bed slope. Chezy roughness coefficient is $C_z = 50 \text{ m}^{0.5}/\text{s}$. The sediment was assumed to have $\rho_s = 2650 \text{ kg/m}^3$, $d_s = 0.32 \text{ mm}$, $p = 0.48$ and sediment transport capacity coefficient $\kappa = 0.000075$ (Ching and Cheng 1964). Langbein and Leopold (1968) suggest $C_{\max} = 245 \text{ kg/m}^2$ (note that $C_b = (1-p)z\rho_s$). In Figure 4.3b, $C_b = 14 \text{ kg/m}^2$ corresponds the bed level $z = 0.01 \text{ m}$ and $C_b = 140 \text{ kg/m}^2$ corresponds the bed level $z = 0.10 \text{ m}$.

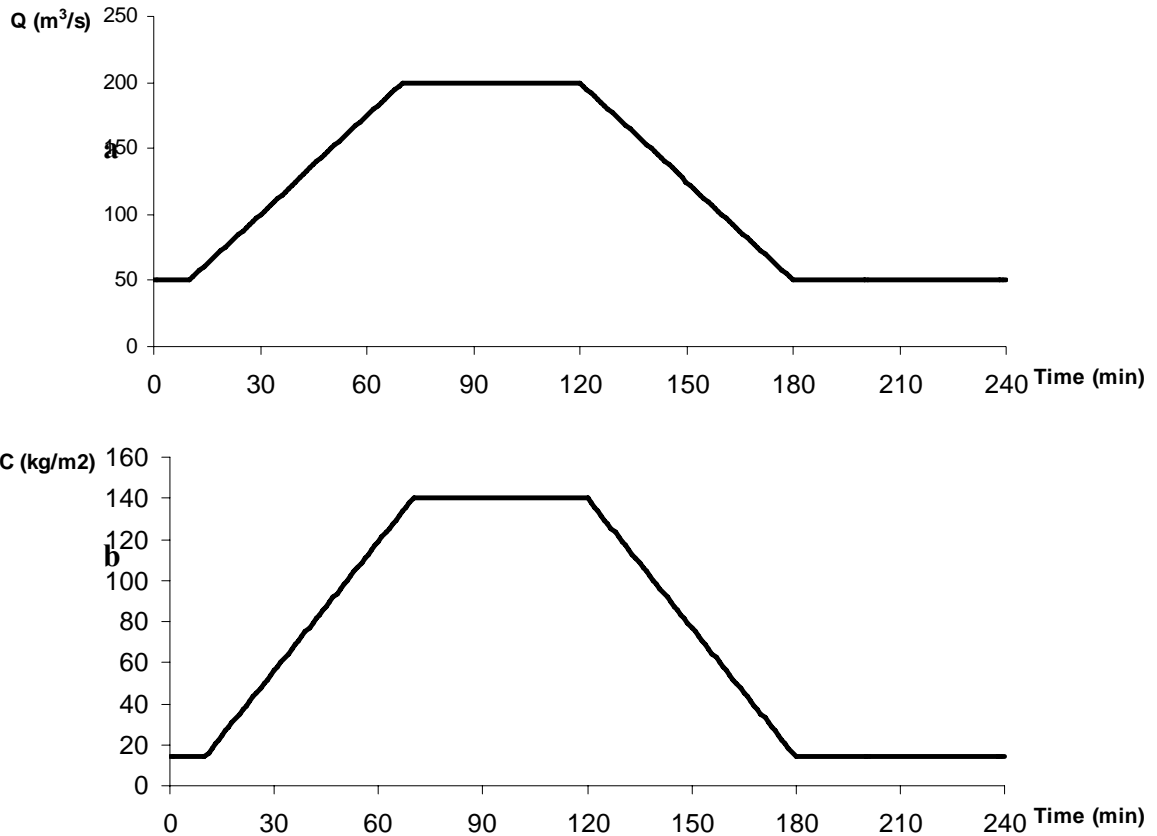


Figure 5.3. (a) Inflow hydrograph (b) Inflow concentration

5.1.1.2.1. Hypothetical Case I: Effect of Inflow Concentration

Figure 5.4a shows that when the inflow concentration increases at the upstream end of the channel, bed level gradually increases. In the Figure 5.4b when the equilibrium feeding of the sediment occurs at the upstream, the bed level continues to increase along the channel length. During the recession limb of the inflow concentration the bed level starts to decrease toward the 10% length of the channel while it increases, toward the 90% length of the channel (Figure 5.4c). Figure 5.4d shows that the bed level decreases to the original level at the upstream section but as time progresses it increases toward the downstream section.

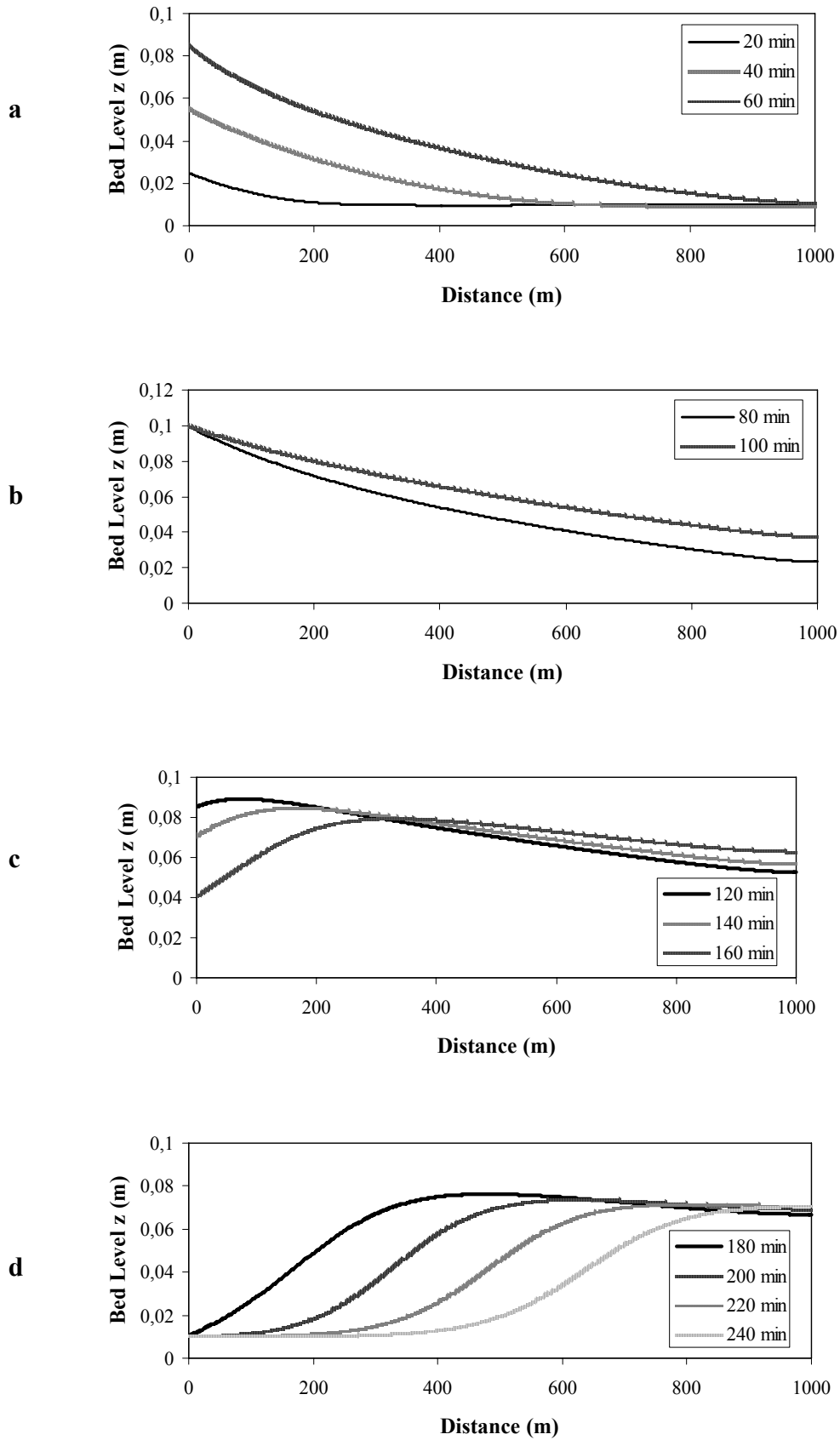


Figure 5.4. Transient bed profile at (a) rising period (b) equilibrium period (c) recession period (d) post recession period of inflow hydrograph and concentration

5.1.1.2.2. Hypothetical Case II: Effect of Particle Velocity and Effect of Particle Fall Velocity

The objective of this case was to compare the sediment particle velocity and particle fall velocity formulations employed in the developed model. The fall velocity must be obtained for calculating the particle velocity. For that reason, first of all we wanted to see four particle velocity formulation's (in literature) performances under the Rouse (1938)'s fall velocity formulation. The fall velocity value is for most natural sands of the shape factor of 0.7 and $d_s = 0.2$ mm is $v_f = 0.024$ m/s (Rouse 1938). Under the same particle fall velocity, the developed model was tested for four different particle velocity formulations (Bor, et al. 2008).

One of the formulations is Chien and Wan (1999) formulation. For $0.08 < d_s < 10\text{mm}$ and $10 < h/d_s < 1550$, Chien and Wan (1999) presented the following relation:

$$v_s = u - \frac{(u_c / 1.4)^3}{u^2} \quad (5.25)$$

where,

u_c = critical flow velocity at the incipient sediment motion (L/T).

u_c can be expressed as a function of the particle fall velocity v_f and the shear velocity Reynolds number R^* as (Yang 1996):

$$u_c = \begin{cases} \frac{2.5v_f}{\log(R^*) - 0.06} + 0.66v_f & 1.2 < R^* < 70 \\ 2.05v_f & R^* > 70 \end{cases} \quad (5.26)$$

The shear velocity Reynolds number R^* (Yang 1996):

$$R^* = \frac{u_* d_s}{\nu} \quad (5.27)$$

where,

ν = kinematic viscosity of water (L^2/T)

u_* = shear velocity (L/T) and defined as (Yang 1996):

$$u_* = \sqrt{ghS_o} \quad (5.28)$$

The second selected formulation is Bridge and Dominic (1984) formulation that is derived though a theoretical consideration of the dynamics of bed load motion.

$$v_s = \delta(u_* - u_{*c}) \quad (5.29)$$

where,

u_{*c} = critical shear velocity (L/T). Bridge and Dominic (1984) expressed the average value of δ between 8 and 12. In this study the employed is $\delta = 10$. The critical shear velocity defined as (Bridge and Dominic 1984):

$$u_{*c} = \frac{v_f (\tan \phi)^2}{\delta} \quad (5.30)$$

where,

$\tan \phi$ = the dynamic friction coefficient (average value between 0.48 and 0.58 (Bridge and Dominic 1984). In this study $\tan \phi = 0.53$ was employed.

The third selected was a constant particle velocity is $v_s = 0.010m / s$.

The fourth particle velocity equation is Kalinske's equation. Kalinske (1947) assumed that

$$v_s = b(u - u_c) \quad (5.31)$$

where,

v_s, u = instantaneous velocities of sediment and fluid

u_c = critical flow velocity at incipient motion

b = a constant close to unity

Secondly we wanted to see these four particle velocity formulation's performances under the Dietrich (1982) fall velocity formulation (Bor, et al. 2008).

$$W_* = R_3 10^{(R_1+R_2)} \quad (5.32)$$

where,

W_* = the dimensionless fall velocity of the particle

The fall velocity of particle is (Dietrich 1982):

$$v_f = \left(\frac{W_* (\rho_s - \rho) g v}{\rho} \right)^{1/3} \quad (5.33)$$

$$R_1 = -3.767 + 1.929(\log D_*) - 0.0982(\log D_*)^2 - 0.00575(\log D_*)^3 + 0.00056(\log D_*)^4 \quad (5.34)$$

$$R_2 = \log \left[1 - \frac{(1 - CSF)}{0.85} \right] - (1 - CSF)^{2.3} \tanh[\log D_* - 4.6] + 0.3(0.5 - CSF)(1 - CSF)^2 (\log D_* - 4.6) \quad (5.35)$$

$$R_3 = \left[0.65 - \left(\frac{CSF}{2.83} \tanh[\log D_* - 4.6] \right) \right]^{1 + \frac{(3.5-P)}{2.5}} \quad (5.36)$$

where,

D_* = the dimensionless particle size

CSF = the Corey shape factor. The mean value of CSF for most naturally occurring sediment is between 0.5 and 0.8 (Dietrich 1982). This study employed a value of $CSF = 0.65$.

P = the Powers value of roughness (the average value of $P = 3.5 \sim 6$ (Dietrich 1982)). This study employed the value of $P = 4.75$.

The dimensionless particle size is expressed as (Dietrich 1982):

$$D_* = \frac{(\rho_s - \rho)gd_s^3}{\rho v^2} \quad (5.37)$$

The third selected particle fall velocity formulation is Yang (1996) formulation. We wanted to see these four particle velocity formulation's performances under the Yang (1996)'s fall velocity formulation (Bor. et al, 2008).

$$v_f = \begin{cases} \frac{1}{18} \frac{(\gamma_s - \gamma_w)}{\gamma_w} \frac{gd_s^2}{v} & d_s \leq 0.1mm \\ F \left[\frac{gd_s(\gamma_s - \gamma_w)}{\gamma_w} \right]^{0.5} & 0.1mm < d_s \leq 2.0mm \\ 3.32 \sqrt{d_s} & d_s > 2.0mm \end{cases} \quad (5.38)$$

where,

$$F = \left\{ \left[\frac{2}{3} + \frac{36v^2\gamma_w}{gd_s^3(\gamma_s - \gamma_w)} \right]^{0.5} - \left[\frac{36v^2\gamma_w}{gd_s^3(\gamma_s - \gamma_w)} \right]^{0.5} \right\} \quad (5.39)$$

In Figures 5.5a, 5.5b and 5.5c it is seen that while Kalinske (1947) and Bridge and Dominic (1984) formula give a faster wavefront, constant $v_s = 0.01m/s$ and Chien and Wan (1999) formula give slower wavefront in rising and equilibrium period. At recession period, as the sediment feeding decreases the bed elevation starts to decrease toward the upstream section (in 20% of the channel length) under constant $v_s = 0.01m/s$. It is seen that Kalinske (1947) and Bridge and Dominic (1984) formula give similar performance and sediment moves faster towards downstream end. This is reasonable, since the transient bed profile moves downstream and thus concentration also increases downstream (Figure 5.5c). In the postrecession period, the bed level increases to original bed level at the upstream section. It is seen that bed profile reached original bed early with Kalinske (1947) and Bridge and Dominic (1984) formula (Figure 5.5d) (Bor, et al. 2008).

The same simulations were obtained under the other three fall velocity formulations.

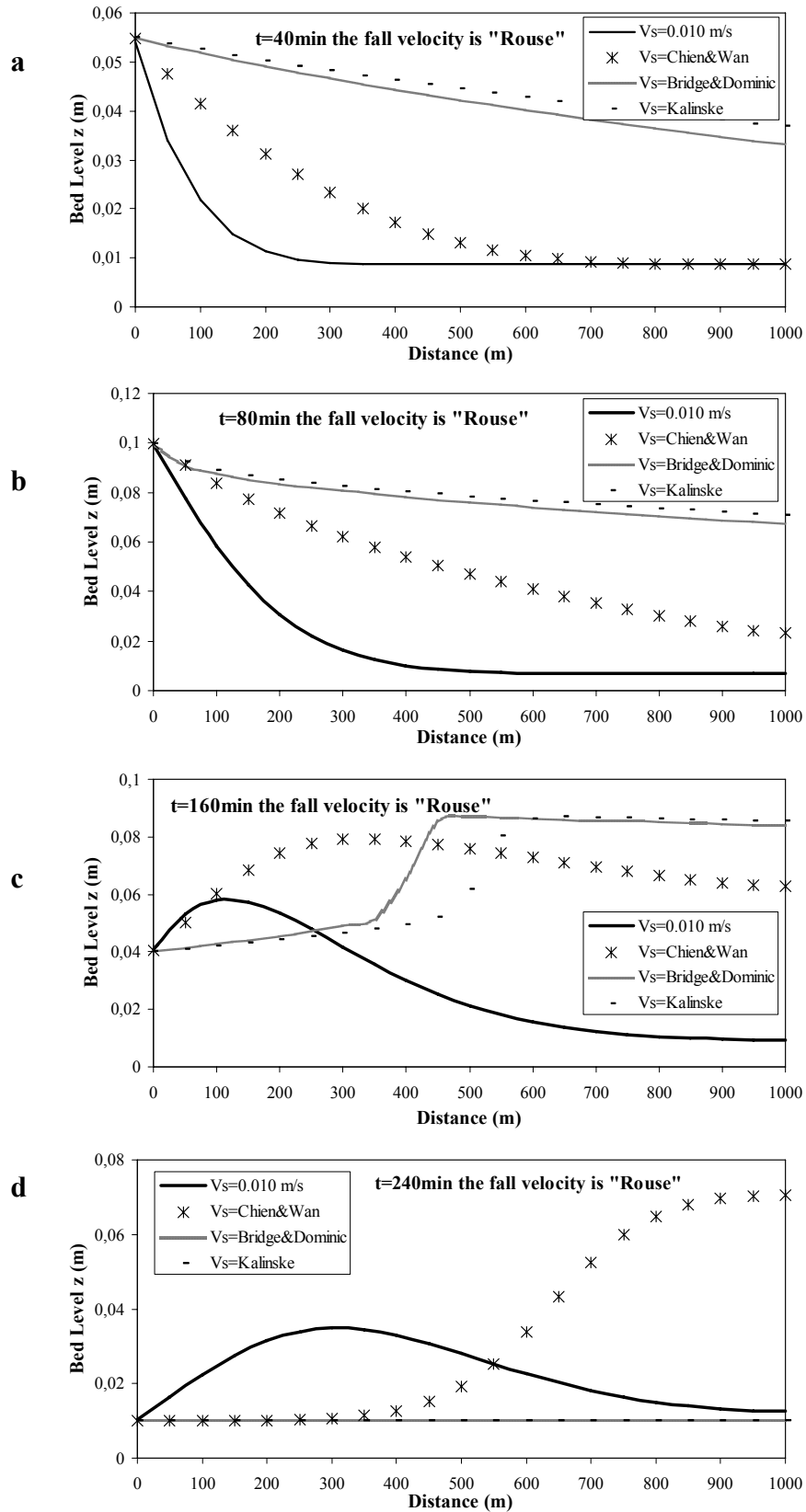


Figure 5.5. Transient bed profile under different particle velocities at (a) rising period (b) equilibrium period (c) recession period (d) postrecession period of inflow hydrograph and concentration. (Source: under Rouse 1938, Dietrich 1982, Yang 1996 formula).

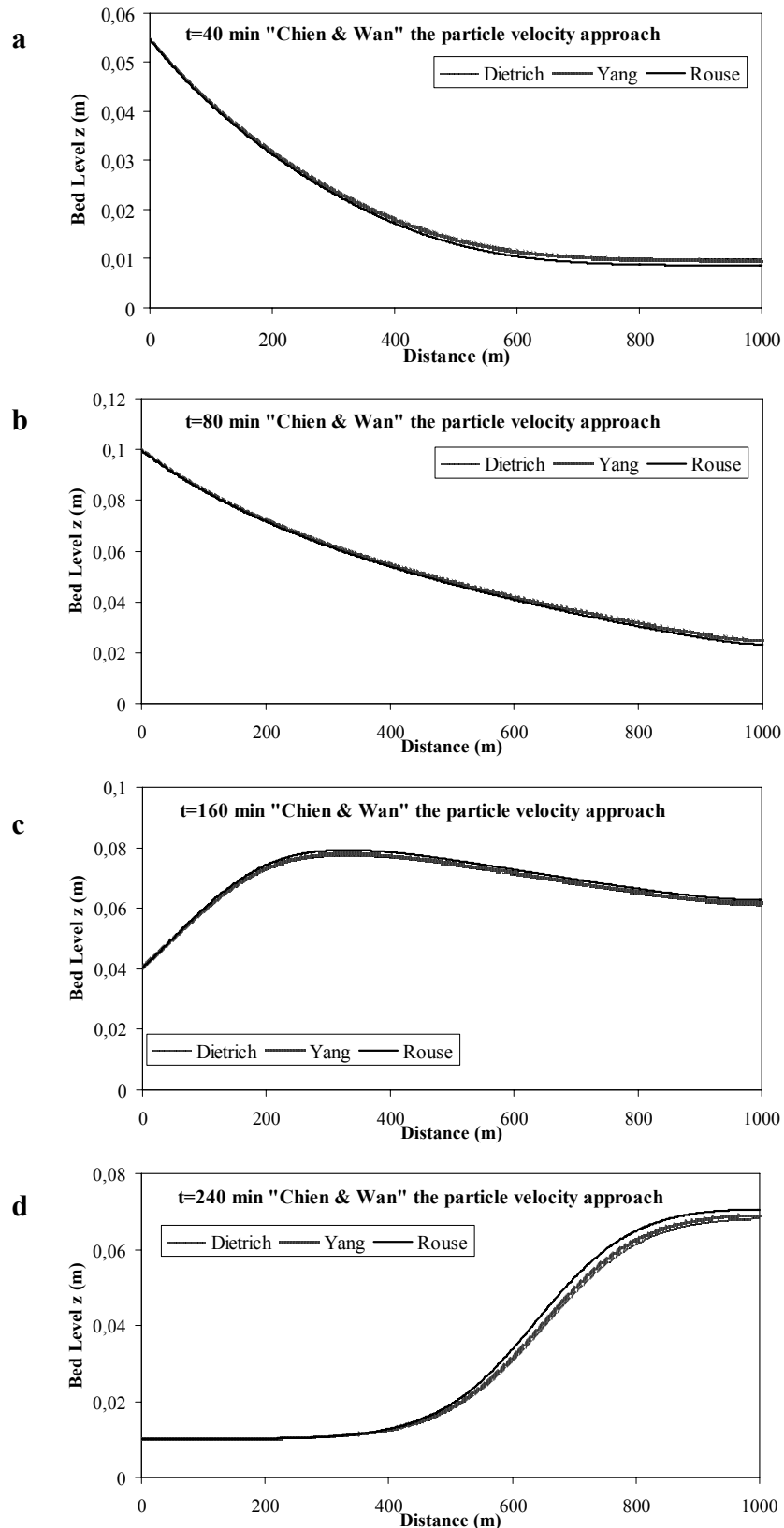


Figure 5.6. Transient bed profiles under different fall velocities at (a) rising period (b) equilibrium period (c) recession period (d) postrecession period of inflow hydrograph and concentration. (Source: under Chien and Wan 1999, Bridge and Dominic 1984, Kalinske 1947 formulation.)

In Figure 5.6a, 5.6b and 5.6c, the effect of the fall velocity on the sediment transport under the different particle velocity formulations is given. Dietrich (1982), Yang (1996) fall velocity formulations and constant $v_f = 0.024m/s$ value (Rouse 1938) give nearly same result under the Bridge and Dominic (1984), Kalinske (1947), and Chien and Wan (1999) particle velocity formulation. For better assessment, the model must be test with experimented results (Bor, et al. 2008).

The same simulation profiles were obtained under the other three particle velocity formulations.

5.1.1.2.3. Hypothetical Case III: Effect of Maximum Concentration

In this case, different maximum concentration values were tested using developed kinematic wave model. For that reason, $C_{max} = 840kg/m^2$ (corresponds to maximum bed level of $z_{max} = 0.60m$), $C_{max} = 630kg/m^2$ (corresponds to maximum bed level of $z_{max} = 0.45m$), $C_{max} = 420kg/m^2$ (corresponds to maximum bed level of $z_{max} = 0.30m$) and $C_{max} = 245kg/m^2$ (corresponds to maximum bed level of $z_{max} = 0.17m$) were selected respectively. It is seen in Figure 5.7 that higher z_{max} value gives higher bed level in the transient bed form profile. The sediment particles move faster downstream under high bed level. The bed levels increased gradually and wavefronts moved slowly at the rising and equilibrium periods of the simulation (Figure 5.7a and 5.7b). At 160 min while the bed wavefront just reached about 400 m under $z_{max} = 0.15m$, it moved the downstream end under $z_{max} = 0.60m$ (Figure 5.7c). While the front under $z_{max} = 0.30m$ closely followed the front under $z_{max} = 0.17m$, front under $z_{max} = 0.45m$ closely followed the front under $z_{max} = 0.60m$ (Figure 5.7a-5.7c).

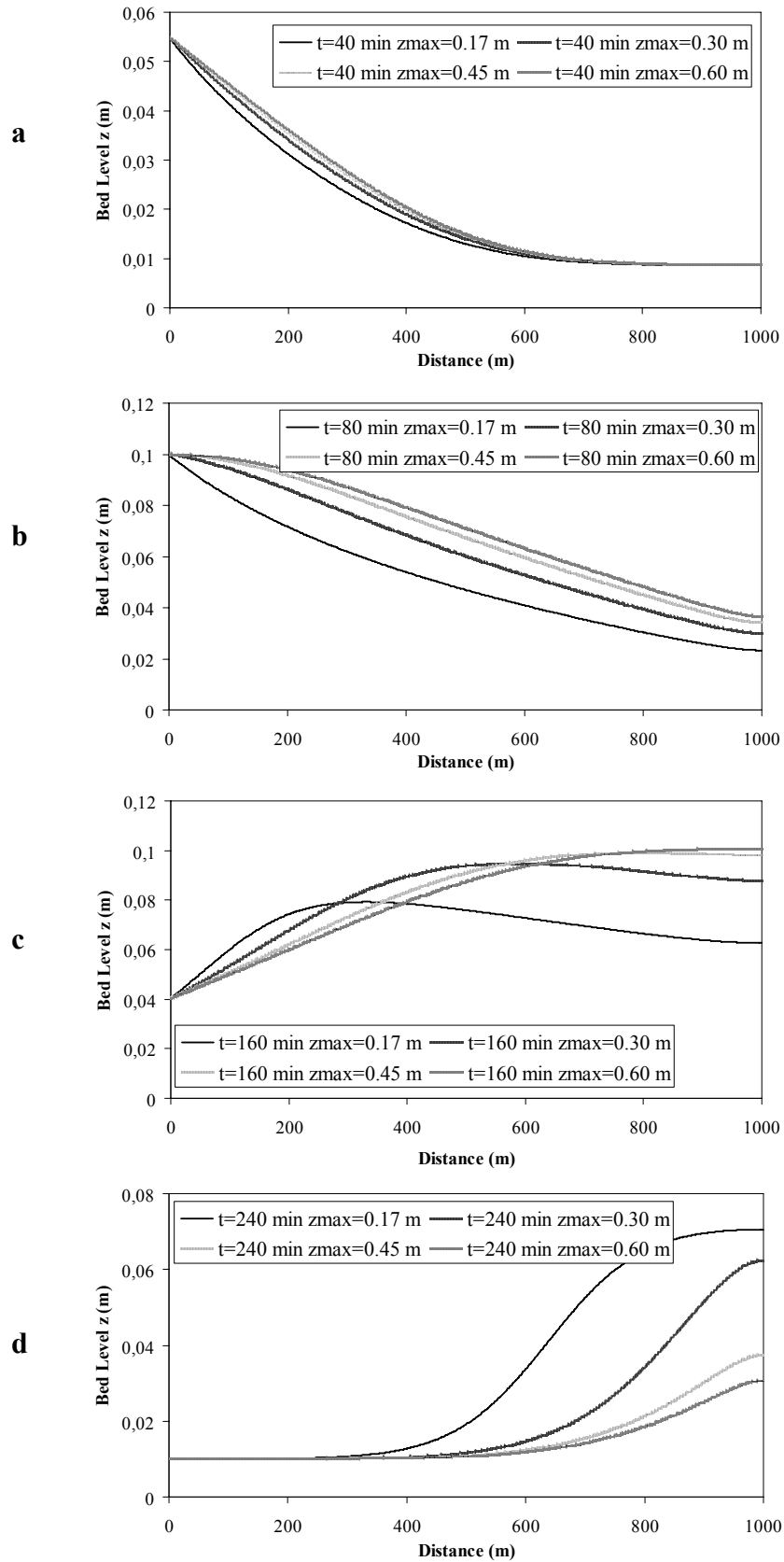


Figure 5.7. Transient bed profile under different z_{max} values at (a) rising period (b) equilibrium period (c) recession period (d) postrecession period of inflow hydrograph and concentration

5.1.2. Diffusion Wave Model of Bed Profiles in Alluvial Channels under Equilibrium Conditions

The diffusion wave model neglects only the local and convective accelerations in the dynamic wave momentum equation. It is the simplified form of the momentum equation which includes also pressure force term. Thus, the momentum equation with these simplifications for a wide rectangular alluvial channel with two layers (Figure 5.1) becomes:

- Momentum equation for water

$$g \frac{\partial h}{\partial x} + g \frac{\partial z}{\partial x} = g(S_0 - S_f) \quad (5.40)$$

The flow velocity in open channels for diffusion waves can be calculated by using either the Manning or Chezy's formulations. We express as $u = \alpha h^{\beta-1}$, α here becomes:

$$\alpha = C_z \left(S_0 - \frac{\partial h}{\partial x} - \frac{\partial z}{\partial x} \right)^{0.5} \quad (5.41)$$

The algorithms for h_i^{j+1} and z_i^{j+1} is presented before by Equations 5.16 and 5.17. The additional algorithm S_{fi}^j is determined as:

$$S_{fi}^j = S_0 - \frac{(h_{i+1}^j - h_{i-1}^j)}{2\Delta x} - \frac{(z_{i+1}^j - z_{i-1}^j)}{2\Delta x} \quad (5.42)$$

The hydrodynamic part of the model is:

$$S_{fi}^j = S_0 - \frac{(h_{i+1}^j - h_{i-1}^j)}{2\Delta x} \quad (5.42a)$$

Equations 5.16, 5.17 and 5.42 are solved simultaneously for each time step.

5.1.2.1. Numerical Solution of Diffusion Wave Equation

Finite difference scheme developed by Lax (1954) is used in this model. The partial derivatives were explained before in Equations 5.14 and 5.15. Initial and boundary conditions were specified before Equations 5.18 – 5.23. And for stability the Courant – Friedrichs – Lewy (CFL) condition was used.

5.1.3. Dynamic Model of Bed Profiles in Alluvial Channels under Equilibrium Conditions

Conservation of mass equations for bed sediment in the movable bed layer, considering there is no exchange of sediment due to the detachment and deposition between two layers, and water for a wide rectangular alluvial channel:

- Continuity equation for water assuming that clear water ($c = 0$):

$$\frac{\partial h}{\partial t} + h \frac{\partial u}{\partial x} + u \frac{\partial h}{\partial x} = q_{1w} \quad (5.43)$$

- Continuity equation for sediment:

$$\frac{\partial hc}{\partial t} + \frac{\partial huc}{\partial x} (1 - p) \frac{\partial z}{\partial t} + \frac{\partial q_{bs}}{\partial x} = q_{1s} \quad (5.44)$$

- Momentum equation for water

The one dimensional partial differential momentum equation of unsteady, equilibrium flow in alluvial channel with dynamic wave assumption is;

$$\frac{\partial u}{\partial t} + u \frac{\partial u}{\partial x} + g \frac{\partial h}{\partial x} + g \frac{\partial z}{\partial x} = g(S_0 - S_f) \quad (5.45)$$

The friction slope S_f in Equation 5.45 can be determined using the Chezy equation (Equation 3.38).

5.1.3.1. Numerical Solution of Dynamic Wave Equations

In dynamic model, a finite difference scheme developed by Lax (1954) is used, as explained as before. With reference to the finite difference grid as shown in Figure 5.2, additional to the partial derivatives, the variables are h_i^j, u_i^j, z_i^j and S_{fi}^j are approximated as follows:

$$h_i^j = \frac{1}{2}(h_{i+1}^j + h_{i-1}^j) \quad (5.46)$$

$$u_i^j = \frac{1}{2}(u_{i+1}^j + u_{i-1}^j) \quad (5.47)$$

$$S_{fi}^j = \frac{1}{2}(S_{fi+1}^j + S_{fi-1}^j) \quad (5.48)$$

Under the assumption there is no suspended sediment (clear water flow ($c = 0$)), the first and second term on the right side of the Equation 5.44 will disappear. Based on the finite difference approximation of (5.14), (5.15), (5.46), (5.47) and (5.48), Equations 5.43 - 5.45 may be written as follows for determining the values h^{j+1}, u^{j+1} and z^{j+1} :

$$h_i^{j+1} = 0.5(h_{i+1}^j + h_{i-1}^j) - 0.5 \frac{\Delta t}{\Delta x} h_i^j (u_{i+1}^j - u_{i-1}^j) - 0.5 \frac{\Delta t}{\Delta x} u_i^j (h_{i+1}^j - h_{i-1}^j) \quad (5.49)$$

$$u_i^{j+1} = 0.5(u_{i+1}^j + u_{i-1}^j) - 0.5 \frac{\Delta t}{\Delta x} u_i^j (u_{i+1}^j - u_{i-1}^j) - 0.5 \frac{\Delta t}{\Delta x} g (h_{i+1}^j - h_{i-1}^j) - 0.5 \frac{\Delta t}{\Delta x} g (z_{i+1}^j - z_{i-1}^j) + g \Delta t (S_o - S_{fi}^j) \quad (5.50)$$

The hydrodynamic part of the model is:

$$u_i^{j+1} = 0.5(u_{i+1}^j + u_{i-1}^j) - 0.5 \frac{\Delta t}{\Delta x} u_i^j (u_{i+1}^j - u_{i-1}^j) - 0.5 \frac{\Delta t}{\Delta x} g (h_{i+1}^j - h_{i-1}^j) + g \Delta t (S_o - S_{fi}^j) \quad (5.50a)$$

$$z_i^{j+1} = 0.5(z_{i+1}^j + z_{i-1}^j) - 0.5 \frac{\Delta t}{\Delta x} \frac{p v_s \left[1 - \frac{2z_i^j}{z_{\max}} \right]}{(1-p)} (z_{i+1}^j - z_{i-1}^j) \quad (5.51)$$

(note that q_{bs} express as before Equation 5.11)

By using the presented algorithm, the unknown values of h and z at the new time level $j+1$ (future time) are determined from every interior node ($i = 2, \dots, N-1$). The values of the dependent variables h and z at the boundary nodes 1 and $N+1$ are determined by using boundary conditions. Also, at the time level $j=1$, initial conditions are already known.

Initial and boundary conditions were specified before Equations 5.18 – 5.23. And for stability the Courant – Friedrichs – Lewy (CFL) condition was used.

Equations 5.49, 5.50 and 5.51 are solved simultaneously for each time step.

Note that, in the case of Dynamic Wave, we assumed that there is no suspended sediment.

5.1.3.2. Model Testing: Comparing the Kinematic, Diffusion and Dynamic Models for Hypothetical Cases

The hypothetical cases were analyzed assuming inflow hydrograph and concentration at the upstream of the channel as shown in Figures 5.3a and 5.3b. The channel was assumed to have a 1000 m length and 20 m width with 0.0025 bed slope. Chezy roughness coefficient $C_z = 50 \text{ m}^{0.5}/\text{s}$ and Manning roughness coefficient $n = 0.021 \text{ sm}^{-1/3}$. The sediment was assumed to have $\rho_s = 2650 \text{ kg/m}^3$, $d_s = 0.32 \text{ mm}$, $p = 0.528$ and sediment transport capacity coefficient $\kappa = 0.000075$ (Ching and Cheng, 1964). Langbein and Leopold (1968) suggest $C_{\max} = 245 \text{ kg/m}^2$ (note that $C_b = (1-p)z\rho_s$).

For three of wave solutions a Courant number was selected 0.2. The numerical solutions are plotted $x = 200\text{m}$, $x = 500\text{m}$ and $x = 800\text{m}$ along the channel, respectively (Figure 5.8 and Figure 5.9). By comparing Figures 5.8a, 5.8b and 5.8c, one can observe the different behavior of the diffusion and kinematic waves, particularly at peak flow points. The diffusion wave reaches faster to maximum flow rate. On the other hand, the

dynamic wave has a smaller peak than the diffusion wave (Figure 5.9a, 5.9b and 5.9c) and kinematic wave has the smallest. It can be said that particle velocity is higher in diffusion and dynamic wave models. Results are acceptable with Kazezyılmaz et al. (2007) paper.

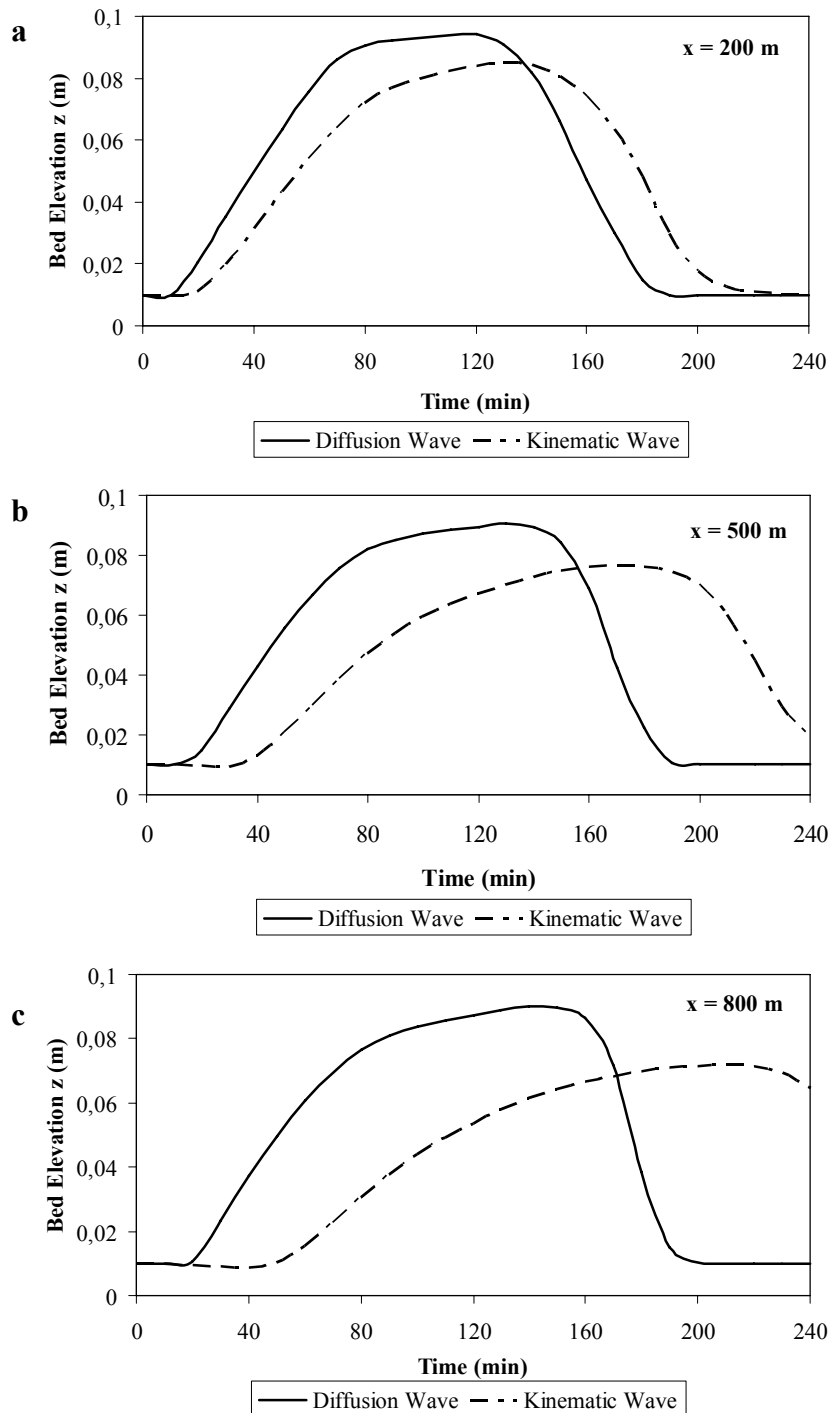


Figure 5.8. Comparison of numerical solution of Diffusion and Kinematic waves at distance (a) $x = 200\text{ m}$ (b) $x = 500\text{ m}$ (c) $x = 800\text{ m}$ of the channel

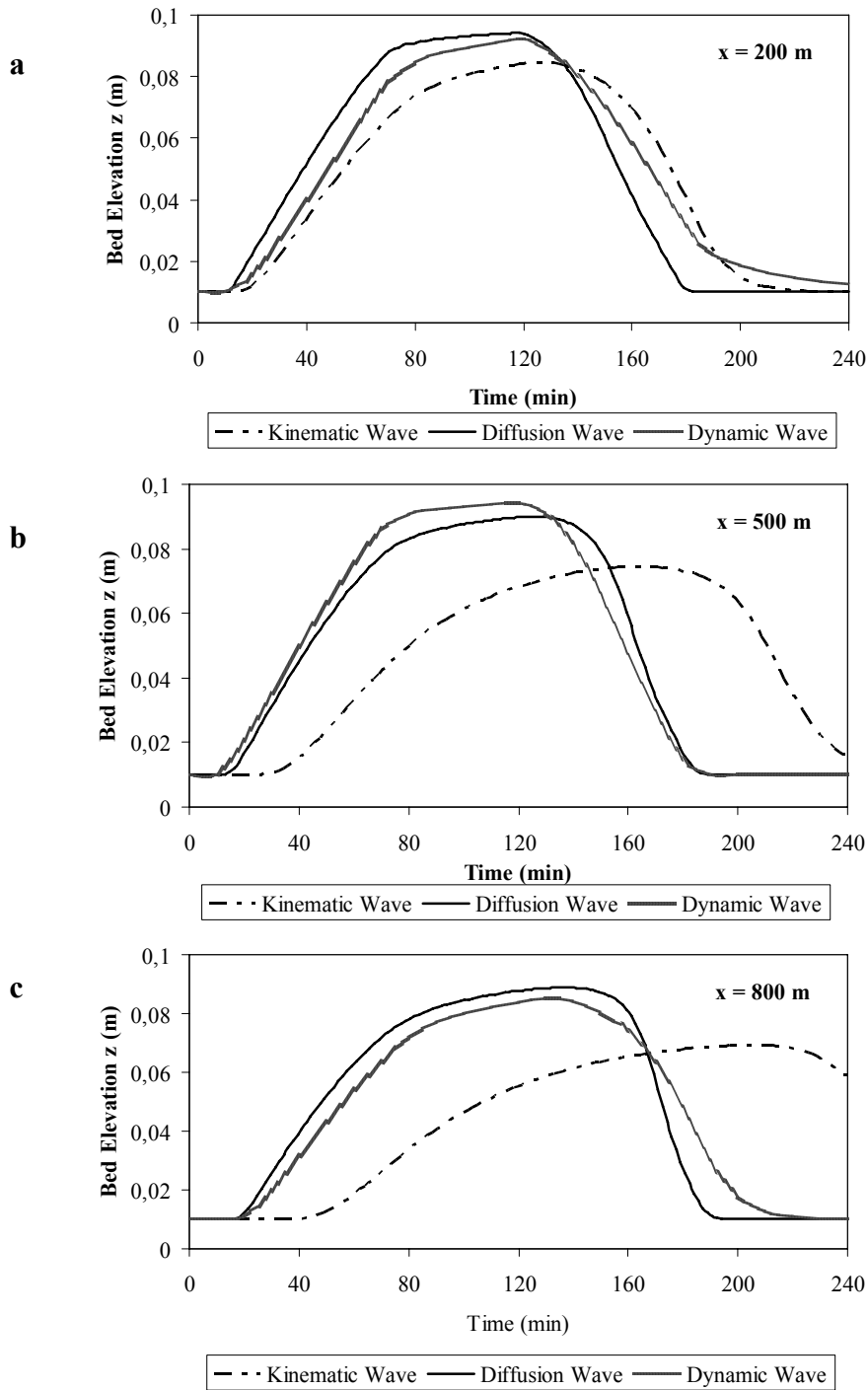


Figure 5.9. Comparison of numerical solution of Dynamic, Diffusion and Kinematic waves at distance (a) $x = 200m$ (b) $x = 500m$ (c) $x = 800m$ (assuming clear water ($c = 0$))

5.1.3.3. Hypothetical Case I: Comparing Three Bed Load Formulas under Kinematic and Diffusion Wave Models

The objective of this case is to compare the bed load transport formulations employed in the developed model. For that reason three bed load formulations were selected from the literature. The formulations are Meyer – Peter (1934) (Equation 3.46), Schoklitsch (1934) (Equation 3.47) and Tayfur and Singh (2006) (Equation 3.69) bed load formulations. First of all, the formulations were tested under Kinematic wave model. While Meyer – Peter and Schoklitsch formula give similar performance, Tayfur and Singh formula gives different performance (Figure 5.10a and 5.10b). The sediment particles moved downstream faster under Tayfur and Singh formula. The second test was under Diffusion wave model, where the same behavior was observed (Figure 5.11a and 5.11b).

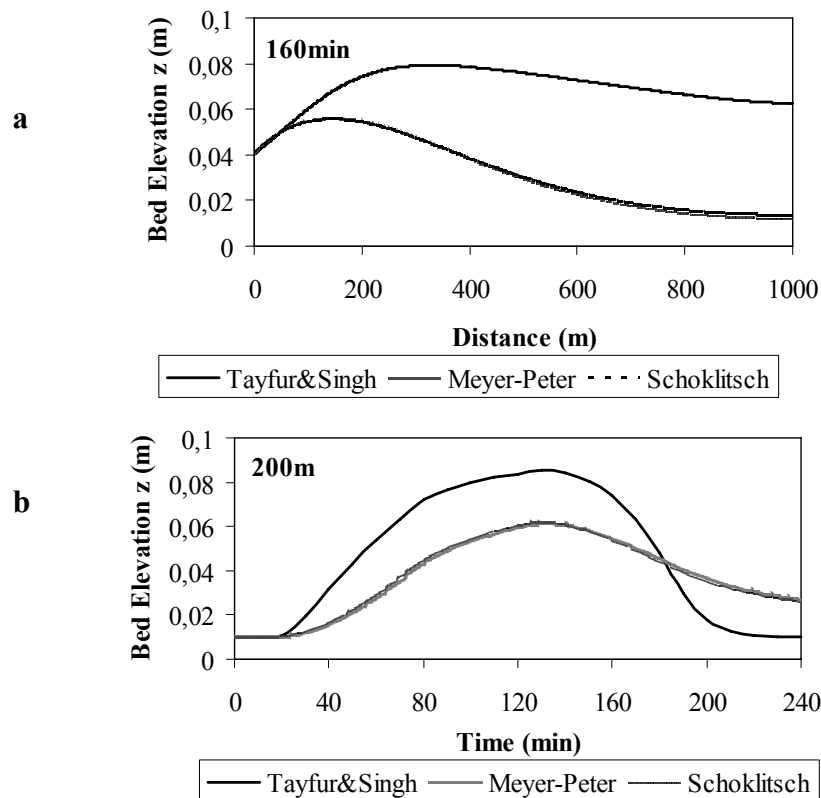


Figure 5.10. (a) Comparison of Tayfur and Singh, Meyer – Peter and Schoklitsch bed load formulations under Kinematic wave model at time 160 min. (b) Comparison of Tayfur and Singh, Meyer – Peter and Schoklitsch bed load formulations under Kinematic wave model at distance $x = 200m$ of the channel

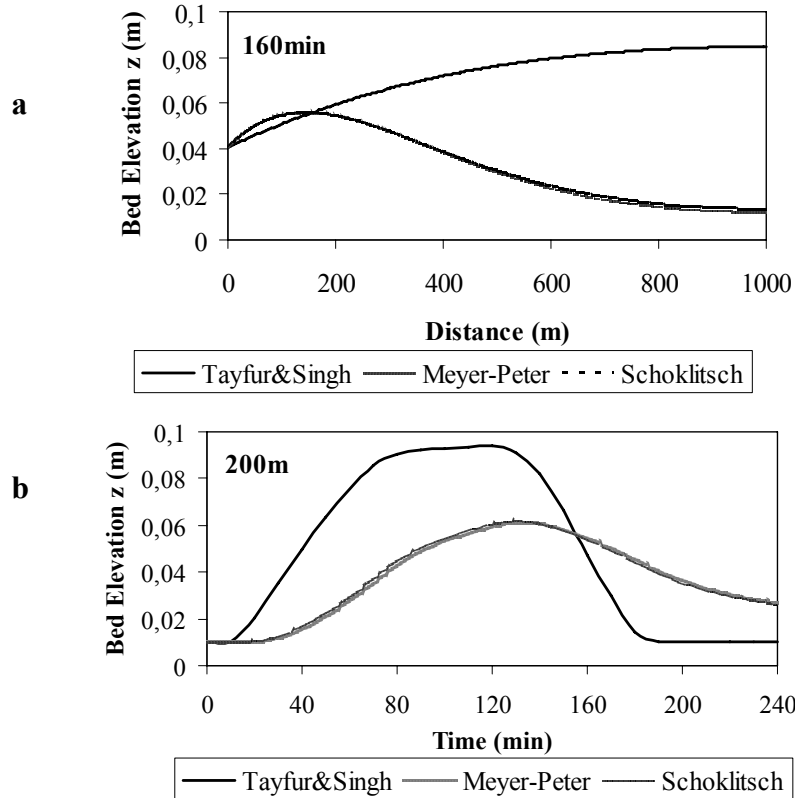


Figure 5.11. (a) Comparison of Tayfur and Singh, Meyer – Peter and Schoklitsch bed load formulations under Diffusion wave model at time 160 min. (b) Comparison of Tayfur and Singh, Meyer – Peter and Schoklitsch bed load formulations under Diffusion wave model at distance $x = 200m$ of the channel

It is seen that while Mayer – Peter (1934) and Schoklitsch (1934) formula give same performance, Tayfur and Singh (2006) gives different. Sediment moves faster towards under Tayfur and Singh (2006) formula.

5.1.3.4. Model Testing Using Experimental Data

5.1.3.4.1. Test I

The one dimensional model in tested by means of the experimental results obtained by Bombar (Güney and Bombar 2008). These experiments are carried out on an experimental system designed and constructed in the scope of TÜBİTAK project no: 106M274. The rectangular flume is 18.6 m long and 0.80 m wide. The bottom slope is

0.001. The input hydrograph constitute the upstream boundary condition. The downstream boundary condition is defined by Equation 5.22 ($h_{N+1}^{j+1} = h_{N-1}^{j+1}$).

The different input hydrographs in the form of isosceles triangle are generated as shown in Figure 5.12. The steady discharge is $0.020 \text{ m}^3/\text{s}$ while the peak discharge value is equal to $0.060 \text{ m}^3/\text{s}$. The hydrographs with rising limb of 90 minutes and 120 minutes are given in Figure 5.12a and 5.12b respectively. The numerical equations, Equation 5.16a and 5.16b are solved simultaneously for each time step under kinematic wave approach. Equation 5.16a and 5.42a are solved simultaneously for each time step under diffusion wave approach. Equation 5.49 and 5.50a are solved simultaneously for each time step under dynamic wave approach.

Figures 5.13 and 5.14 represent the variations of water depths with time at section 10.5 m and 15 m far from upstream end of the channel. These figures involve the experiment results as well as those obtained from numerical solutions performed by using various approaches; namely, kinematic diffusion and dynamic wave assumptions.

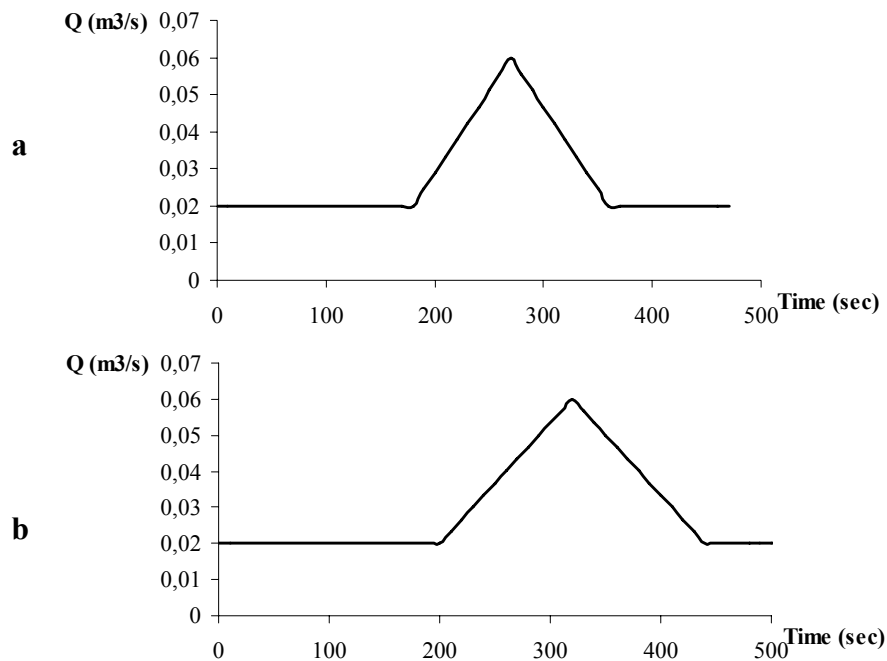


Figure 5.12. (a) The input hydrograph a) Rising limb = 90 second (b) Rising limb = 120 second

The results corresponding to the first hydrograph (rising limb = 90 sec) are given in Figure 5.13 and those obtained from the second hydrograph (rising limb = 120 sec) are depicted in Figure 5.14.

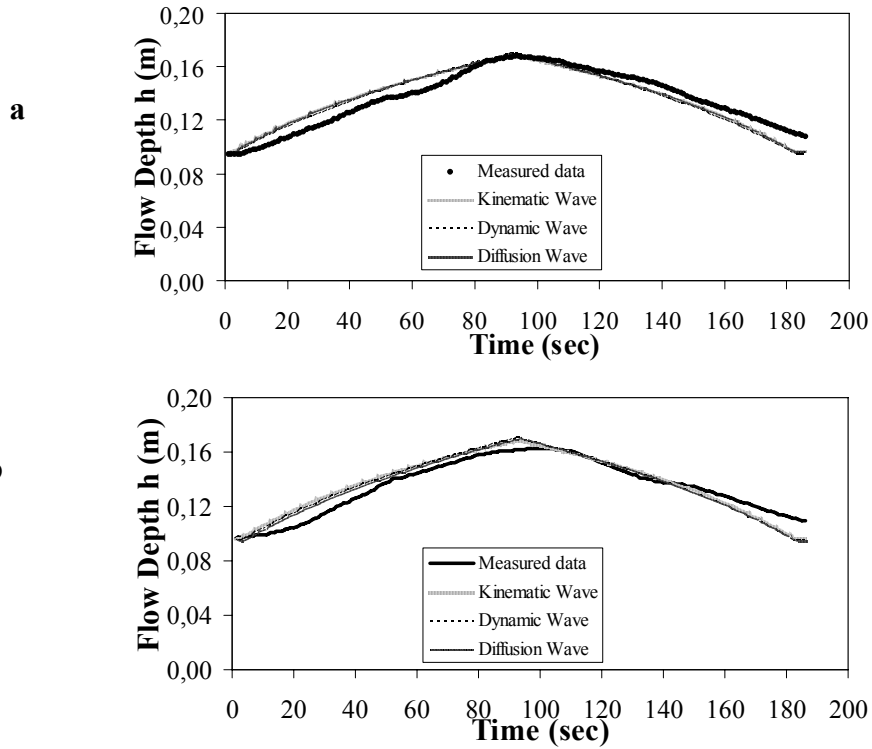


Figure 5.13. Measured and computed water depths at (a) 10.5 m (b) 14 m (the hydrograph that has 90 second in rising limb)

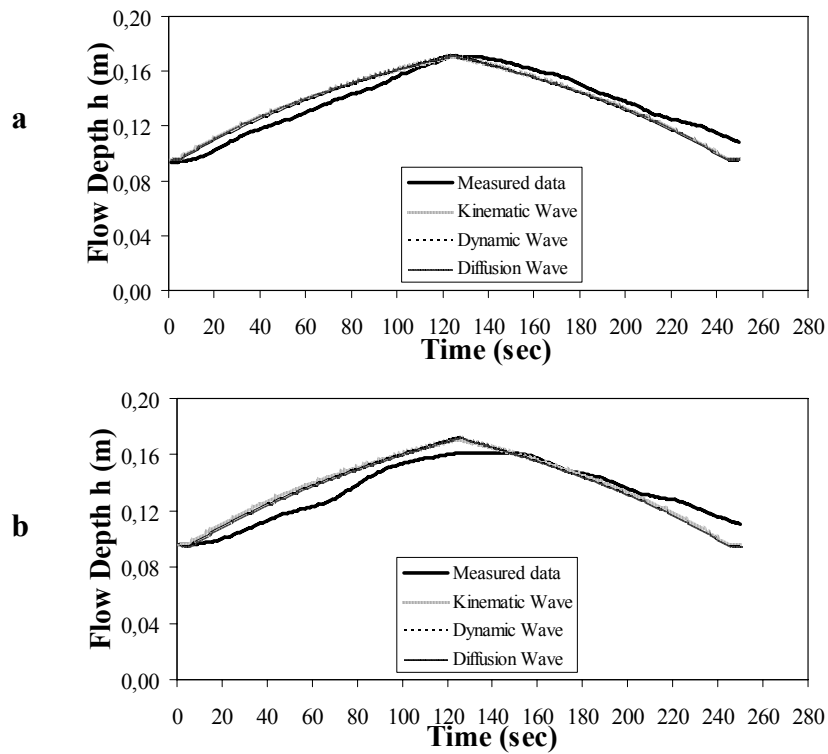


Figure 5.14. Measured and computed water depths at (a) 10.5 m (b) 14 m (the hydrograph that has 120 second in rising limb)

The overall computed error measures for simulations are presented in Table 5.1. As seen, the mean relative error of $MRE = 5.2$ implies that the developed model makes about 5% error in predictions. The computed values of $RMSE$ (root mean square error) and MAE are 0.007 and 0.006 cm, respectively.

Table 5.1. Computed $RMSE$, MAE , MRE

<u>RMSE, cm</u>		
Kinematic W.	Dynamic W.	Diffusion W.
0,0074	0,0072	0,0073
<u>MAE, cm</u>		
Kinematic W.	Dynamic W.	Diffusion W.
0,0065	0,0064	0,0064
<u>MRE, %</u>		
Kinematic W.	Dynamic W.	Diffusion W.
5,1952	5,0646	5,0789

5.1.3.4.2. Test II

The second test was against the experimental data of aggradation depths measured by Soni (1981a) in a laboratory flume of rectangular cross section. The flume used by Soni was 30.0 m long, 0.20 m wide and 0.50 m deep. In the experimental run constant equilibrium flow discharge was $Q = 0.02m^3/s$ and uniform flow depth was $h_0 = 0.092m$. The sand used for bed material and sediment feed in the experiments had a median diameter of $d_s = 0.32mm$ and specific gravity of 2.65. Soni performed experiments in the mobile bed condition to better represent natural rivers. Initially the flume was filled with sand to a depth of 15 cm. Then the rectangular flume was filled slowly with water and control valve was used to attain the specified discharge. The tail gate height was adjusted in a way so that uniform flow was obtained in the flume by allowing the bed to adjust by erosion or deposition. A uniform flow condition in the flume was achieved when the measured bed and water surface were parallel to each other. After reaching the uniform flow condition, sediment was dropped at the upstream of the flume at a constant rate. The sediment injection section was located far enough from the entrance of the flume to avoid entrance disturbances. The aggradation in the bed started due to the excess load of the sediment. Bed and water surface elevation were measured at regular time intervals (from 10 to 20 min at eleven sections). Aggradation

runs were continued until the end point of the transient profiles reached the downstream end.

For computing the maximum bed elevation z_{\max} , Langbein and Leopold (1968)'s given a value of $C_{b\max} = 245 \text{ kg} / \text{m}^2$. The porosity was assumed to be $p = 0.4$. The flow was uniform and steady and suspended sediment was negligible in this experiment, so Equation 5.2 would suffice to model the bed aggradation.

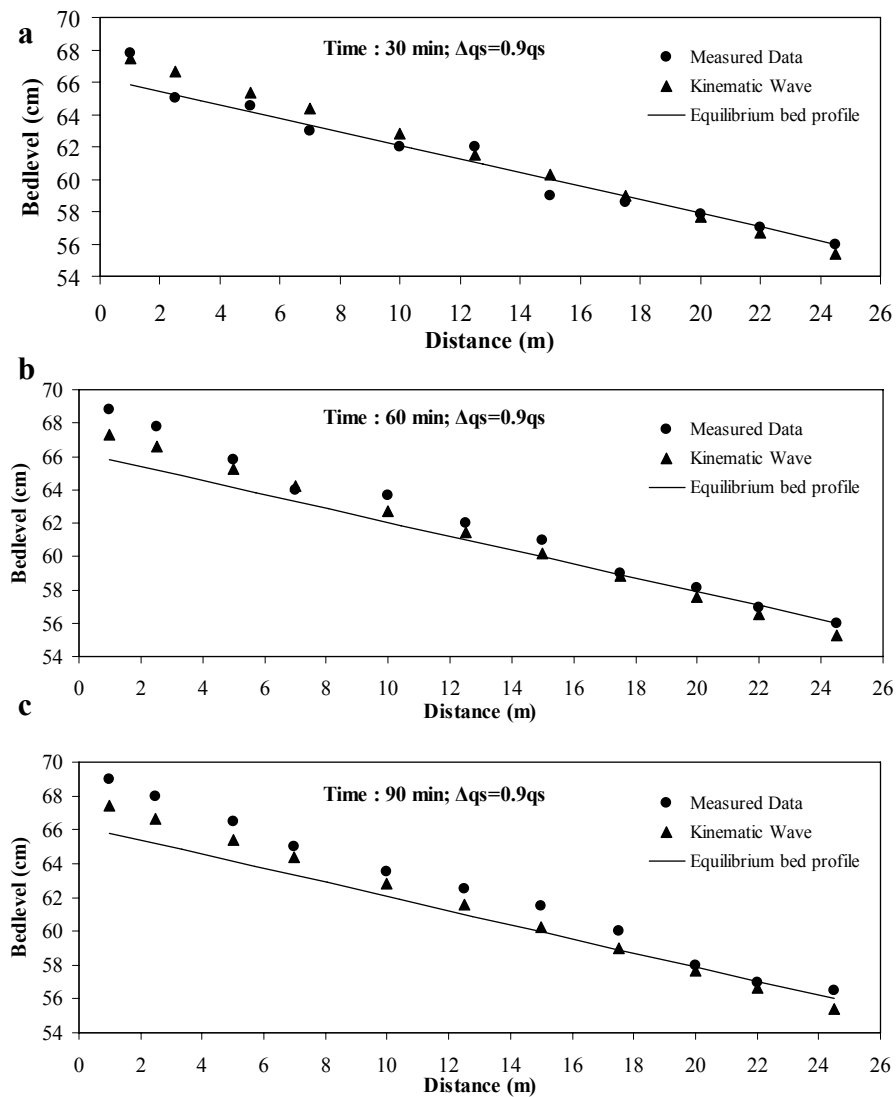


Figure 5.15. Simulation of measured bed profile at (a) 30 min (b) 60 min (c) 90 min

Figures 5.15a-5.15c show, respectively, simulations of bed profiles measured at 30, 60 and 90 min during the experimental run. The equilibrium flow conditions are $Q = 0.02 \text{ m}^3 / \text{s}$ (equilibrium flow discharge), $q_{seq} = 111 \times 10^{-6} \text{ m}^2 / \text{s}$ (equilibrium

sediment discharge), $S_o = 0.00212$ (bed slope), $h_o = 0.092m$ (uniform flow depth) and an excess sediment rate of $\Delta q_s = 0.9q_{seq}$.

Figures 5.15 and 5.16 show the model simulations of the experiments. Figure 5.15 corresponds to the measured data under the rate of $\Delta q_s = 0.9q_{seq}$. As seen that the earlier parts of the transient profiles were closely captured by the model in downstream end. It is observed that the transient profiles were faster than those of the measured ones in reaching the equilibrium bed profile (Figure 5.16 and 5.16c). Figure 5.16 corresponds to the measured data under the rate of $\Delta q_s = 1.35q_{seq}$. The simulations of bed profiles measured at 15, 45, 75 and 105 min during the experimental run. The measured and predicted profiles moved very closely toward the downstream end and reached the equilibrium bed profile at the same time (Figure 5.16b). The measured and predicted profiles moved together and reached the equilibrium bed profile at the same time (Figure 5.16c). The predicted bed profile reached the equilibrium bed profile slightly earlier than did the measured one (Figure 5.16d).

The overall computed error measures for simulations are presented in Table 5.2. As seen, the mean relative error of $MRE = 1.21$ implies that the developed model makes about 1.21% error in predictions for $\Delta q_s = 0.9q_{seq}$ and for $\Delta q_s = 1.35q_{seq}$ the error is 1.5%. The computed values of $RMSE$ (root mean square error) and MAE are 0.89 and 0.75 cm, respectively. For $\Delta q_s = 1.35q_{seq}$ the computed values of $RMSE$ and MAE are 1.23 and 0.95 cm, respectively.

Table 5.2. Computed $RMSE$, MAE , MRE

Experiment	<u>RMSE, cm</u>	<u>MAE, cm</u>	<u>MRE, %</u>
	KW	KW	KW
$\Delta q_s = 0.9q_{seq}$	0,89	0,75	1,21
$\Delta q_s = 1.35q_{seq}$	1,23	0,95	1,50

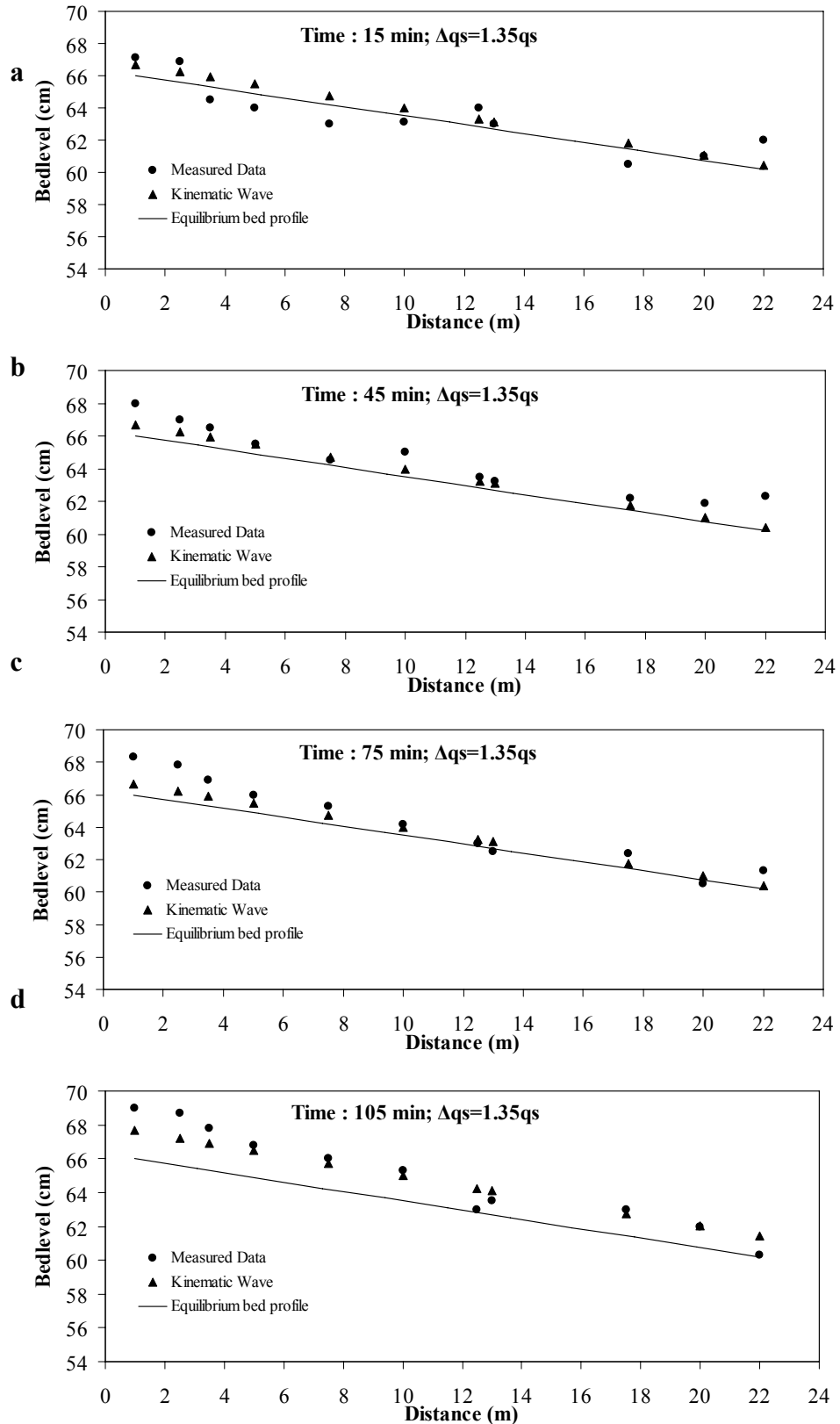


Figure 5.16. Simulation of measured bed profile at (a) 15 min (b) 45 min (c) 75 min (d) 105 min

5.2. One Dimensional Numerical Model for Sediment Transport under Unsteady and Nonequilibrium Conditions

All the sediment transport functions or equations presented earlier have been intended for the estimation of bed levels at the equilibrium condition with no scour or deposition, at least from a statistical point of view. It has been assumed that the amount of wash load depends on the supply from upstream and is not a function of the hydraulic conditions at a given station. Also, the amount of wash load is not high enough to significantly affect the fall velocity of sediment particles, flow viscosity or flow characteristics in a river in comparison with these values in clear water. When the wash load or concentration of fine material is high, non equilibrium bed material sediment transport may occur.

The floods may cause heavy erosion and landslides in a river basin causing sediment overloading within a river reach. During the aggradation and degradation, there may be an exchange of sediment particles between bed layer and suspended layer exceeding the flow capacity. The nonequilibrium sediment transport condition results in an unstable streambed elevation. In such cases a numerical sediment transport model provides the computational framework for analysis.

There are significant differences between the calculations of equilibrium and nonequilibrium conditions. The nonequilibrium condition solution can be obtained by numerical sediment modeling using control volume approach.

5.2.1. Governing Equations

Tayfur and Singh (2007) studied transport movement in a wide rectangular alluvial channels represented in two layers. Figure 5.17 shows the possible exchange of sediment between two layers: the water flow layer and movable bed layer, depending upon flow transport capacity and sediment rate in suspension.

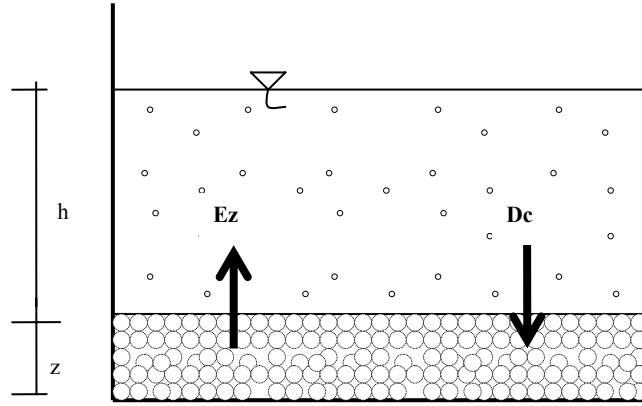


Figure 5.17. Definition Sketch of two layer system in nonequilibrium condition
(Source: Tayfur and Singh 2007)

The water flow layer may contain suspended sediment. The movable bed layer consists of both water and sediment particles; therefore bed layer includes porosity (Tayfur and Singh 2007). Equations 5.1 and 5.2 are for equilibrium conditions, where the entrainment rate (E_z) is equal to the deposition rate (D_c) (i.e., $E_z = D_c$). Under nonequilibrium condition entrainment rate is not equal to the deposition rate ($E_z \neq D_c$). This makes the solution more complex than equilibrium approach. Pianese (1994) employed one more equation, adaptation equation relating the change in bed level in time to flow variables (u, h), equilibrium suspended sediment concentration (c_{eq}) and suspended sediment concentration (c) to simplifying the solution. The adaptation equation is,

$$(1 - p) \frac{\partial z}{\partial t} = \frac{uh}{\lambda} (c_{eq} - c) \quad (5.52)$$

where,

λ =adaptation length

If the right hand side of the equation is negative, it represents detachment rate, if it is positive, it represents deposition rate (Pianese 1994). When deposition occurs, z increases, but c decreases. Otherwise, when detachment occurs, z decreases, c increases. Mohammadian et al. (2004) employed an equation for the conservation of water

(Equation 5.1) (assuming clear water $c = 0$) and an equation for conservation of suspended sediment in the water flow layer as:

$$\frac{\partial hc}{\partial t} + \frac{\partial huc}{\partial x} = \frac{\partial}{\partial x} \left(V_x h \frac{\partial c}{\partial x} \right) + \frac{v_f}{\eta} (c_{eq} - c) \quad (5.53)$$

where,

V_x = the sediment mixing coefficient

η = a coefficient

As explained before, the right side of the equation represents deposition (negative) or detachment rate (positive). They also used an additional equation which represents the change in bed level in time to the particle fall velocity, equilibrium suspended sediment concentration (c_{eq}), and suspended sediment concentration (c) as:

$$(1 - p) \frac{\partial z}{\partial t} = \frac{v_f}{\eta} (c_{eq} - c) \quad (5.54)$$

There are some deficiencies in Equations 5.53 and 5.54. One of them is that when the last term on the right hand side of the Equation 5.53 is negative, it acts a sink of concentration in the bed layer, so there should be a negative sign in front of the term on the right hand side of the equation. The second deficiency is concern with Equation 5.54. It does not fully represent the conservation of mass equation for the sediment in the movable bed layer, since it ignores the major term of the sediment flux gradient $\left(\frac{\partial q_{bs}}{\partial x} \right)$. Mohammadian et al. (2004) who did not employ Equation 5.2, ignored the bed sediment flux term. To avoid any confusion, the conservation of mass for suspended sediment in the water flow layer and the conservation of mass for bed sediment in the movable bed layer are written separately (Tayfur and Singh 2007);

$$\frac{\partial hc}{\partial t} + \frac{\partial huc}{\partial x} = q_{1sus} + \frac{1}{\rho_s} [E_z - D_c] \quad (5.55)$$

$$(1-p)\frac{\partial z}{\partial t} + \frac{\partial q_{bs}}{\partial x} = q_{bed} + \frac{1}{\rho_s} [D_c - E_z] \quad (5.56)$$

where,

q_{1sus} = the lateral suspended sediment (L/T)

q_{bed} = the lateral bed load sediment (L/T)

ρ_s = the sediment mass density (M/L³)

E_z = the detachment rate (M/L²/T)

D_c = the deposition rate (M/L²/T)

The equations include the exchange of sediment due to the detachment and deposition between the two layers. The process is $E_z \neq D_c$ in the non equilibrium condition. The process is $E_z = D_c$ in the equilibrium condition. When $E_z > D_c$, there is entrainment from the bed layer (reducing the bed elevation, increasing the suspended sediment concentration). When $E_z < D_c$, there is deposition from the bed layer (increasing the bed elevation, reducing the suspended sediment concentration).

According the Equations 5.1, 5.55 and 5.56, there are five unknowns, h, u, c, z and q_{bs} . Therefore, two more equations are needed for solving the system. One more equation can be obtained from the momentum equation for water flow. In this study, the kinematic wave approximation was employed for the momentum equation (Equation 5.4). The fifth equation can be obtained by relating sediment transport rate to sediment concentration in the movable bed layer. In this study, the kinematic theory was employed (Tayfur and Singh 2006) (Equation 3.69).

Combining the Equations 3.69, 5.1, 5.4, 5.55 and 5.56 can be written in a compact form as:

$$\frac{\partial h}{\partial t} + \alpha\beta h^{\beta-1} \frac{\partial h}{\partial x} + \frac{p}{(1-c)} \frac{\partial z}{\partial t} - \frac{h}{(1-c)} \frac{\partial c}{\partial t} - \frac{\alpha h^\beta}{(1-c)} \frac{\partial c}{\partial x} = \frac{q_{1w}}{(1-c)} \quad (5.57)$$

$$\frac{\partial c}{\partial t} + \alpha h^{\beta-1} \frac{\partial c}{\partial x} + \frac{c}{h} \frac{\partial h}{\partial t} - c\alpha\beta h^{\beta-2} \frac{\partial h}{\partial x} = \frac{q_{1sus}}{h} + \frac{1}{\rho_s h} [E_z - D_c] \quad (5.58)$$

$$\frac{\partial z}{\partial t} + v_s \left[1 - \frac{2z}{z_{\max}} \right] \frac{\partial z}{\partial x} = \frac{q_{1bed}}{(1-p)} + \frac{1}{\rho_s(1-p)} [D_c - E_z] \quad (5.59)$$

These equations are kinematic wave equations for modeling unsteady state, nonuniform transient channel bed profiles under nonequilibrium conditions. For calculating the detachment rate E_z , the shear stress approach was used (Yang 1996);

$$E_z = \sigma T_c = \sigma [\Phi(\tau - \tau_{cr})^k] \quad (5.60)$$

where,

$$\tau = \gamma_w h S_o \quad (5.61)$$

$$\tau_{cr} = \kappa(\gamma_s - \gamma_w) d_s \quad (5.62)$$

where,

σ = the transfer rate coefficient (1/L)

T_c = the flow transport capacity (M/L/T)

Φ = the soil erodibility coefficient

τ = the shear stress (M/L²)

τ_{cr} = the critical shear stress (M/L²)

k = an exponent

γ_w, γ_s = the specific weight of water and sediment respectively (M/L³)

κ = a constant

d_s = the sediment particle diameter (L)

The deposition rate D_c can be expressed as (Yang 1996);

$$D_c = \sigma \rho_s q_{ss} = \sigma [\rho_s h u c] \quad (5.63)$$

where,

q_{ss} = the unit suspended sediment discharge (M/L/T)

5.2.1.1. Numerical Solution of Kinematic Wave Equations

Equations 5.57, 5.58 and 5.59 were solved using the finite difference scheme developed by Lax (1954) as explained before (Equations 5.14 and 5.15). Note that the finite difference equations were written for both the layers not only at the central nodes of the domain but also at the downstream nodes. All the equations were solved simultaneously for each time step. The finite difference equations are:

$$h_i^{j+1} = 0.5(h_{i+1}^j + h_{i-1}^j) - \frac{\Delta t \alpha \beta}{2\Delta x} h_{ij}^{\beta-1} (h_{i+1}^j - h_{i-1}^j) - \frac{P}{(1-c_i^j)} [z_i^{j+1} - 0.5(z_{i+1}^j + z_{i-1}^j)] \\ + \frac{h_i^j}{(1-c_i^j)} [c_i^{j+1} - 0.5(c_{i+1}^j + c_{i-1}^j)] + \frac{\Delta t \alpha}{2\Delta x} \frac{h_{ij}^\beta}{(1-c_i^j)} (c_{i+1}^j - c_{i-1}^j) + \frac{q_{1w}\Delta t}{(1-c_i^j)} \quad (5.64)$$

$$c_i^{j+1} = 0.5(c_{i+1}^j + c_{i-1}^j) - \frac{\Delta t \alpha}{2\Delta x} h_{ij}^{\beta-1} (c_{i+1}^j - c_{i-1}^j) - \frac{c_i^j}{h_i^j} [h_i^{j+1} - 0.5(h_{i+1}^j + h_{i-1}^j)] \\ - \frac{\Delta t \alpha \beta}{2\Delta x} c_i^j h_{ij}^{\beta-2} (h_{i+1}^j - h_{i-1}^j) + \frac{q_{1sus}\Delta t}{h_i^j} + \frac{\Delta t}{\rho_s h_i^j} [E_z^{ij} - D_c^{ij}] \quad (5.65)$$

$$z_i^{j+1} = 0.5(z_{i+1}^j + z_{i-1}^j) - \frac{\Delta t v_s}{2\Delta x} \left(1 - \frac{2z_i^j}{z_{\max}}\right) (z_{i+1}^j - z_{i-1}^j) + \frac{q_{1sus}\Delta t}{(1-p)} + \frac{\Delta t}{\rho_s(1-p)} [D_c^{ij} - E_z^{ij}] \quad (5.66)$$

where,

i = stands for space node

j = stands for time node

Δt = time increment

Δx = space increment

By using presented algorithm, the unknown values of h , c and z at the new time level $j+1$ (future time) are determined at every interior node ($i = 2, \dots, N-1$). The values of the dependent variables h , c and z at the boundary nodes 1 and $N+1$ are determined by using boundary conditions. Also, at the time level $j=1$, initial conditions are already known (Figure 5.2)

Initial conditions can be specified as:

$$h(x,0) = h_o \quad (5.67)$$

$$c(x,0) = c_o \quad (5.68)$$

$$z(x,0) = z_o \quad (5.69)$$

where,

h_o, c_o and z_o = the initial flow depth (L), concentration (L^3/L^3) and the bed level (L), respectively.

The upstream boundary conditions can be specified as inflow hydrograph and inflow sedimentograph.

$$h(0,t) = h(t) \quad t > 0.0 \quad (5.70)$$

$$c(0,t) = c(t) \quad t > 0.0 \quad (5.71)$$

$$z(0,t) = z(t) \quad t > 0.0 \quad (5.72)$$

The downstream boundary conditions can be specified as:

$$\frac{\partial h((N,t))}{\partial x} = 0 \quad (h_{N+1}^{j+1} = h_{N-1}^{j+1}) \quad t > 0.0 \quad (5.73)$$

$$\frac{\partial c((N,t))}{\partial x} = 0 \quad (c_{N+1}^{j+1} = c_{N-1}^{j+1}) \quad t > 0.0 \quad (5.74)$$

$$\frac{\partial z((N,t))}{\partial x} = 0 \quad (z_{N+1}^{j+1} = z_{N-1}^{j+1}) \quad t > 0.0 \quad (5.75)$$

- Stability

The numerical scheme has to satisfy the stability conditions. For this reason, the Courant – Friedrichs – Lewy (CFL) condition was used. Since the water waves travel at a much higher velocity than the bed transients this condition is given as before Equation 5.24.

Equations 5.64, 5.65 and 5.66 are solved simultaneously for each time step.

5.2.1.2. Model Application

The channel was assumed to have a 1000 m length and 30 m width with 0.0015 bed slope. The model parameters basically are as follows: $C_z, p, S_o, z_{\max}, \rho_s, \gamma_s, \sigma, \Phi, \phi, k, \kappa, CSF, P$ and d_s . Parameters ρ_s, γ_s , and d_s can be obtained from experimental sediment data. Chezy roughness coefficient is assumed to be $C_z = 36m^{0.5}/s$. The sediment was assumed to have $\rho_s = 2650kg/m^3$, $d_s = 0.32mm$ and $p = 0.528$. Maximum concentration was assumed $C_{\max} = 500kg/m^2$ (note that $z_{\max} = C_{\max}/(1-p)\rho_s$). Gessler (1965) suggested a value of 0.047 for κ for most flow conditions. The value of transfer rate can be calculated in flumes by $\sigma = 1/(7h)$, where h is flow depth, parameter Φ has a range of 0.0 – 1.0 and exponent k_i has a range of 1.0 – 2.5 in literature (Foster 1982, Tayfur 2002, Yang 1996). The inflow hydrograph and inflow concentration were given in Figure 5.18 for upstream boundary conditions.

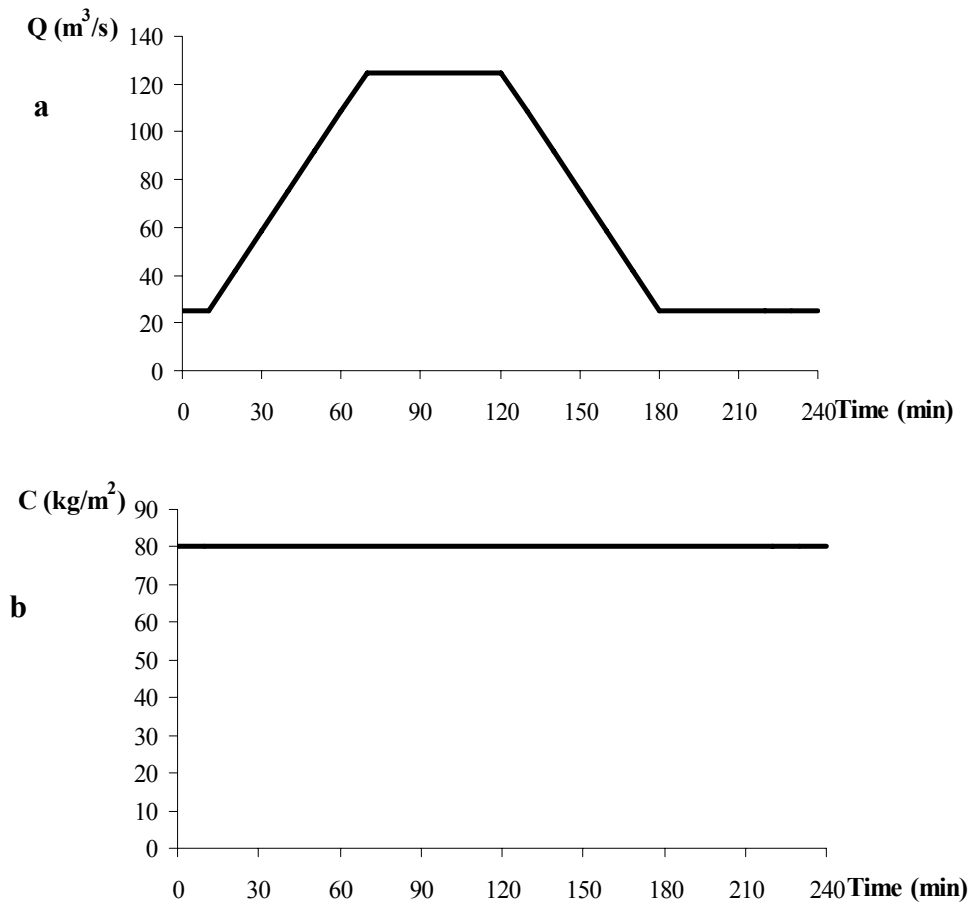


Figure 5.18 (a) Inflow hydrograph. (b) Inflow concentration

Figures 5.19a-5.19d present bed profiles during the rising limb, equilibrium, recession limb and postrecession limb of the inflow hydrograph and concentration, respectively. It is seen that while inflow concentration increases, the bed level gradually increases in upstream and it decreases after about 200 m in the downstream (Figure 5.19a). The bed elevation continues to increase in the equilibrium period at the upstream end (Figure 5.19b). In rising period the bed level reaches at equilibrium after the 200 m of the channel (Figure 5.21c). In procession period the bed level nearly same afert the 200 m (Figure 5.19d).

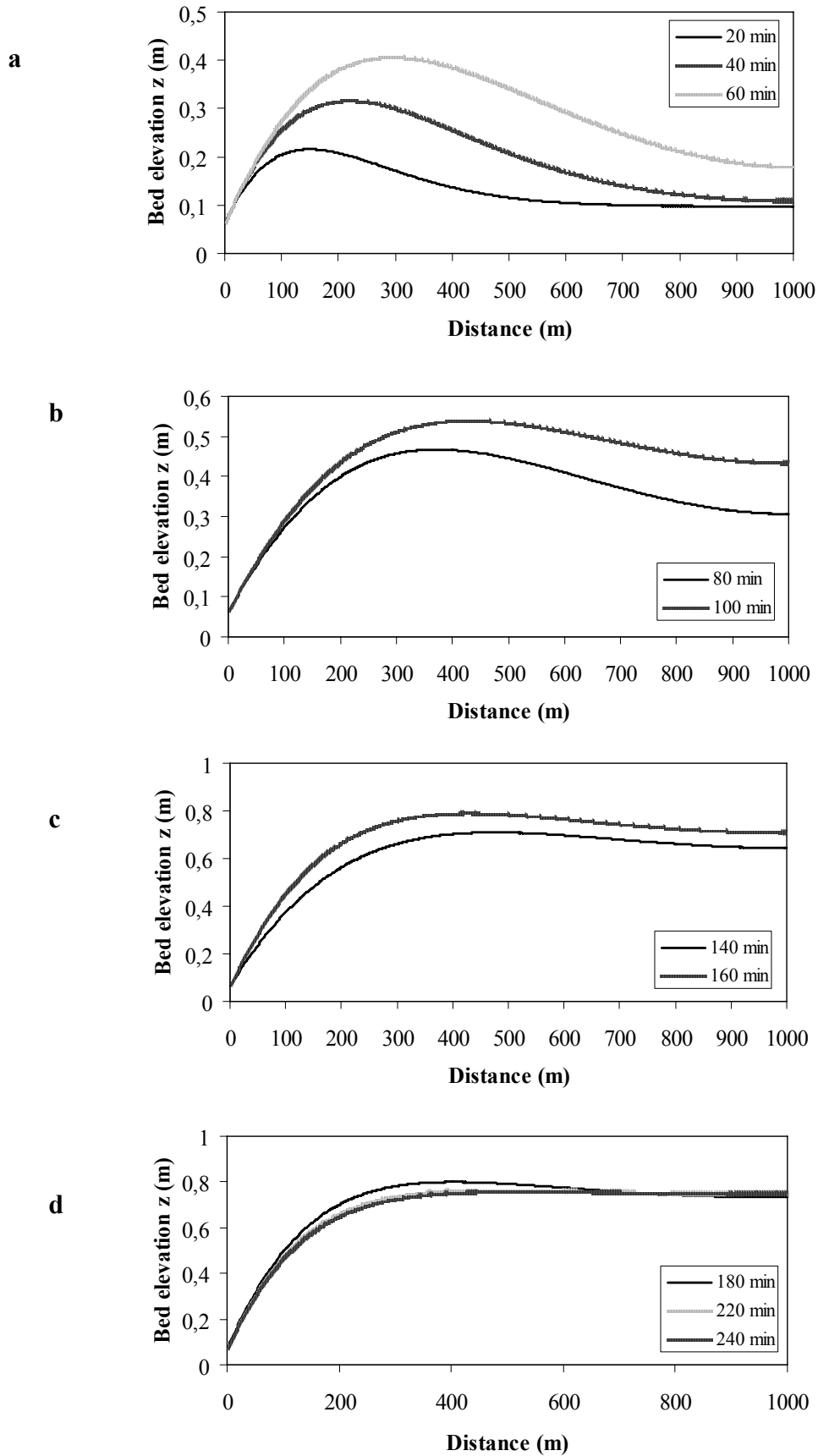


Figure 5.19. Transient bed profile at (a) rising period (b) equilibrium period (c) recession period (d) post recession period of inflow hydrograph and concentration

5.2.1.3. Model Testing Using Experimental Data

The model was tested against the experimental data of aggradation depths measured by Yen et al. (1992) in laboratory flume. The flume used for present experiments is 72 m long and 1 m wide. The water discharge was maintained at a constant rate of $0.12\text{m}^3 / \text{s}$ for all experiments. The initial bed slope is 0.0035 and sediment median diameter is 1.8 mm. At the beginning of an experiment, a sediment supply rate of 3.3 kg/min (dry mass) was continuously released from the upstream end until the channel bed reached a state of equilibrium. The sediment supply rate was then increased to 9.9 kg/min until a new equilibrium was reached. The rate of sediment supply was thereafter reduced back to and kept at 3.3 kg/min until another new equilibrium was reached. Finally, the sediment supply was cut off, and only clear water was released from the upstream end until the channel bed was fully armored. Each period lasted for about 30 hours. Bed elevations were measured 5 m apart from each other. A sluice gate at the downstream end of the flume was employed to maintain a constant tailwater level. The details of the experiment can be obtained from Yen et al. (1992).

Simulations of bed profiles measured at 30, 60, 90 and 120 hours during the experiment run (Figure 5.20.). The model and measured data nearly closed at each location along the bed. At 120 hr predicted and measured data were nearly same (Figure 5.20d).

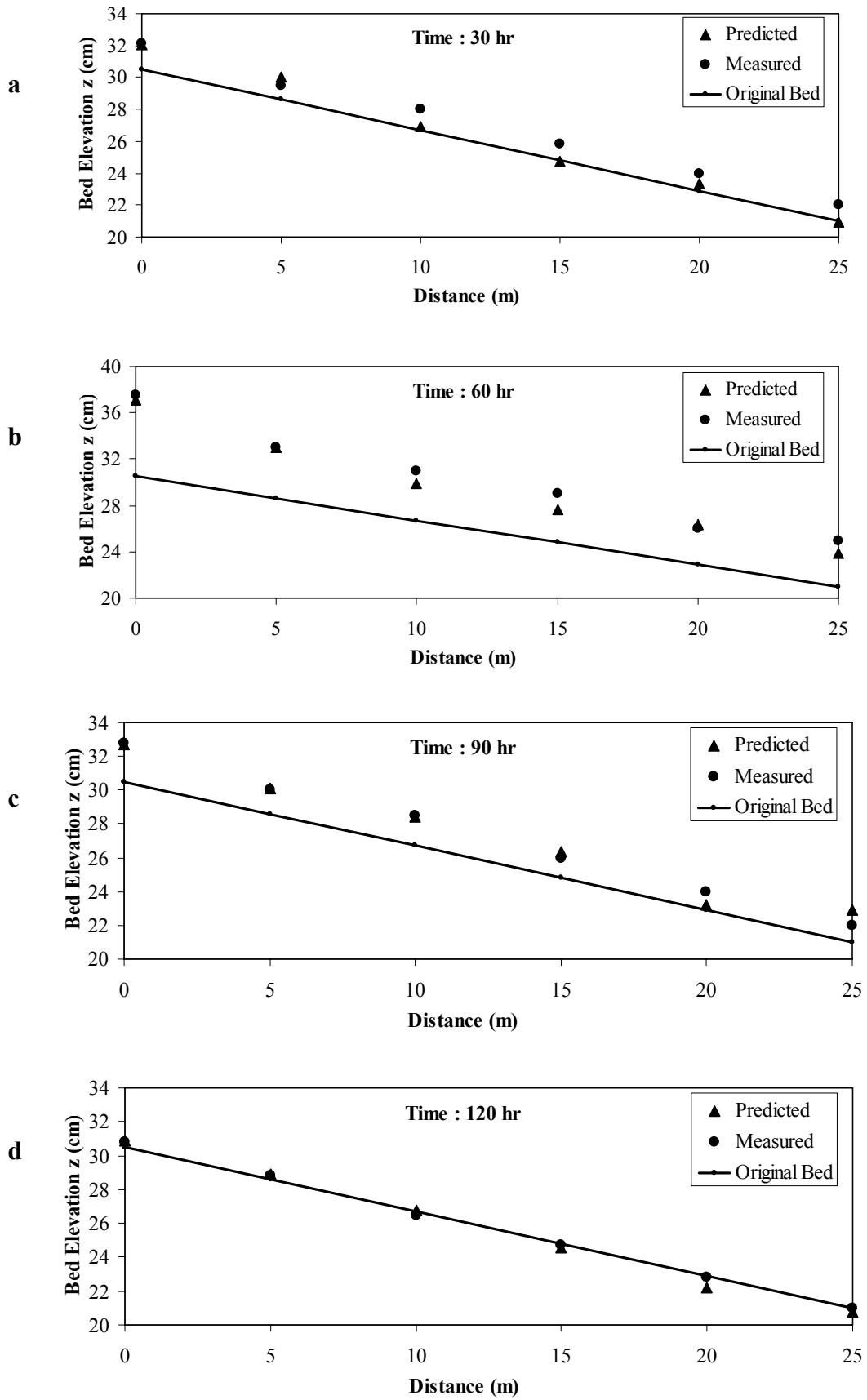


Figure 5.20. Simulation of bed profiles along a channel bed at (a) 30 h, (b) 60 h, (c) 90 h and (d) 120 h of the laboratory experiment

Figure 5.21 presents simulation of bed level measured at 10 m away from the upstream end during the experiment period of 120 hours. The model simulations of transient bed levels at the specified locations are satisfactory. The model closely predicted bed levels during, rising equilibrium and recession periods satisfactory.

The overall computed error measures for simulations are presented in Table 5.3 Location #1. As seen, the mean relative error of $MRE = 1.99$ implies that the developed model makes about 1.99% error in predictions. The computed values of $RMSE$ (root mean square error) and MAE are 0.82 and 0.66 cm, respectively.

Table 5.3. Computed $RMSE$, MAE , MRE

RMS, cm	MAE, cm	MRE, %
0,820	0,663	1,992

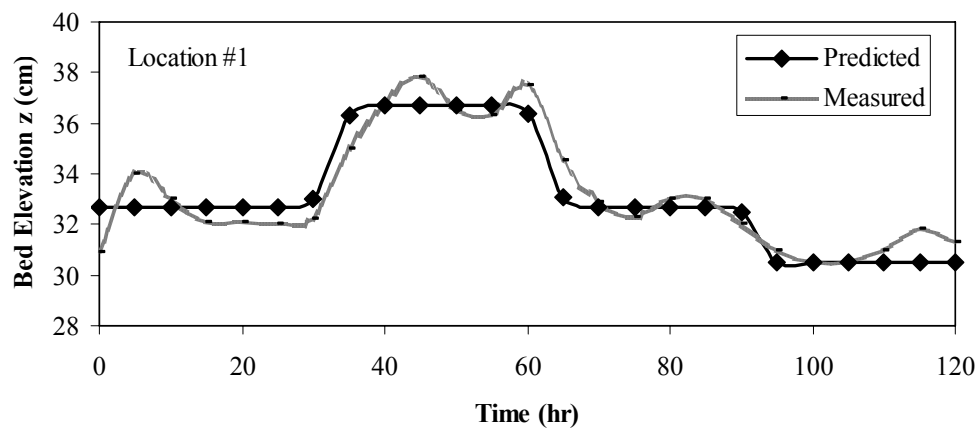


Figure 5.21. Simulation of bed profiles in time during the laboratory experiment at six different locations of the experimental channel. Location #1 is 10 m away from the upstream end (Yen, et al. 1992)

5.2.1.4. Model Testing: Comparing the Equilibrium and Nonequilibrium models for Hypothetical Cases

The hypothetical cases were analyzed assuming inflow concentration hydrograph at the upstream of the channel as shown in Figures 5.22. The channel was assumed a flume and to have a 20 m length and 1 m width with 0.0001 bed slope. The sediment was assumed to have $\rho_s = 2650 \text{ kg/m}^3$, $d_s = 0.09 \text{ mm}$, $p = 0.45$ and sediment transport capacity coefficient $\kappa = 0.000075$ (Ching and Cheng 1964). Langbein and

Leopold (1968) suggest $C_{\max} = 500 \text{ kg/m}^2$ (note that $C_b = (1 - p)z\rho_s$). The water discharge is $Q = 0.5 \text{ m}^3/s$ at the beginning. In equilibrium part $Q = 1\text{m}^3/s$ (in trapezoidal).

For two model solutions a Courant number was selected 0.2. The numerical solutions are plotted $x = 500\text{m}$ along the channel (Figure 5.23). It is seen that the different behavior of equilibrium and nonequilibrium model, particularly at peak flow points. The equilibrium model reaches faster to maximum flow rate. On the other hand, the nonequilibrium model has a smaller peak. It can be said that bed material decreases because of suspended sediment increases.

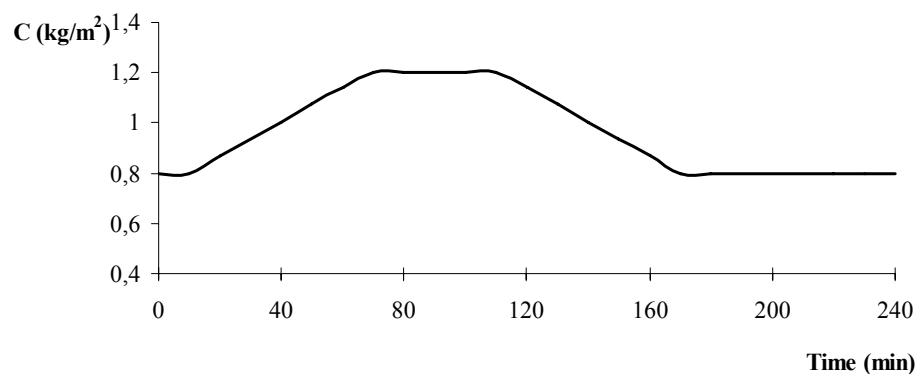


Figure 5.22. (a) Inflow hydrograph. (b) Inflow concentration

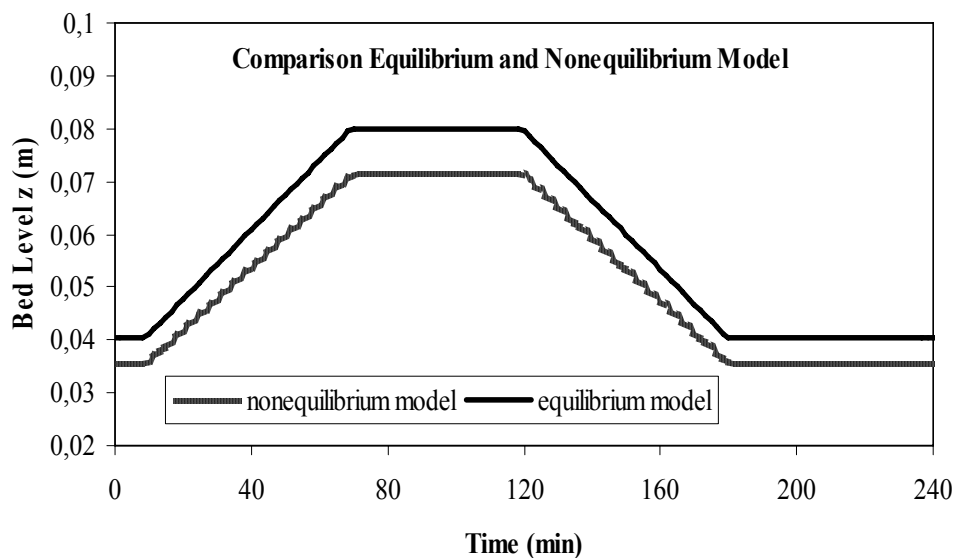


Figure 5.23. Comparing the equilibrium and nonequilibrium models

5.3. One Dimensional Numerical Model for Nonuniform Sediment Transport under Unsteady and Nonequilibrium Conditions

One dimensional sediment transport models are simulated in uniform gravel bed in this chapter. In this part, the proposed one dimensional model simulates the nonequilibrium sediment transport of nonuniform total load under unsteady flow conditions in rivers. For this reason, de Saint Venant equations are solved for complex material. Models simulated suspended sediment transport using the nonequilibrium transport approach. In this research, the mathematical model is developed using diffusion wave theory under nonequilibrium condition. The bed profile evolution of complex gravel in alluvial channels can be presented in Figure 5.24.

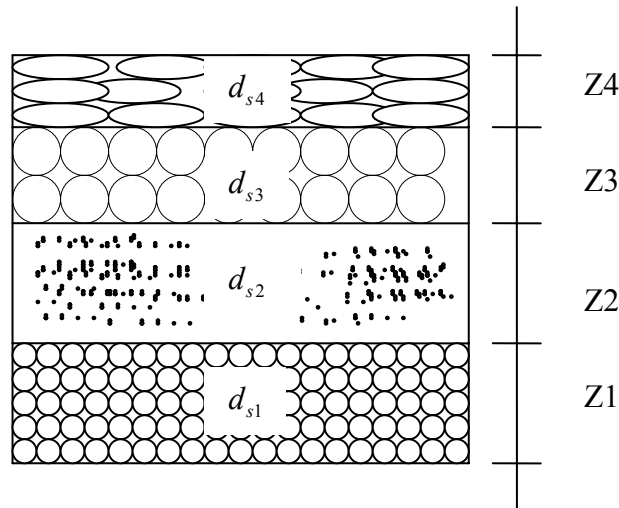


Figure 5.24. Multiply – layer model for bed load column

5.3.1. Governing Equations

The conservation of mass for suspended sediment in the water flow layer and the conservation of mass for bed sediment in the movable bed layer separately can be written for nonuniform and nonequilibrium sediment transport;

$$\frac{\partial h \sum_{k=1}^N c_k}{\partial t} + \frac{\partial hu \sum_{k=1}^N c_k}{\partial x} = q_{1sus} + \frac{1}{\rho_s} \left[\sum_{k=1}^N E_{zk} - \sum_{k=1}^N D_{ck} \right] \quad (5.76)$$

$$\left(1 - \sum_{k=1}^N p_k\right) \sum_{k=1}^N \left(\frac{\partial z_b}{\partial t}\right)_k + \frac{\partial \sum_{k=1}^N q_{bsk}}{\partial x} = q_{lbed} + \frac{1}{\rho_s} \left[\sum_{k=1}^N D_{ck} - \sum_{k=1}^N E_{zk} \right] \quad (5.77)$$

where,

c_k = section – averaged sediment concentration of size class k

E_{zk} = the detachment rate of size class k ($M / L^2 / T$)

D_{ck} = the deposition rate of size class k ($M / L^2 / T$)

q_{bsk} = the sediment flux in the movable bed layer of size class k (L^2 / T)

$(\partial z_b / \partial t)_k$ = bed change rate corresponding to the k th size class of sediment

p_k = bed material porosity of size class k

5.3.1.1. Numerical Solutions of Nonuniform Model

Equations 5.40, 5.41, 5.76 and 5.77 were solved using the finite difference scheme developed by Lax (1954) as explained before (Equations 5.14 and 5.15). The finite difference equations are:

$$S_{fi}^j = S_o - \frac{(h_{i+1}^j - h_{i-1}^j)}{2\Delta x} - \frac{\left(\sum_{k=1}^N (z_{i+1}^j)_k - \sum_{k=1}^N (z_{i-1}^j)_k\right)}{2\Delta x} \quad (5.78)$$

$$\begin{aligned} h_i^{j+1} = & 0.5(h_{i+1}^j + h_{i-1}^j) - \frac{\Delta t \alpha \beta}{2\Delta x} h_{ij}^{\beta-1} (h_{i+1}^j - h_{i-1}^j) \\ & - \frac{p}{\left(1 - \sum_{k=1}^N c_i^j\right)} \left[\sum_{k=1}^N z_i^{j+1} - 0.5 \left(\sum_{k=1}^N z_{i+1}^j + \sum_{k=1}^N z_{i-1}^j \right) \right] \\ & + \frac{h_i^j}{\left(1 - \sum_{k=1}^N c_i^j\right)} \left[\sum_{k=1}^N c_i^{j+1} - 0.5 \left(\sum_{k=1}^N c_{i+1}^j + \sum_{k=1}^N c_{i-1}^j \right) \right] \\ & + \frac{\Delta t \alpha}{2\Delta x} \frac{h_{ij}^\beta}{\left(1 - \sum_{k=1}^N c_i^j\right)} \left(\sum_{k=1}^N c_{i+1}^j - \sum_{k=1}^N c_{i-1}^j \right) + \frac{q_{1w} \Delta t}{\left(1 - \sum_{k=1}^N c_i^j\right)} \end{aligned} \quad (5.79)$$

$$\begin{aligned}
c_{i\ k}^{j+1} &= 0.5((c_{i+1}^j)_k + (c_{i-1}^j)_k) - \frac{\Delta t \alpha}{2\Delta x} h_{ij}^{\beta-1} ((c_{i+1}^j)_k - (c_{i-1}^j)_k) \\
&- \frac{(c_i^j)_k}{h_i^j} [h_i^{j+1} - 0.5(h_{i+1}^j + h_{i-1}^j)] \\
&- \frac{\Delta t \alpha \beta}{2\Delta x} (c_i^j)_k h_{ij}^{\beta-2} (h_{i+1}^j - h_{i-1}^j) \\
&+ \frac{q_{1sus} \Delta t}{h_i^j} + \frac{\Delta t}{(\rho_s)_k h_i^j} [(E_z^{ij})_k - (D_c^{ij})_k]
\end{aligned} \tag{5.80}$$

$$\begin{aligned}
z_{i\ k}^{j+1} &= 0.5((z_{i+1}^j)_k + (z_{i-1}^j)_k) - \frac{\Delta t (v_s)_k}{2\Delta x} \left(1 - \frac{2(z_i^j)_k}{(z_{max})_k} \right) ((z_{i+1}^j)_k - (z_{i-1}^j)_k) \\
&+ \frac{q_{1sus} \Delta t}{(1-p_k)} + \frac{\Delta t}{(\rho_s)_k (1-p_k)} [(D_c^{ij})_k - (E_z^{ij})_k]
\end{aligned} \tag{5.81}$$

By using the presented algorithm, the unknown values of h and z at the new time level $j+1$ (future time) are determined from every interior node ($i = 2, \dots, N-1$). The values of the dependent variables h and z at the boundary nodes 1 and $N+1$ are determined by using boundary conditions. Also, at the time level $j=1$, initial conditions are already known.

Initial and boundary conditions were specified before Equations 5.18 – 5.23. And for stability the Courant – Friedrichs – Lewy (CFL) condition was used.

Equations 5.49, 5.50 and 5.51 are solved simultaneously for each time step.

5.3.1.2. Model Application

The channel assumed as a flume has 20 m length and 1 m width with 0.0005 bed slope. The model parameters basically are as follows: $C_z, p, S_o, z_{max}, \rho_s, \gamma_s, \sigma, \Phi, \phi, k, \kappa, CSF, P$ and d_s . Parameters ρ_s, γ_s , and d_s can be obtained from experimental sediment data. Chezy roughness coefficient is assumed to be $C_z = 50m^{0.5}/s$. It is assumed that there are four different sediment types in the sediment column. Sediment characteristics that used in the model are summarized in Table 5.4.

Table 5.4. Sediment Characteristics

type	ρ_s (kg/m ³)	d_s (mm)	p
1	2700	0.5	0.40
2	2650	0.7	0.45
3	2600	0.9	0.55
4	2500	1.2	0.60

Maximum concentration $C_{\max} = 500 \text{ kg} / \text{m}^2$ was assumed for each particle sizes (note that $z_{\max} = C_{\max} / (1 - p)\rho_s$). Gessler (1965) suggested a value of 0.047 for κ for most flow conditions. The value of transfer rate can be calculated in flumes by $\sigma = 1/(7h)$, where h is flow depth, parameter Φ has a range of 0.0 – 1.0 and exponent k_i has a range of 1.0 – 2.5 in literature (Foster 1982, Tayfur 2002, Yang 1996). The inflow hydrograph and inflow concentration were given in Figure 5.25 for upstream boundary conditions.

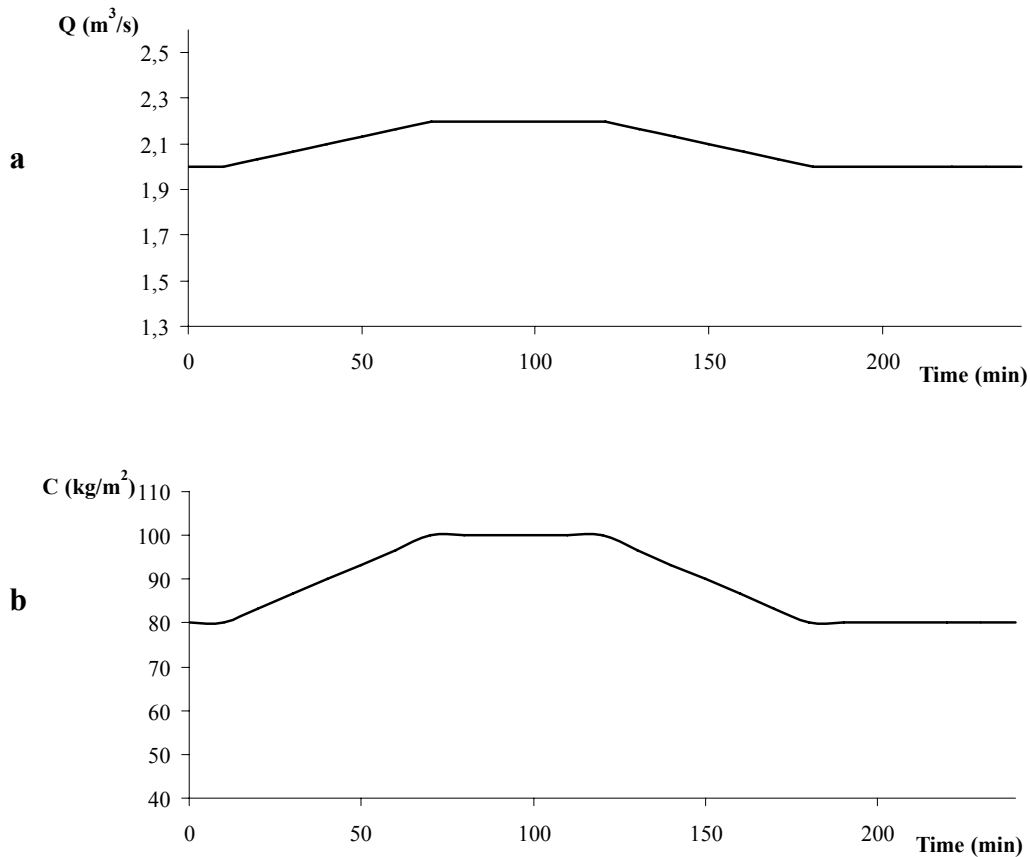


Figure 5.25 (a) Inflow hydrograph. (b) Inflow concentration

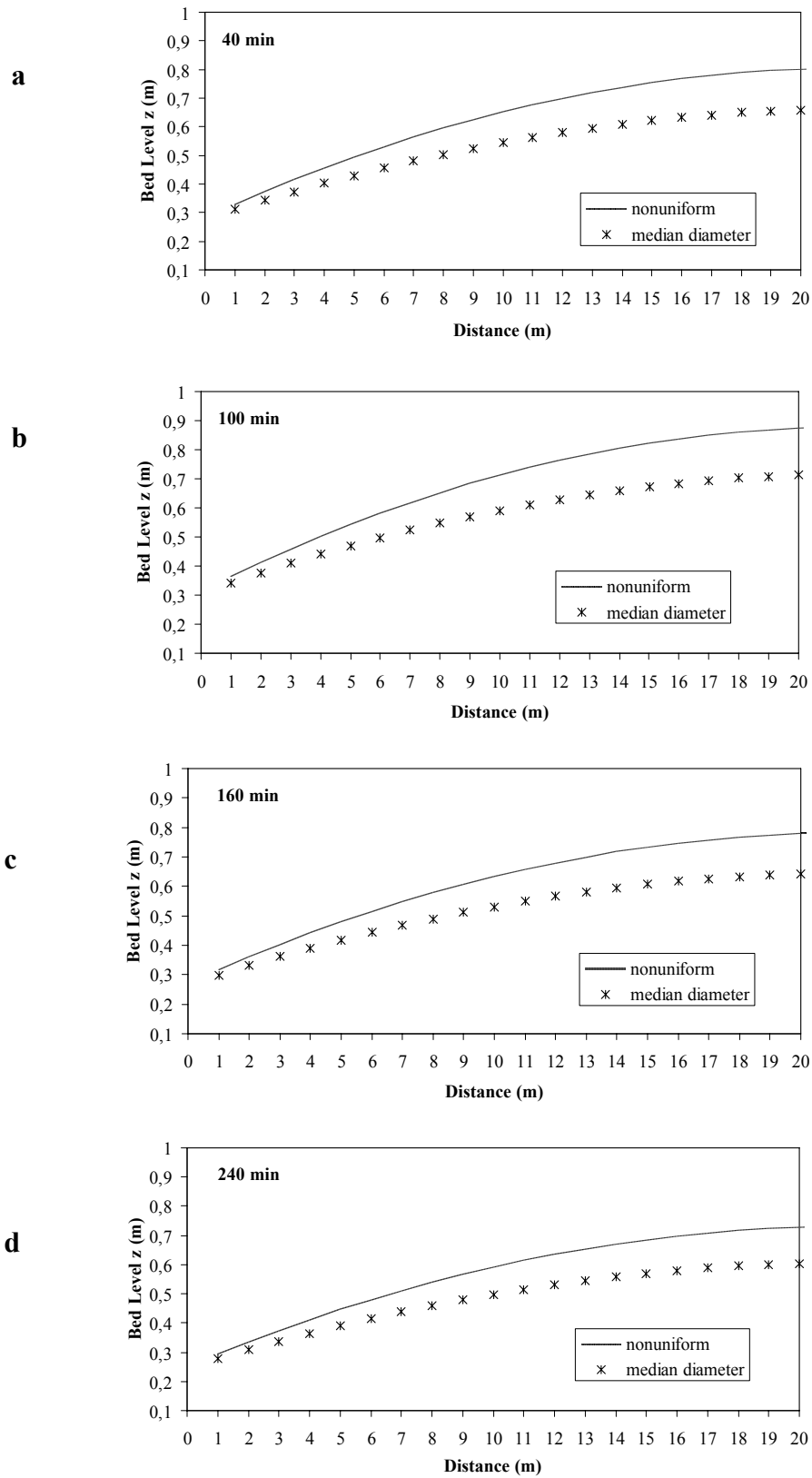


Figure 5.26. Transient bed profiles of nonuniform sediment and uniform sediment model at (a) rising period (b) equilibrium period (c) recession period (d) post recession period of inflow hydrograph and concentration in unsteady flow conditions

Simulations were significantly under d_{50} (median diameter) and nonuniform mixture for all the periods of the simulations. Under d_{50} (median diameter) conditions, bed levels were lower than nonuniform flow case (Figure 5.26).

In another simulation for the same flume we considered constant inflow hydrograph with $Q = 1.2m^3/s$ and the same inflow sedimentograph seen in Figure 5.25.b. The simulations for the case are presented in Figure 5.27. While nonuniform and uniform sediment transport model give similar performance under steady flow condition, give different performance under unsteady flow conditions (Figure 5.27).

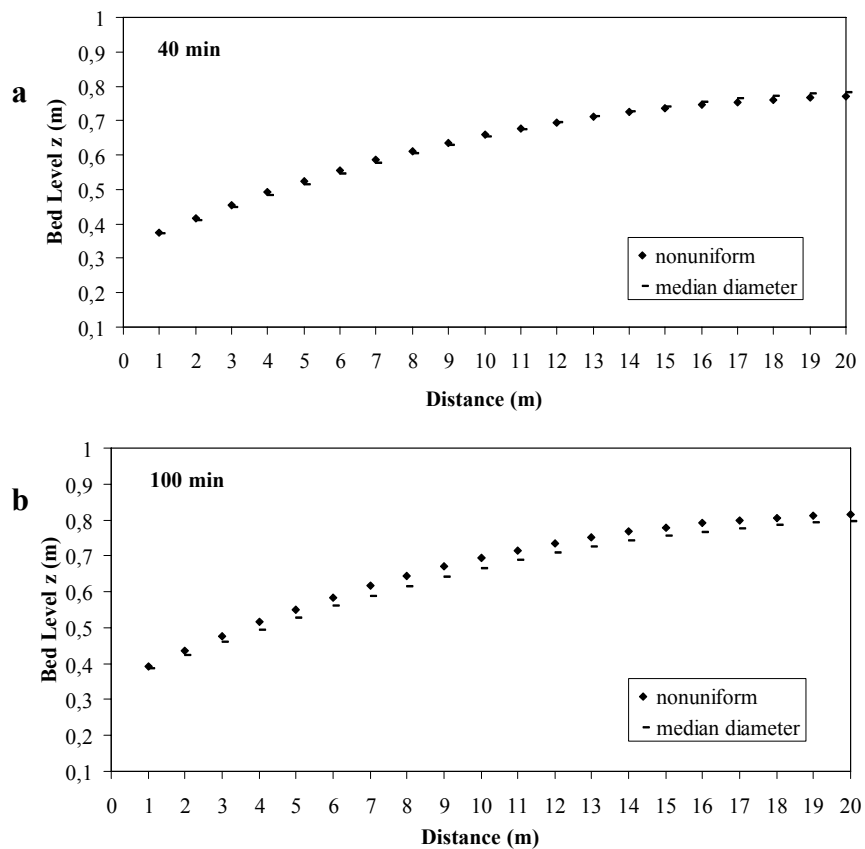


Figure 5.27. Transient bed profiles of nonuniform sediment and uniform sediment model at (a) rising period (b) equilibrium period (c) recession period (d) post recession period of inflow hydrograph and concentration in steady flow conditions

(cont. on next page)

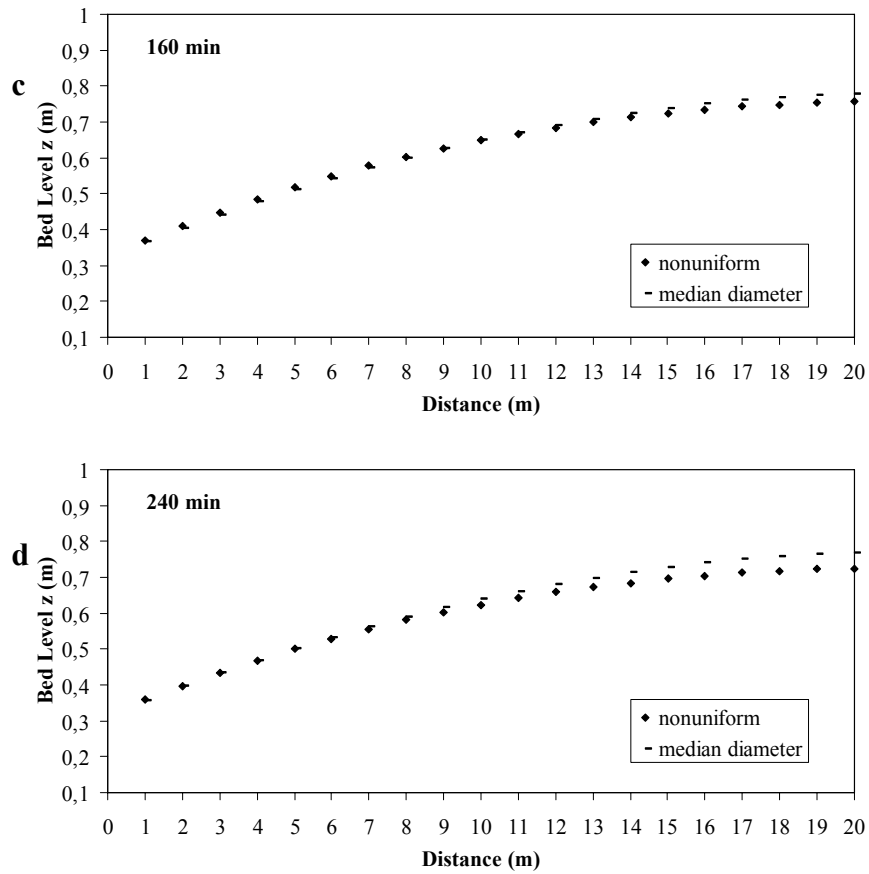


Figure 5.27. (cont.) Transient bed profiles of nonuniform sediment and uniform sediment model at (a) rising period (b) equilibrium period (c) recession period (d) post recession period of inflow hydrograph and concentration in steady flow conditions

CHAPTER 6

SUMMARY AND CONCLUSION

6.1. Summary

Three mathematical and numerical models have been developed under kinematic, diffusion and dynamic wave approaches for simulating bed profiles in alluvial channels under unsteady and equilibrium conditions. Transient bed profiles are also simulated for several hypothetical cases, comparing different particle velocities and different particle fall velocities. The model tested with flume experiments. Also different wave models (kinematic, diffusion and dynamic) were compared. The kinematic wave model was developed for simulating transient bed profiles in alluvial channels under unsteady and nonequilibrium conditions and tested against experimental data. The diffusion wave model was developed for simulating transient bed profiles in alluvial channels under unsteady, nonuniform and nonequilibrium conditions.

6.2. Conclusion

1. Numerical model is able to capture the effects of suspended sediment and bed load sediment on the transport. When the transport capacity is greater than the suspended load, deposition occurs, otherwise detachment occurs. The model is able to capture this phenomenon.
2. The application of the developed model to hypothetical cases revealed that the model is able to capture the behavior of the process in alluvial channels.
3. Modeling the process under nonequilibrium conditions give different results than those under equilibrium conditions. Therefore, if the flow conditions in nonequilibrium, it should be so modeled.
4. The model was not tested against experimental data under unsteady and nonequilibrium flow and sediment loadings. The next aim is to test the model for that general case.

5. The selected on particle velocity, particle fall velocity and hydrodynamic wave (kinematic, diffusion and dynamic) would be better decided with testing of the model with the general case (unsteady, nonequilibrium) experimental data.
6. Another shortcoming is the application of the model is field conditions. This is able one of the future plans.
7. The investigation of different particle velocity formulations revealed that under the same flow conditions, wave front is faster in Kalinske and Bridge and Dominic's formulation.
8. The investigation of different particle fall velocity formulations revealed that under the same flow conditions, they produced nearly the same results.
9. The investigation of the effect of z_{\max} (maximum bed level) on the transport revealed that it is an important parameter. It significantly affects the wavefront speed and bed level. The higher the z_{\max} , the faster the wavefront and the higher the bed level.
10. The numerical investigation of different sediment flux (bed load) formulations revealed that under the same transport flow condition, the kinematic wave theory produced different results than Meyer – Peter and Schoklists. Meyer – Peter and Schoklists produced nearly the same profiles. Under kinematic wave theory, the wavefronts move faster.
11. The numerical comparison of kinematic, diffusion and dynamic wave for hypothetical cases of sediment transport revealed under the same sediment flux function of the wavefront is slower in the case of kinematic wave.
12. The hydrodynamic part the developed numerical model was tested successfully tested experimental flume data. It satisfactorily (less than 5%) simulated the measured data.
13. The developed numerical model was tested against measured sediment data from the literature. It predicted measured bed levels satisfactorily.
14. The numerical model revealed that modeling sediment mixtures with only mean particle diameter d_{50} approximation might lead to misleading results. In other words, it's better model with the mixture with corresponding particle characteristics i.e. d_{50} (median diameter), ρ_s (density) and p (porosity).

REFERENCES

- Ackers, P. and White, W. R. 1973. Sediment Transport: New Approach and Analysis. *Journal of the Hydraulics Division, ASCE* 99: 2041-2060.
- Al-Khafif, S. M. 1965. Study of open channels degradation and corresponding bed roughness. *University of California. Thesis of PhD.*
- Bagnold, R. A. 1966. An approach to the sediment transport problem from general physics. *Geological survey prof. paper 422-I*. Washington. D.C.
- Begin, Z. B., Meyer, D. F. and Schumm, S. A. 1981. Development of longitudinal profiles of alluvial channels in response to base-level lowering. *Earth Surface Processes and Land Forms* 6(1): 49-68.
- Bhallamudi, S. M. and Chaudhry, M. H. 1989. Numerical Modeling of Aggradation and Degradation in Alluvial Rivers. *Journal of Hydraulic Engineering* 117(9).
- Bhamidipaty, S. and Shen, W. H. 1971. Laboratory Study of Degradation and Aggradation. *Journal of Waterways, Harbors and Coastal Engineering Division* 97: 615- 630.
- Blumberg, A. and Mellor, G. L. 1987. A description of A three-dimensional Coastal Ocean Circulation Model. *In Three-Dimensional Coastal Ocean Models*. American Geophysical Union, N. S. Heaps (Ed.), 1-16, Washington, DC.
- Boer, S., DeVriend, H. J. and Wind, H. G. 1984. A Mathematical Model for the Simulation of Morphological Processes in the Coastal Area. *Proc. 19th ICCE, Houston, USA*: 1437-1453.
- Bor, Asli, Tayfur, G. and Elçi, Ş. 2008. Parçacık Hızı ve Düşüm Hızının Katı Madde Taşınımına Etkisinin Kinematik Dalga Yaklaşımı ile Modellenmesi. *Havza Kirliliği Konferansı*. DSİ II. Bölge Müdürlüğü, Gümüşdüz, 2008, İzmir: 89-96.
- Bor, A., Elçi, Ş. and Çalışkan A. 2008. Prediction of Sedimentation in Reservoirs by Acoustic Methods. *River Flow International Conference on Fluvial Hydraulics, Cesme, Izmir, Turkey*. River flow 2008, 2: 1251-1260.
- Bridge, J. S. and Dominic, D. F. 1984. Bed Load Grain Velocities and Sediment Transport Rates. *Water Resources Res.* 20(4): 476-490.
- Cao, Z. and Egiashira, S. 1999. Coupled Mathematical Modelling of Alluvial Rivers. *Journal of Hydraulic Engineering* 17(2): 71-85.
- Cao, Z., Day, R. and Egiashira, S. 2001. Coupled and Decoupled Numerical Modelling of Flow and Morphological Evolution in Alluvial Rivers. *Journal of Hydraulic Engineering, ASCE* 128(3): 306-321.

- Cao, Z. and Carling, P. A. 2003. On evolution of bed material waves in alluvial rivers, *Earth Surf. Processes Landforms* 28: 437-441.
- Capart, H. 2000. Dam break induced geomorphic flows and the transition from solid to fluid like behavior across evolving interfaces. *Catholic University. Thesis of PhD.*
- Capart, H. and Young, D. L. 2002. Two Layer Shallow Water Computation of Torrential Geomorphic Flows. *River Flow International Conference on Fluvial Hydraulics*, Louvain-la-Neuve, Belgium, River flow 2002, 2: 1003.
- Casulli, V. 1990. Semi-Implicit Finite Difference Methods for the Two-dimensional Shallow Water Equations. *J. Comput. Phys.* 86: 56-74.
- Chang, F. M., Simons, D. B. and Richardson, E. V. 1965. Total Bed-Material Discharge in Alluvial Channels. *U.S. Geological Survey Water-Supply* I: 1498.
- Chang, H. H. 1982. Mathematical Model for Erodible Channels. *J. Hydraul. Div. Am. Soc. Civ. Eng.* 108(5): 678-689.
- Chaudhry, M. H. 1993. *Open – Channel Flow*. New Jersey: Prentice Hall, Englewood Cliffs, 07632.
- Chaudhry, M. H. 1996. *Principles of flow of water*. Chapter 2 in Handbook of Water Resources. L.Mays (ed.). McGraw-Hill.
- Chien, H. H. and Wan, Z. H. 1999. *Mechanics of Sediment Transport*. Am. Soc. of Civ. Eng. Reston, Va.
- Ching, H. H. and Cheng, C. P. 1964. Study of River Bed Degradation and Aggradation by The Method of Characteristics. *Journal of Hydraulic Engineering* 5: 41.
- Colby, B. R. and Hembree, C. H. 1955. Computation of total sediment discharge, Niobrara River near Cody, Nebraska. *Supply Paper 1357*. U.S. Geological Survey, Water. Washington, D.C.
- Collins, W., Gregory, R., Anderson, J. 1996. A digital approach to seabed classification. *Sea Technology* 37(8): 83–87.
- Correia, L., Krishnappan, B. G. and Graf, W. H. 1992. Fully Couplad Unsteady Mobile Boundary Flow Model (FCM). *Journal of Hydraulic Engineering* 118(3): 476-494.
- Cui, Y., Parker, G. and Paola, C. 1996. Numerical Simulation of Aggradation and Downstream Fining. *Journal of Hydraulic Res.* 34(2): 195-204.
- Cunge, J. A., Holly, F. M. and Verwey, A. 1980. *Practical Aspects of Computational River Hydraulics*. Pitman, USA.

- Cunge, J.A. and Verwey, N. 1973. Mobile bed fluvial mathematical models. *La Houille Blanch.* 7: 561-580.
- Curran, J. C. and Wilcock, P. R. 2005. Effect of Sand Supply on Transport Rates in a Gravel-bed Channel. *Journal of Hydraulic Engineering* 131(11): 961 – 967.
- Demuren, A. O. and Rodi, W. 1986. Calculation of Flow and Pollutant Dispersion in Meandering Channels. *Journal of fluid mechanics* 172: 63-92, Cambridge, U.K.
- de Vries, M. 1965. Consideration About Non – Steady Bed Load Transport in Open Channels. *XI Congress, Int Assoc. of Hydraul. Eng. and Res.* St. Petersburg, Russia.
- de Vries, M. 1973. River Bed Variation – Aggradation and Degradation. *Publ. 107, Delft Hydraulic Lab.* Delft, Netherlands.
- de Vries, M. 1975. A Morphological Time Scale for Rivers. *XVI Congress, Int Assoc. of Hydraul. Eng. and Res.* Sao Paulo, Brazil.
- DHI Inc. 2003. MIKE21 user guide. <http://www.dhisoftware.com/> 301 South State Street, Newtown, PA, 18940, USA.
- Di Cristo, C., Leopardi, A. and Greco, M. 2002. A Bed-Load Transport Model for Non-Uniform Flows. *River Flow International Conference on Fluvial Hydraulics*, Louvain-la-Neuve, Belgium. *River flow 2002*, 2: 859.
- Dietrich, W. E. 1982. Settling Velocity of Natural Particles. *Water Resources Res.* 18(6): 1615-1626.
- Dubois, M. P. 1879. Le Rhone et les Rivieres a Lit affouillable. *Annales de Ponts et Chaussée*, sec. 5, 18: 141-195.
- Dyer, K. 1986. *Coastal and Estuarine Sediment Dynamics*. John Wiley & Sons, Inc., New York.
- ECOMSED 2002. *Users Manual*. HydroQual Inc. Mahwah N.J.
- Einstein, H. A. 1950. The Bed Load Function for Sediment Transportation in Open Channel Flows. *Technical Bulletin no. 1026*, U.S. Department of Agriculture. Washington, D.C.
- Engelund, F. and Hansen, E. 1972. *A Monograph on Sediment Transport in Alluvial Streams*. Teknisk Forlag. Copenhagen.
- Foster, G. R. 1982. *Modelling the erosion process in hydraulic modeling of small Watersheds*. edited by C. T. Haan, H. P. Johnson, and D. L. Brakensiek. Am. Soc. of Agric. Eng. St. Joseph. Mich.

- Gessler, J. 1965. *The beginning of bed – load movement of mixtures investigated as natural armoring in channels*. W. M. Keck Lab. of Hydraul. and Water Resour. Calif. Inst. of Tech. Pasedana, California.
- Gill, M. A. 1983a. Diffusion Model for Aggrading Channels. *Journal of Hydraulic Research, IAHR* 21(5): 355-367.
- Gill, M. A. 1983b. Diffusion Model for Degrading Channels. *Journal of Hydraulic Research, IAHR* 21(5): 21:369-378.
- Gill, M. A. 1987. Nonlinear Solution of Aggradation and Degradation in Channels. *Journal of Hydraulic Research* 25(5), 537-547.
- Guy, H.P., Simons, D.B., Richardson, E.V. 1966. Summary of alluvial channel data from flume experiments. *Professional Paper 462-I*. United States Geological Society, Washington, D.C.
- Güney, M. Ş. and Bombar, G. 2008. TÜBİTAK Araştırma Projesi Gelişme Raporu. Proje no. 106M274, Rapor no. 4, Rapor dönem no. 4.
- Hamrick, J.M. 1996. Users manual for the environmental fluid dynamic computer code. *Virginia Institute of Marine Science*. Special Report 328, 224.
- Hayter, E. j., Bergs, M. A., Gu, R., McCutcheon, S., Simth, S. J. and Whiteley, H. J. 1995. *HSCTM- 2D*. A finite element model for depth averaged hydrodynamics, sediment and contaminant transport.
- Higginbottom, I., Hundley, A., Pauly, T. 1994. A Desktop Study of Some Acoustic Seabed Classification Systems. *Unpublished report by Sonar Data Tasmania/Offshore Scientific Pty Ltd*. 21.
- Holly, Jr., F. M. and Rahuel, J. L. 1990a. New Numerical/Physical Framework for Mobile-Bed Modeling, Part I: Numerical and Physical Principles. *Journal of Hydraulic Engineering* 28(4): 401-416.
- Holly, Jr., F. M. and Rahuel, J. L. 1990b. New Numerical/Physical Framework for Mobile-Bed Modeling, Part II: Test Applications. *Journal of Hydraulic Engineering* 28(4): 545-564.
- Holly, Jr., F. M. Yang, J. C., Schwarz, P., Schaefer, J., Hsu, S. H. and Einhelling, R. 1993. Numerical Simulation of Unsteady Water and Sediment Movement in Multiply Connected Networks of Mobile Bed Channels. *IIHR report no. 343*, Iowa Institute of Hydraulic Research. The University of Iowa, Iowa City, Iowa.
- Hotchkiss, R. H., and Parker, G. 1991. Shock fitting of aggradational profiles due to backwater. *Journal of Hydraulic Engineering* 117(9): 1129-1144.
- Jain, S. C. 1985. River Bed Aggradation due to Increase in Sediment Load. *Pre-workshop Proc. of 2nd International Workshop on Alluvial Problems*. University of Roorkee. Roorkee, India.

- Jaramillo, W. F. Torres 1983. Aggradation and degradation of alluvial-channel beds. *University of Iowa. Thesis of PhD.*
- Jaramillo, W. F. and Jain, S. C. 1984. Aggradation and Degradation of Alluvial-Channel Beds. *Journal of Hydraulic Engineering, ASCE* 110(8): 1072-1085.
- Kalinske, A. A. 1947. Movement of Sediment as Bed-Load in Rivers. *Transactions of The American Geophysical Union* no:4.
- Kassem, A. and Chaudhry, M. H. 1998. Comparison of Coupled and Semicoupled Numerical Models for Alluvial Channels. *Journal of Hydraulic Engineering, ASCE* 124(8): 794-802.
- Kazezyilmaz, C. M. and Medina, M. A. 2007. Kinematic and Diffusion Waves: Analytical and Numerical Solutions to Overland and Channel Flow. *J. Hydrologic Eng. No.2.*
- Krishnappan, B. G. 1985. Modeling of Unsteady Flows in Alluvial Streams. *Journal of Hydraulic Engineering, ASCE* 111(2).
- Lane, E. W. 1947. Report of the subcommittee on sediment terminology. *Trans., Amer. Soc. Civil Engineers* 119:1069-79.
- Lane, E. W. and Borland, W. M. 1954. River Bed Scour during Floods. *Transactions of the American Geophysical Union* 28(6): 936-938.
- Lane, E. W. and Kalinske, A. A. 1941. Engineering Calculations of Suspended Sediment. *Transactions of the American Geophysical Union* 20(3): 603-607.
- Langbein, W. B. and Leopold, L. B. 1968. River channel bars and dunes – Theory of kinematic waves. *Geological survey prof. paper 422-L.* Washington. D.C.
- Langendoen, E. J. 1996. Discretion diffusiveiffusive wave model. *Technical Report No. CCHE-TR-96-1.* Center for Computational Hydroscience and Engineering. The University of Mississippi, University, Miss.
- Laursen, E. M. 1958. The Total Sediment Load of Streams. *Journal of Hydraulics Division. ASCE* 84(1): 1530-1-1530-36.
- Lax, P. D. 1954. *Weak solutions of Nonlinear Hyperbolic Equations and Their Numerical Computation.* Commun. Pure crnd Appl. Math. 7, 159.
- Leopold, L. B. and Maddock, T. 1953. The hydraulic geometry of stream channels and some physiographic implications. *Geological survey prof. paper.* Washington. D.C. 252.
- Li, S. S. and Millar, R. G. 2007. Simulating Bed-Load Transport in A Complex Gravel-Bed River. *Journal of Hydraulic Engineering* 133(3): 323-328.

- Lin, B. L. and Falconer, R. A. 1996. Numerical Modelling of Three Dimensional Suspended Sediment for Estuaries and Coastal Waters. *Journal of Hydraulic Research, Delft*. The Netherlands 34(4): 435-456.
- Lisle, T. E., Pizzuto, J. E., Ikeda, H., Iseya, F., and Kodama, Y. 1997. Evolution of a sediment wave in an experimental channel. *Water Resources Research* 33: 1971 – 1981.
- Lisle, T. E., Cui, Y. T., Parker, G., Pizzuto, J. E. and A. Dodd, A. M. 2001. The dominance of disperssion in the evolution of bed material waves in gravel-bed rivers. *Earth Surf. Processes Landforms* 26: 1409 – 1420.
- Little, W. C. and Mayer, P. G. 1972. *The role of sediment gradation on channel armoring*. School of Civil Eng. In Cooperation With Environmental Resources Center. Georgia Inst. of Tech., ERC-0672: Atlanta, Ga.
- Lyn, D. A. and Altinakar, M. 2002. St-Venant Exner Equations for Near-Critical and Transcritical Flows. *Journal of Hydraulic Engineering* 128(6): 579-587.
- Lyn, D. A. and Goodwin, P. 1987. Stability of A general Preissmann Scheme. *Journal of Hydraulic Engineering* 117(1): 16-28.
- Mahmood, K. 1987. *Reservoir Sedimentation: Impact, Extent and Mitigation*. Technical Paper Number 71, The World Bank, Washington D.C.
- Manual on Sediment Management and Measurement. 2003. *World Meteorological Organization Operational Hydrology*. Report No. 47.
- McAnally, Jr., W. H., Heltzel, S. B. and Donnell, B. P. 1991. *The Atchafalaya River Delta; Report 1, A Plan for Predicting the Evolution of Atchafalaya Bay, Louisiana*. Technical Report HL-82-15. US Army Engineer Waterways Experiment Station. Vicksburg, MS.
- Mehta, P. J. 1980. Study of aggradation in alluvial streams. *University of Roorkee, Roorkee. Thesis of PhD*.
- Meyer-Peter, E., Favre, H. and Einstein, A. 1934. Neuere Versuchsergebnisse über den Geschiebetrieb. *Schweiz Bauzeitung* 103(13).
- Meyer-Peter, E. and Müller, R. 1948. Formulas for Bed-Load Transport. *International Association of Hydraulic Research. IAHR. 2nd meeting*. Stockholm, Sweden.
- Minh Duc, B., Wenka, T. and Rodi, W. 2004. Numerical Modeling of Bed Deformation in Laboratory Channels. *Journal of Hydraulic Engineering* 130 (9): 894-904.
- Mohammadian, A., Tajrishi, M. and Azad, F. L. 2004. Two-dimensional numerical simulation of flow and geo-morphological processes near headlands by using unstructured grid. *Int. J. Sediment Res.* 19(4): 258-277.

- Mohapatra, P. K. and Bhallamudi, S. M. 1994. Leel Variation in Channel Expansions with Movable Beds. *Journal of Irrigation and Drainage Engineering, ASCE* 120(6): 1114 – 1121.
- Mosconi, C. E. 1988. River bed variations and evolution of armor layers. *The University of Iowa. Thesis of PhD.*
- Newton, C. T. 1951. *An experimental investigation of bed degradation in an open channel.* Boston Society of Civil Engineers, Boston.
- Odhiambo, B.K. and Boss, S.K. 2004. Integrated Echo Sounder, Gps, and Gis for Reservoir Sedimentation studies: Examples from Two Arkansas Lakes. *Journal of the American Water Resources Association, Paper no: 02061.*
- Park, I. and Jain, S. C. 1986. River-Bed Profiles with Imposed Sediment Load. *Journal of Hydraulic Engineering, ASCE* 112(4).
- Parker, G., Klingeman, P. C. and McLean, D. G. 1982. Bed Load and Size Distribution in Paved Gravel-Bed Streams. *Journal of Hydraulics Division, ASCE* 108(HY4): 544-571.
- Perdreau, N. and Cunge, J. A. 1971. Sedimentation dans les Estuaires et les Embouchures Bouchon Marin et Bouche on Fluvial. *Proc. 14th Congress IAHR, Paris.*
- Pianese, D. 1994. Comparison of different mathematical models for river dynamics analysis. *International Workshop on Floods and Inundations related to Large Earth Movements, Int. Assoc. of Hyraul. Eng. and Res. Trento, Italy. 4-7 Oct.*
- Prandtl, L. 1926. Uber die Ausgebildete Turbulenz. *Proceedings of the Second International Congress of Applied Mechanics. Zurich.*
- Rahuel, J.L. and Holly, F. M. 1989. Modeling of River Bed Evolution for Bed Load Sediment Mixtures. *Journal of Hydraulic Engineering, ASCE* 115(11): 1521-1542.
- Ribberink, J. S. and Van Der Sande, J. T. M. 1985. Aggradation in rivers due to overloading: Analytical approaches. *Journal of Hydraulic Engineering* 23(3): 273 – 283.
- Roberson, J.A., Cassidy, J. J. and Chaudhry, M. H. 1997. *Hydraulic Engineering. 2nd Edition: John Wiley and Sons, Inc. New York, NY.*
- Rottner, J. 1959. A Formula for Bed-Load Transportation. *LaHouille Blanche* 14(3): 285-307.
- Rouse, H. 1937. Modern Conceptions of the Mechanics of Turbulence. *Transact,ons of the ACSE* 102.
- Rouse, H. 1938. *Fluid Mechanics for Hydraulic Engineers.* NewYork: Dover.

- Schlichting, H. 1955. *Boundary Layer Theory*. New York: McGraw-Hill.
- Schoklitsch, A. 1934. Der Geschiebetrieb und die Geschiebefracht. *Wasserkraft und Wasserwirtschaft* 29(4): 37-43.
- Schoklitsch, A. 1949. Berechnung der Geschiebefracht. *Wasser und Energiewirtschaft*. Nr.1.
- Schulz, E. F., Wilde, R. H. and Albertson, M. L. 1954. Influence of Shape on the Fall Velocity of Sediment Particles. *MRD Sediment Series*. No:5.
- Shields, A. 1936. *Application of Similarity Principles and Turbulence Research to Bed-Load Movement*. California Institute of Technology. Pasadena.
- Shimizu, Y. and Itakura, T. 1989. Calculation of Bed Variation in Alluvial Channels. *Journal of Hydraulic Engineering, ASCE* 115(3): 367-384.
- Simons, D. B. and Richardson, E. V. 1966. Resistance to Flow in Alluvial Channels. *U.S. Geological Survey Professional*. 422-j.
- Singh, T., Beerenwinkel, N. and Lengauer, T. 2004. Learning Mixtures of Localized Rules by Maximizing The Area under the ROC Curve. *Proceedings of the 1st International Workshop on ROC Analysis in Artificial Intelligence*. Valencia, Spain. 89–96.
- Singh, V. 2005. Two dimensional sediment transport model using parallel computers. *B.Tech., Banaras Hindu University. Thesis of MSc.*
- Soni, J. P., Garde, G. J. and Raju, K. G. 1980. Aggradation in Streams due to Overloading. *J. Hydrol. Division. Proc. Amer. Soc. Civil Eng.* 106(1) :117-32.
- Soni, J.P. 1981a. Laboratory Study of Aggradation in Alluvial Channels. *Journal of Hydrology* 49: 87-106.
- Soni, J. P. 1981b. An Error Function Solution of Sediment Transport in Aggradation Channels. *Journal of Hydraulic Engineering* 49: 107 – 119.
- Soni, J. P. 1981c. Unsteady Sediment Transport Law and Prediction of Aggradation Parameters. *Journal of the American Water Resources Association* 17(1): 33 – 40.
- Spasojevic, M. and Holly, F.M. 1990. MOBED2 - Numerical Simulation of wo-Dimensional Mobile-Bed Processes. *IIHR Report No.344*. IowaInstitute of Hydraulic Research. The University of Iowa, Iowa City, Iowa,USA, October.
- Stokes, G. G. 1851. On the Effect of the Internal Friction of Fluids on the Motion of Pendulums. *Transactions of the Cambridge Philosophical Society* 9(2): 8-106.
- Straub, L. G. 1935. Missouri River Report. *In-House Document 238, 73rd Congress, 2nd Session*. U.S. Government Printing Office. Washington, D. C. p.1135.

- Strickler, A. 1923. *Beitrage zur Frage der Geschwindigkeitsformel und der Rauheitszahlen für Ströme Kanäle und Geschlossene Leitungen*. Mitteilungen des Eidgenössischen Amtes für Wasserwirtschaft. Bern.
- Struiksma, N., Oleson, K. W., Flokstra, C. and De vriend, H. J. 1985. Bed Deformation in Curved Alluvial Channels. *Journal of Hydraulic Research* 23(1).
- Suryanarayana, B. 1969. Mechanics of degradation and aggradation in laboratory flume. *Ph.D. Thesis*, Colorado State University, Ft. Collins Colorado.
- Tang, X. and Knight, D. W. 2006. Sediment Transport in River Models with Overbank Flows. *Journal of Hydraulic Engineering* 132(1): 77-86.
- Tayfur, G. 2002. Applicability of Sediment Transport Capacity Models for Nonsteady State Erosion from Steep Slopes. *J. Hydrologic Eng.* 7(3).
- Tayfur, G. and Singh, V. P. 2006. Kinematic Wave Model of Bed Profiles in Alluvial Channels. *Water Resour. Res.* 42: W06414.
- Tayfur, G., and Singh, V. P. 2007. Kinematic Wave Model For Transient Bed Profiles In Alluvial Channels Under Nonequilibrium Conditions. *Water Resour. Res.* 143: W12412.
- Thomas, W. A., McAnally, W. H., Jr. 1990. *User's Manual for the Generalized Computer Program Systems for Open Channel Flow and Sedimentation: TABS-2 system*. US Army Corps of Engineers, Waterways Experiment Station, Hydraulics Laboratory, Vicksburg, MS.
- Tinney, E. R. 1955. A study of the mechanics of degradation of a bed of uniform sediment in an open channel. *University of Minnesota. Thesis of PhD.*
- Tsai, C. W. 2003. Applicability of Kinematic, Noninertia and Quasi-steady Dynamic Wave Models to Unsteady flow Routing. *J. Hydrologic Eng.* 60(1-4): 43-58.
- Urick, R. J. 1983. *Principles of Underwater Sound*. Peninsula Publishing, Los Altos.
- USACE 2008. US Army Corps of Engineers. <http://www.usace.army.mil>.
- Van, R. 1987. Mathematical Modeling of Morphological Processes in The Case of Suspended Sediment Transport. *Delft hydr. Communication no. 382*.
- Vanoni, V. A. 1971. Sedimentation Engineering. *ASCE Task Committee for the Preparation of The Manual on Sedimentation of The Sedimentation Committee of The Hydraulics Division*.
- Vanoni, V. A. 1975. Sediment transport mechanics, H. sediment discharge formulas. *Journal of the Hydraulics Division*. ASCE 97: 523.
- Velikanov, M. A. 1954. Gravitational theory of sediment transport. *J. Sci. Soviet Union*, 4.

- Vreugdenhill, C. B. and de Vries, M. 1973. Analytical approaches to on-steady bedload transport. *Delft Hydraul. Lab. Delft, Netherlands*. 78(IV): 16.
- Wang, Z. Y. and Adeff, S. E. 1986. Three Dimensional Modelling of River Sedimentation Processes. *Proceeding 3rd International symposium on river sedimentation*. University of Mississippi.
- Wathen, S. J., and Hoey, T. B. 1998. Morphological controls on the downstream passage of a sediment wave in a gravel bed stream. *Earth Surf. Process Landforms* 23: 715-730.
- Wilcock, P. R. and Southard, J. B. 1989. Bed Load Transport of Mixed Size Sediment: Fractional Transport Rates, Bed forms and the Development of a Course Bed Surface Layer. *Journal of the American Water Resources Association* 25(7): 1629-1641.
- Wilcock, P. R., Kenworthy, S. T. and Crowe, J. C. 2001. Experimental Study of The Transport of Mixed Sand and Gravel. *Journal of the American Water Resources Association* 37(12): 3349-3358.
- WL|Delft Hydraulics. 2002. Grensproject Bovenrijn/Grenzprojekt Niederrhein – Investigation of Individual Engineering Measures with 2D Morphological Model I. *WL Project Rep. Q2496. Delft Hydraulics Laboratory. July*. Delft, Netherlands.
- Wu, W., Rodi, W. and Wenka, T. 2000. 3-D Numerical Modeling of Water Flow and Sediment Transport in Open Channels. *Journal of Hydraulic Engineering* 126(1): 4 – 15.
- Wu, W. 2001. CCHE2D-2.1, Sediment Transport model. Technical report no. NCCHE-TR-2001-3. *National Center for Computational Hydroscience and Engineering*. The University of Mississippi.
- Wu, W. 2004. Depth-Averaged 2-D Numerical Modeling of Unsteady Flow and Nonuniform Sediment Transport in Open Channels. *Journal of Hydraulic Engineering, ASCE* 130(10): 1013-1024.
- Wu, Q., Zhang, Y., Xu, J. and Shen, P. 2005. Regulation of hunger-driven behaviors by neural ribosomal S6 kinase in *Drosophila*. *Proc. Natl. Acad. Sci. USA* 102(37): 13289-13294.
- Yang, C. T. 1973. Incipient motion and sediment transport. *Journal of hydraulic division, ASCE* 99(HY10): 1679 – 1704.
- Yang, C. T. 1977. The movement of sediment in rivers. *Geophysical Survey* 3, D. Reidel, Dordrecht, 39-68.
- Yang, C. T. and Stall, J. B. 1976. Applicability of unit stream power equation. *Journal of hydraulic division ASCE* 102(HY5): 12103, 559 – 568.

- Yang, C. T. 1996. *Sediment transport: Theory and Practice*. San Francisco: The McGraw-Hill Companies, Inc.
- Yen, C. L., Wang, R. Y. and Chang, S.Y. 1985. *Mechanics and Numerical Simulation of Aggrading/Degrading Alluvial Stream with Application to the Choshui River – (I)*. Report No. 74-65. Disaster Prevention Research Program, National Science Council, Taipei, R.O.C.
- Yen, C. L., Wang, R. Y. and Chang, S.Y. 1988a. A study on Aggradation of Coarse Sediment in Open Channel. *Proc., 6th Congress of IAHR-APD*. Kyoto, Japan.
- Yen, C., Chang, S. and Lee, H. 1992. Aggradation and Degradation Process in Alluvial Channels. *Journal of Hydraulic Engineering, ASCE* 118(12): 1651-1669.
- Zhang, H. and Kahawita, R. 1987. Nonlinear Model for Aggradation in Alluvial Channels. *Journal of Hydraulic Engineering* 113(3): 353-369.

APPENDIX A

CODES

Sub equilibrium()

Dim h(502), u(502), z(502), hnew(502), znew(502)

'equilibrium'

'Kinematic wave approach'

'Vf Rouse, Vs Chien and Wan'

'DATA'

L = 1000 'Channel Length'

W = 20 'Channel Width'

So = 0.0025 'Channel Slope'

tn = 14400

dx = 2

dt = 0.1

nn = L / dx + 1

mm = tn / dt

g = 9.81

K = 0.756 * 10 ^ -4

Cz = 50

Cmax = 245

p = 0.528

ros = 2650

ro = 1000

ds = 0.32 * 10 ^ (-3)

al = Cz * So ^ 0.5

bet = 1.5

nu = 3

CSF = 0.65

pp = 4.75

fi = 0.53

trakd = 10

zmax = Cmax / (p * ros)

vis = 1.139 * 10 ^ -6

'Initial and Boundary Conditions'

'Discharge Hydrograph'

Q1 = 50

Q2 = 200

h1 = 1

h2 = 2.5198

'Sedimentgraph'

c1 = 14

c2 = 140

'trapeziodal hydrograph'

t1 = 0

t2 = 600
t3 = 4200
t4 = 7200
t5 = 10800
t6 = 14400

'Time started t=0s'

t = 0

Do

'Initial Conditions'

If t = 0 Then GoTo 1 Else GoTo 2

1 For i = 0 To nn

z(i) = c1 / (p * ros)

Next i

For i = 0 To nn

h(i) = h1

Next i

GoTo 3

2 For i = 0 To nn

z(i) = znew(i)

Next i

For i = 0 To nn

h(i) = hnew(i)

Next i

'Upstream Boundary Conditions'

3 If t < t2 Then GoTo 8 Else GoTo 9

8 h(0) = h1

z(0) = c1 / (p * ros)

GoTo 17

9 If t2 <= t And t < t3 Then GoTo 10 Else GoTo 11

10 h(0) = 4.2217 * 10⁻⁴ * (t - 600) + h1

z(0) = (0.035 * (t - 600) + c1) / (p * ros)

GoTo 17

11 If t3 <= t And t < t4 Then GoTo 12 Else GoTo 13

12 h(0) = h2

z(0) = c2 / (p * ros)

GoTo 17

13 If t4 <= t And t < t5 Then GoTo 14 Else GoTo 15

14 h(0) = -4.2217 * 10⁻⁴ * (t - 10800) + h1

z(0) = (-0.035 * (t - 10800) + c1) / (p * ros)

GoTo 17

15 h(0) = h1

z(0) = c1 / (p * ros)

17 For i = 1 To nn

$$u_ = (g * h(i) * So) ^ 0.5$$

$$Vf = 0.024$$

$$R_ = u_ * ds / vis$$

$$\text{If } 1.2 < R_ < 70 \text{ Then } uc_ = 2.5 * Vf / (\text{Log}(R_) - 0.06) + 0.66 * Vf$$

$$\text{If } R_ > 70 \text{ Then } uc_ = 2.05 * Vf$$

$$u(i) = al * h(i) ^ (\text{bet} - 1)$$

$$Vs = ((u(i) - (uc_ / 1.4) ^ 3 / u(i) ^ 2)) \text{ 'Chien \& Wan'}$$

$$VON = K / (g * Vf)$$

$$AA = 1 - VON * \text{bet} * al ^ 3 * h(i) ^ (\text{bet} - 1)$$

$$BB = al * \text{bet} * h(i) ^ (\text{bet} - 1) - VON * \text{bet} * al ^ 4 * h(i) ^ (2 * \text{bet} - 2)$$

$$CC = VON * \text{bet} * al ^ 3 * h(i) ^ (\text{bet} - 1)$$

$$DD = VON * (2 * \text{bet} - 1) * al ^ 4 * h(i) ^ (2 * \text{bet} - 2)$$

$$EE = p * Vs * (1 - 2 * z(i) / zmax)$$

$$hnew(i) = 0.5 * (h(i + 1) + h(i - 1)) - dt * BB * (h(i + 1) - h(i - 1)) / (2 * dx * AA)$$

$$znew(i) = 0.5 * (z(i + 1) + z(i - 1)) - dt * DD * (h(i + 1) - h(i - 1)) / (2 * p * dx) - dt * EE * (z(i + 1) - z(i - 1)) / (p * 2 * dx) - CC * (hnew(i) - 0.5 * (h(i + 1) + h(i - 1))) / p$$

$$hnew(i) = 0.5 * (h(i + 1) + h(i - 1)) - dt * BB * (h(i + 1) - h(i - 1)) / (2 * dx * AA) - (1 - p) * (znew(i) - 0.5 * (z(i + 1) + z(i - 1))) / AA$$

'Downstream Boundary Conditions'

$$hnew(nn) = hnew(nn - 1)$$

$$znew(nn) = znew(nn - 1)$$

$$dt = (dx / (u(i) + (g * hnew(i) ^ 0.5)) * 0.1$$

Next i

'New time'

$$t = t + dt$$

Loop

End Sub

Sub nonequilibrium()

Dim h(502), u(502), z(502), hy(502), hk(502), zk(502), c(502), uk(502), hkapdate(502),
ck(502), zg(502), Sf(502), uy(502), QQ(502), hky(502), unewp(502), unewpp(502), Ez(502),
Dc(502)

'nonequilibrium sediment transport'

'kinematic Wave approach'

'DATA'

'channel length in m'

$$L = 1000$$

'channel width in m'

$$W = 30$$

'channel slope'

$$So = 0.0015$$

$$tn = 14400$$

```

dx = 2
dt = 0.1
nn = L / dx + 1
mm = tn / dt
g = 9.81
K = 0.756 * 10 ^ -4
Cz = 36.5
Cmax = 500
p = 0.528
ros = 2650
ro = 1000
spww = ro * g
spws = ros * g
ds = 0.32 * 10 ^ (-3)  'm'
bet = 1.5
nu = 3
CSF = 0.65
pp = 4.75
fi = 0.53
trakd = 10
vis = 1.139 * 10 ^ -6
n = 0.02
zmax = Cmax / (p * ros)
'Boundary and initial Conditions'
'Hydrographs'
Q1 = 25  'dischare m^3/s'
Q2 = 125
h1 = (Q1 / (W * Cz * (So) ^ 0.5)) ^ (1 / 1.5)
h2 = (Q2 / (W * Cz * (So) ^ 0.5)) ^ (1 / 1.5)
c1 = 80  'kg/m^2 sediment'
c2 = 80

'trapeziodal hydrograph'
'in s'
t1 = 0
t2 = 600
t3 = 4200
t4 = 7200
t5 = 10800
t6 = 14400

t = 0  'time started at t=0 s'

Do
  'initial conditions'
  If t = 0 Then GoTo 1 Else GoTo 2
1  For i = 0 To nn
    h(i) = h1
  Next i
  For i = 0 To nn
    u(i) = Q1 / (h1 * W)
  Next i

  For i = 0 To nn
    z(i) = c1 / (p * ros)

```

```

Next i

For i = 0 To nn
c(i) = c1 / ros
Next i

GoTo 3

2 For i = 0 To nn
h(i) = hkapdate(i)
Next i

For i = 0 To nn
z(i) = zk(i)
Next i

For i = 0 To nn
c(i) = ck(i)
Next i

'Boundary conditions upstream'

3 If t < t2 Then GoTo 8 Else GoTo 9
8 h(0) = h1
z(0) = c1 / (p * ros)
u(0) = Q1 / (h1 * W)
c(0) = c1 / ros
GoTo 17

9 If t2 <= t And t < t3 Then GoTo 10 Else GoTo 11
10 h(0) = ((h2 - h1) * (t - t2)) / (t3 - t2) + h1
z(0) = (((c2 - c1) * (t - t2)) / (t3 - t2) + c1) / (p * ros)
QQ(0) = ((Q2 - Q1) * (t - t2)) / (t3 - t2) + Q1
u(0) = QQ(0) / (h(0) * W)
c(0) = (((c2 - c1) * (t - t2)) / (t3 - t2) + c1) / ros
GoTo 17

11 If t3 <= t And t < t4 Then GoTo 12 Else GoTo 13
12 h(0) = h2
z(0) = c2 / (p * ros)
QQ(0) = Q2
u(0) = Q2 / (h2 * W)
c(0) = c2 / ros
GoTo 17

13 If t4 <= t And t < t5 Then GoTo 14 Else GoTo 15
14 h(0) = ((h2 - h1) * (t - t5)) / (t4 - t5) + h1
z(0) = (((c2 - c1) * (t - t5)) / (t4 - t5) + c1) / (p * ros)
QQ(0) = ((Q2 - Q1) * (t - t5)) / (t4 - t5) + Q1
u(0) = QQ(0) / (h(0) * W)
c(0) = (((c2 - c1) * (t - t5)) / (t4 - t5) + c1) / ros
GoTo 17

15 h(0) = h1
z(0) = c1 / (p * ros)
u(0) = Q1 / (h1 * W)
c(0) = c1 / ros

```

```

17 For i = 1 To nn
  al = Cz * So ^ 0.5
  bet = 1.5

  Vf = 0.024 'fall velocity ROUSE'
  Vs = 0.01 'constant particle velocity'
  von = K / (g * Vf) 'velikanov'

  all = 0.5

'Flume'
lamda = 7 * h(i)
transferrate = 1 / lamda
transferrate2 = all * Vf / (h(i) * u(i))
tto = 1000 * h(i) * So
kk = 0.047
k1si = 0.5
ki = 2.5
ttocr = kk * (2650 - 1000) * ds
Tc = (k1si * (tto - ttocr) ^ ki)

'detachment rate'
Ez(i) = transferrate * Tc

'deposition rate'
Dc(i) = transferrate2 * ros * h(i) * u(i) * c(i)

'Boundary conditions downstream'
u(nn + 1) = u(nn - 1)
h(nn + 1) = h(nn - 1)
z(nn + 1) = z(nn - 1)
c(nn + 1) = c(nn - 1)

zk(i) = 0.5 * (z(i + 1) + z(i - 1)) - dt * Vs * (1 - 2 * z(i) / zmax) * (z(i + 1) - z(i - 1)) / (2 * dx) +
dt * (Dc(i) - Ez(i)) / ((1 - p) * ros)

hk(i) = 0.5 * (h(i + 1) + h(i - 1)) - dt * al * bet * h(i) ^ (bet - 1) * (h(i + 1) - h(i - 1)) / (2 * dx) - p
* (zk(i) - 0.5 * (z(i + 1) + z(i - 1))) / (1 - c(i)) + dt * al * h(i) ^ bet * (c(i + 1) - c(i - 1)) / (2 * dx
* (1 - c(i)))
ck(i) = 0.5 * (c(i + 1) + c(i - 1)) - dt * al * bet * h(i) ^ (bet - 1) * (c(i + 1) - c(i - 1)) / (2 * dx) -
c(i) * (hk(i) - 0.5 * (h(i + 1) + h(i - 1))) / h(i) - dt * al * bet * c(i) * h(i) ^ (bet - 2) * (h(i + 1) -
h(i - 1)) / (2 * dx) + dt * (Ez(i) - Dc(i)) / (h(i) * ros)
hkapdate(i) = 0.5 * (h(i + 1) + h(i - 1)) - dt * al * bet * h(i) ^ (bet - 1) * (h(i + 1) - h(i - 1)) / (2 *
dx) - p * (zk(i) - 0.5 * (z(i + 1) + z(i - 1))) / (1 - c(i)) + dt * al * h(i) ^ bet * (c(i + 1) - c(i - 1)) /
(2 * dx * (1 - c(i))) + h(i) * (ck(i) - 0.5 * (c(i + 1) + c(i - 1))) / (1 - c(i))

uk(i) = al * hkapdate(i) ^ 0.5

hkapdate(502) = hkapdate(500)
ck(502) = ck(500)
zk(502) = zk(500)

'stability'
dt = (dx / (uk(i) + (g * hk(i) ^ 0.5))) * 0.2

```

```
Next i  
'new time'  
t = t + dt
```

```
Loop  
End Sub
```